MAGNETIC PROPERTIES OF SOME DILUTE SOLID SOLUTIONS OF TRANSITION METALS IN VARIOUS SOLVENTS

Thesis Submitted

for the

Degree of Doctor of Philosophy

of the University of London

by

JAN HENDRIK WASZINK.

Physics Department,
Imperial College of Science & Technology,
London, January 1965.

ABSTRACT

The magnetic susceptibility of some dilute alloys was measured between 2 and 300°K by a force method. The main part of the work was on 0.1 at % solutions of Cr, Mn, Fe or Co in the η, ε and γ -phases of the copper-zinc system. The results show a striking variation of the atomic moment per solute atom with composition of the matrix. Mn carries a moment in all these phases. This moment varies strongly with Cu-Zn ratio in the ε-phase, but less strongly in the γ-phase where the value is surprisingly small (about $1\mu_B$ per atom). Fe is not magnetized in either Zn or the Zn-rich end of the ε-phase; but at the Cu-rich end of this phase the moment is about $1.5\mu_B$. The solutions of Co in the γ-phase have a temperature-independent susceptibility, but for Cr dissolved in this matrix a small moment is observed. Co and Cr in the γ-phase give moments of about $1.2\mu_B$. A survey is made of recent theoretical models for alloys and the results of this investigation compared with these.

Measurements were also made on solutions of Fe in Mo, Rh and Ir, the results of which can not be easily interpreted in terms of any existing theory.

ACKNOWLEDGEMENTS

The author wishes to express his sincere thanks to Dr. B.R. Coles for his interest and advice during the progress of this work which was carried out at his suggestion and under his supervision. He is greatly indebted to Dr. J.G. Park for many helpful discussions. Further he would like to thank Dr. D. Griffiths for handing on the susceptibility-balance used in this investigation.

During this work, the following financial support was gratefully received: a bursary from the Nederlandse Organisatie voor Zuiver Wetenschappelijk Onderzoek (from February to September 1961), a scholarship from the British Council (from October 1961 to December 1962) and a research bursary from the United Kingdom Atomic Energy Authority (from December 1962 to April 1964).

CONTENTS

INTRODUCTION

It was shown by Jones[1] in 1953 that the valency of a transition metal in solid solution can be expected to vary with the electron concentration in the conduction band of the solvent. Coles[2] then pointed out that experimental data which can be interpreted rather directly in terms of these ideas are the magnetic properties of dilute solutions of a transition metal. In the last ten years a large amount of work has been done on the electrical and magnetic properties of these solutions, mainly with a noble metal as solvent. In all the alloys investigated, anomalies in these properties were observed. The results also show that the state of the solute is strongly dependent on the electronic structure of the solvent. Theoretical models have been developed which describe some of the observed anomalies qualitatively but no complete interpretation of the experimental data has been given.

It seems likely that some information about the factors which determine the state of a solute atom can be obtained from measurements on solutions of a given transition metal in a binary alloy system in which the ratio of the two components is varied in small steps. A system with a large range of solid solutions in which small amounts of some transition metals are expected to dissolve is the Cu-Zn system.

In this work measurements have been made of the magnetic susceptibility of ternary solutions of 0.1 at % of a transition metal of the first long period in η, ε and γ-phase Cu-Zn alloys to investigate the correlation

between the magnetic behaviour of the solute and the properties of the matrix. Also measured was the susceptibility of some dilute alloys of two transition metals for which anomalies in the electrical resistivity have been reported.

CHAPTER I

THE THEORY OF DILUTE SOLID SOLUTIONS

Section A. Impurity States

§.1 Introduction

A dilute metallic solid solution of a solute B in a solvent A is a homogeneous mixture of the two metals which has the crystal structure of the solvent metal and in which the concentration of B atoms is low enough for mutual interactions between these atoms to be weak.

If an atom B is brought into the lattice, the one-electron wave functions of its outer electrons will overlap and interact with those of the band states of the host lattice. The energy levels and wave functions of these outer electrons will now be different from those of the corresponding states in the pure B lattice. It can be expected that the electronic structure of these states will be different for different solvents. On the other hand the impurity atom will perturb the periodic potential of the lattice and modify the structure of the Bloch states. In transition metals of the first long period the outer electrons are those in 3d and 4s states, the lower lying states will remain tightly bound to the nucleus and resemble those on free atoms. Because the 3d electrons are responsible for the magnetic properties of these pure metals, it can be expected that in alloys the magnetic moment per atom of solute and any coupling between these moments depends on the electronic structure of the host lattice, as is found from experiments. Qualitatively, three different ways of describing the effect of solute atoms on the band structure of the matrix can

be distinguished.

Consider an alloy of two elements of the first transition group and assume that a solute atom, on entering the lattice contributes all its 3d and 4s electrons to the band. The effect of the alloying process will be, apart from a change in the total number of electrons, an increase in the positive charge at some of the lattice points. The question is then how the extra charge will be screened. If this perturbation is small, the band structure will be deformed in such a way that around the impurity site the charge density is modified and screens the perturbing potential. In this case the alloy retains a common band structure. A second possibility is that the perturbing potential is strong enough to hold a bound state which is then subtracted from the band. Finally, there is, for intermediate values of the perturbing potential, the possibility of a virtual bound state, which is mainly localised in a certain volume around the impurity site without being a proper bound state.

These three models will be discussed in the following paragraphs.

§.2 The Band Model

If the perturbation is small the lattice potential can be written as the sum of the unperturbed periodic potential and a perturbing term V_p, which is localised at the impurity site[3]. The change in energy of a Bloch state $\psi_{\underline{k}}$, due to V_p is to first order $\Delta E = \int \psi_{\underline{k}}^*(\underline{r})\, V_p\, \psi_{\underline{k}}(r)\, d^3\underline{r}$.

If $\underline{k}$ is not too near a Brillouin zone boundary $\psi_{\underline{k}} \approx \psi_o \; e^{i\underline{k}\cdot\underline{r}}$ and $\Delta E = \int_{\cdot} \psi_o(\underline{r})\, V_p \psi_o(\underline{r})\, d^3\underline{r}$, i.e. independent of $\underline{k}$. This means that the energy of every state will be shifted by the same amount ΔE, so that the shape of the density of state vs energy curve will remain unchanged. The relation $N(E) = N_o(E \pm \Delta E)$ will hold depending on the sign of the perturbation. Here $N(E)$ is the density of states for the alloy, $N_o(E)$ that for the pure solvent. The results of this description remain qualitatively the same if $N(E) = N'_o(E \pm \Delta E)$ where $N'_o(E)$ is a function slightly different from $N_o(E)$, the difference being the result of the alloying process.

The introduction of the impurity potential will also cause a redistribution of charge in space. It is convenient to define the density $\rho(E,\underline{r})$ as the number of electrons with energy below energy E per unit volume at position $\underline{r}$. If the rigid band model holds $\rho(E,\underline{r}) = \rho_o(E - V_p, r)$ where ρ_o is the density for the pure solvent. The potential V_p at the impurity site is related to the resultant screening charge density by Poissons equation[4]: $\Delta V_p = -4\pi e \Delta\rho = 4\pi e^2 \left\{ \rho(E_F,) - \rho_o(E_F) \right\}$, where E_F is the Fermi-energy. This leads to the equation $V_p = \frac{e^2}{r} e^{-r/r_s}$, where $r_s^2 = \frac{1}{4\pi e^2 N(E_F)}$ From this result it is clear that a high density of Bloch states at the Fermi level is essential for effective screening. A typical value of $N(E_F)$ for a transition metal is 1 state per eV per atom which gives a screening radius $r_s = \frac{1}{3}$ Å, in this case the perturbing potential will be screened within the impurity atom.

The dependence of the saturationmagnetization on alloy composition of the binary alloys systems Ni-Fe, Ni-Co and Fe-Co (see Fig I) can be explained on the common band model[3]

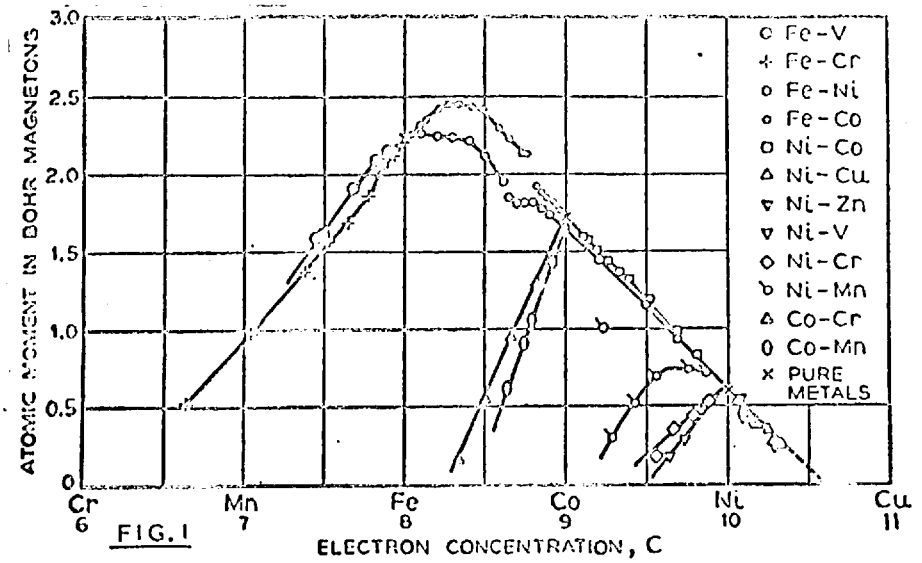

FIG. 1

Assume a 3d band as in Fig.2a, decoupled into two parts for different spin states. If an impurity is dissolved, the perturbing potential, i.e. the excess nuclear charge Z will be screened by the part of the band with the highest value of $N(E_F)$, in this case that for spin down states. If the screening radius is small, the moment at an impurity site will be the moment on a matrix atom μ_m minus $Z\mu_B$, while μ_m remains unchanged.

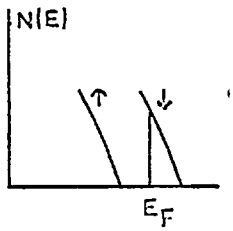

FIG. 2a

Neutron diffraction measuremonts[5] show that in Ni-Fe, Fe-Mn, Ni-Co and Fe-Co an atomic magnetic moment is localized at a lattice site. This does not necessarily mean that the charge density is also localized nor that a band model is the only explanation possible but the results are

consistent with the common band picture. The transition metals of the 4th and 5th period do not show ferromagnetism and an analysis as for the alloys of elements of the first transition group can not be given. It seems however likely that in general a picture as given above will be justified for alloys of elements with a difference in atomic number of one or possibly two units.

The common band picture has been applied mainly to alloys of non-transition elements. Many binary alloy systems of Cu and Ag with different elements of the IIB, IIIB and IVB sub group have similar phase diagrams. The values of the average number of conduction electrons per atom $\frac{e}{a}$ at which a given phase boundary occurs in different systems lie close together. That the ratio $\frac{e}{a}$ is an essential parameter in the description of these alloys indicates that the band model is applicable here.

§.3 Bound Impurity States.

A different situation arises if the potential V_p, defined in the previous paragraph is increased so that a bound state can exist. Slater and Koster[6] made a calculation for a simple cubic lattice, containing an impurity potential at one site, and showed, that the potential, if larger than a certain critical value, will remove a bound state, having a wave function of the form $\frac{e^{-ar}}{r}$, from the top or the bottom of the band, depending on the sign of the perturbation. For values of V_p smaller than the critical value the energy levels of the band were found to remain almost unperturbed.

If the screening of the impurity is done by electrons in bound states, it can be expected that the screening radius will be small.

The variation of the saturation magnetization of Co-Mn, Co-Cr, Ni-Mn, Ni-Cr and Ni-V (see Fig.1) with alloy composition was described by Friedel[3] in the following way.

Assume a 3d-band split into two parts corresponding to different spin states. The solute perturbs the lattice potential strongly, and a bound state is removed from the top of the full sub-band to an energy above the Fermi-surface of the alloy (Fig.2.b). This state is five-fold degenerate and five electrons will make a transition from a spin-up state, mainly to the other 3d sub-band. Neutron diffraction experiments[8] for Co-Cr, Ni-Cr and Ni-V show that the presence of the Cr or V atoms affects the moment at neighbouring Co or Ni sites, consequently the bound state must extend over a rather large volume.

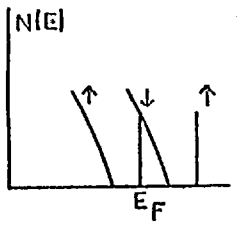

FIG 2·b

§.4 The Virtual Bound State.

a. General remarks.

Between the two extremes of a weak perturbing potential which causes a shift of the density of states curve and a strong one which pushes a bound state out of the collective band an intermediate situation is possible, the virtual bound state[9] which, although not being a proper bound state, is localized in energy and space. The concept can be introduced from the

consideration of the scattering of an electron by a spherically symmetric potential. The wave equation for a particle with angular momentum l in such a potential is

$$-\frac{\hbar^2}{2m}\frac{d^2\chi}{dr^2}+\left\{V(r)+\frac{l(l+1)\hbar^2}{2mr^2}\right\}\chi=E\chi,$$

the wave function for the particle is $\psi(r,\vartheta,\varphi) = R(r)\, y(\vartheta,\varphi)$ and $R(r) = \frac{\chi(r)}{r}$ $V(r)$ is assumed to be a localized potential, $V(r) = 0$ for $r>a$. The angular momentum term $\frac{\hbar^2\, l(l+1)}{2mr^2}$ can be seen as an additional potential energy. If the potential $V(r)$ is not strong enough to contain a bound state, the effective potential $V(r) + \frac{\hbar^2\, l(l+1)}{2mr^2}$ can have the form as in Fig.3a, with a potential barrier at r=a.

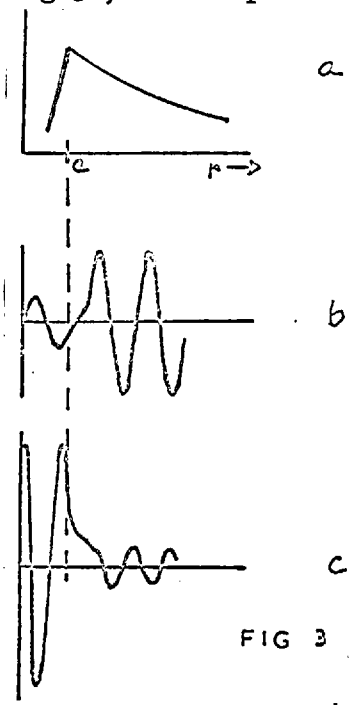

FIG 3

In general, the wave function of an electron of positive energy $<V_b$ in this kind of potential will be of the form as given in Fig.3b, but for some values of energy E_v with $0<E_v<V_b$, solutions as in Fig.3c are possible. This situation can be imagined as an incident electron, being "trapped" for a certain time between the barriers, before being scattered again. In this case a resonance maximum will occur in the scattering cross-section as function of energy at the energy E_v.

A state as in Fig.3c is called a virtual bound state. An electron will have a certain lifetime τ in this semi-bound state, to this time corresponds an uncertainty in energy $\Delta E \approx \frac{\hbar}{\tau}$.

This means that if $l \neq 0$, it is possible to have in a localized potential field a state with positive energy, which is localized in energy and space without being either a bound or a free electron state.

The phase shift δ as function of energy for a particle, scattered by a square well which is not deep enough to hold a bound state, is shown in Fig.4a. If the well is deep enough for a bound state to exist, δ will vary as shown in Fig.4b. A maximum in the scattering cross-section $\sigma = \frac{4\pi}{k^2} \sum_l (2l+1) \sin^2\delta_l$ will be observed at the energy for which $\delta = \frac{\pi}{2}$, this energy can be taken as the centre of the virtual state.

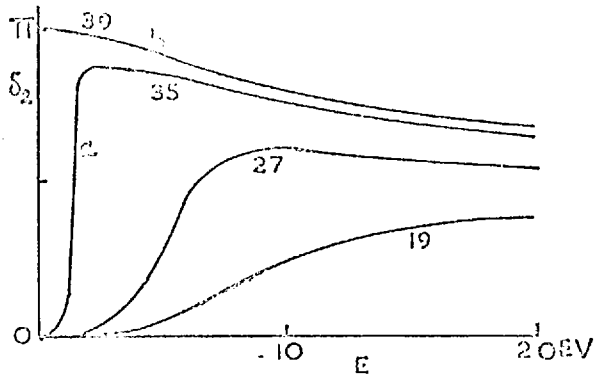

FIG.4 The phase-shift of the l = 2 partial wave for a free particle of energy E, scattered by a square potential well of radius 1.4 Å. The depth of the well in eV is indicated on the curves. After ref. 10

A different approach to the concept of a virtual bound state is to consider a bound 3d-state having a sharp energy level which lies in the range of the energies of a band. Interactions between this state and the states of the band will cause a broadening of the energy level. Qualitatively this can be seen as follows. Consider two non-interacting states A and B, having Energy E_a

and E_b respectively. If an interaction H is introduced the perturbed energy-levels are found from

$$\begin{vmatrix} E_a - E & H_{ab} \\ H_{ab} & E_b - E \end{vmatrix} = 0 \quad \text{giving} \quad E = \frac{E_a + E_b}{2} \pm \sqrt{(E_a - E_b)^2 + 4H_{ab}^2}$$

The effect of the perturbation is largest when $E_a = E_b$. If B is a state from a band and the interaction of A with all states B is considered, the perturbed energy E_a' will be broadened in energy and shifted with respect to E_a. The perturbed wave function of A will contain terms that depend on the B-states, i.e. the wave function of A will become mixed with those of the band-states. A proper treatment along these lines (§.4d) shows that the broadened A-state is identical with the resonant state discussed above.

The work by Friedel, who was the first to apply the concept of a virtual bound state is solid solutions, will be discussed in section 6 below. In section c and d a summary of the more precise formulation as given by Wolff, Clogston and Anderson will be given.

b. <u>The work of Friedel.</u>

Friedel showed [11] that the total number of states, bound and unbound, introduced in a Fermi-gas below an energy E by a localized potential V_p is equal to $n(E) = \frac{2}{\pi} \sum_l (2l+1)\, \delta_l(E)$ where $\delta_l(E)$ is the phase shift of the l'th partial wave for the scattering by V_p of an electron of energy E.

The density of states for the virtual state as a function of energy can now be written in terms of the phase shifts as $N(E) = \frac{dn(E)}{dE} = \frac{2}{\pi} \Sigma_l (2l+1) \frac{d\delta_l}{dE}$ and an alternative definition of the centre of the level is that energy where $\frac{d\delta_l}{dE}$ is greatest.

Blandin and Friedel, when investigating the behaviour of solutions of transition metals in noble metals (in particular Cu-Mn) calculated phase shifts for l=2 waves as function of energy of the incoming wave for a square well of different depths.[10] The radius of the well was taken as 2.7 atomic units = 1.4Å i.e. the atomic radius of copper. The numerical results showed:

a) that the energy of the virtual state can be taken to be limited to a certain energy range. The centre of the state was defined as the energy E_o for which N(E) reaches a maximum and the width as follows. Let n(E) be the total number of states up to energy E. The width is then defined as the difference E"-E' with these two energies defined by the relations $n(E') = \frac{1}{2} n(E_o)$ and $n(E'') = \frac{3}{2} n(E_o)$.

b) That E_o moves to higher energy if the depth of the potential well is reduced.

c) that the width of the state is proportional to the energy E_o, measured from the top of the well. Earlier calculations showed that for a given depth of the well the width of the state decreases with increasing angular momentum.

Friedel first introduced the concept of the virtual bound state to describe the observed variation of the residual resistivity of a number

of dilute alloys of Cu and elements of the first transition group[12]. In Fig. 5 the difference between the residual resistivity of binary alloys containing 1% of solute and that of Cu, $\Delta\rho$, is plotted as a function of atomic number of the solute, Z.

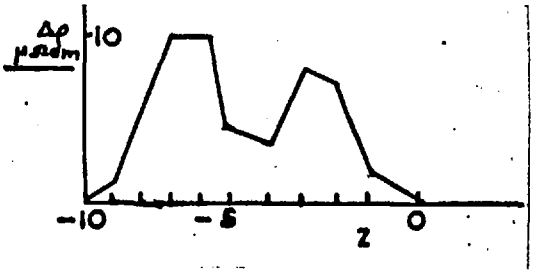

FIG.5 The difference in the residual resistivity of binary solutions of 1% of a transition metal in Cu and pure Cu. Z is the difference in atomic number between the solute and Cu. After ref. 3.

The experimental results could be explained on the assumption that the 3d states of the transition metal lie close to the Fermi level of the alloy. Further it had to be assumed that this state is split into two parts with different energy, this can be due to :

a) crystal field splitting, removing the degeneracy of the 3d states. In a lattice of cubic symmetry a charge distribution as shown in Fig. 6a, belonging to a state of symmetry $\frac{xy}{r^2}$ will have a different energy from that shown under B, belonging to states like $\frac{x^2-y^2}{r^2}$,

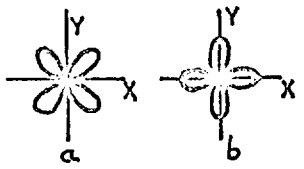

FIG. 6 (AFTER REF. 13)

b) Coulomb interactions between d-states,

c) exchange interactions between d states, this was taken as the cause of the greatest splitting, as a result the two sub-levels will contain states with different spin functions α and β.

The resistivity and magnetic susceptibility results were explained in terms of the following picture. (See Fig.7).

FIG. 7

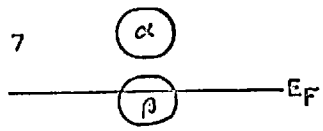

Both halves of the 3d level, containing 5 states each, lie near or coincide with the Fermi-level E_F and are broadened because of interactions with conduction electrons. The extra residual resistivity observed is due to resonance scattering of conduction electrons of energy E_F via the 3d state and related to the density of virtual states at E_F. A maximum in the $\Delta\rho$ vs Z curve is now ascribed to the fact that for the corresponding solute the energy of one of the 3d states, either α or β, coincides with E_F. The magnetic moment is proportional to the difference in occupation between α and the β state. The splitting between these states has to be greater than or at least comparable to the width of the state to have any meaning as such. If the splitting is swamped by the broadening no atomic moment will be observed, and only one peak in the $\Delta\rho$vs Z curve. Both conditions are fulfilled in solutions of the metals of the firsttransition group in Al.

c. The Model by Wolff and Clogston[14,15]

The possibility of the existence of a virtual state and the conditions under which it can carry a magnetic moment were investigated in more detail by Wolff and Clogston. The general approach is that of Friedel, a single band of conduction electrons is perturbed by the potential of a single impurity atom. It is shown that a resonance in the scattering can occur at a certain energy and that the wave function of the state, having this energy is concentrated around this potential.

The Schrodinger equation for the scattering of a conduction electron by the impurity potential V(r) is written as $\left\{ H_o + V(r) \right\}\psi = E\psi$ (1), where H_o is the unperturbed one-electron energy operator, E the energy and ψ the wave function of the electron. A solution ψ now satisfies the relation

$$\psi(\underline{r}) = \varphi_{\underline{k}}(\underline{r}) - \int g(\underline{r}\,\underline{r}')\, V(\underline{r}')\ \psi(\underline{r}')\ d\underline{r}' \qquad (2)$$

where $\varphi_{\underline{k}}(\underline{r})$ is the unperturbed Bloch wave function having a wave vector $\underline{k}$ and energy E_k and $g(\underline{r}\ \underline{r}')$ a function which satisfies the relation $(H_o - E)g(\underline{r}\ \underline{r}') = \delta(\underline{r}-\underline{r}')$.

Equation (2) can be written as

$$\psi(\underline{r}) = \varphi_{\underline{k}}(\underline{r}) + \left(\frac{1}{2\pi}\right)^3 \lim_{s \to o} \iint \frac{\varphi_{k'}(\underline{r})\varphi^*_{k'}(\underline{r}')}{E - \underline{k}'^2 + is} V(\underline{r}')\psi(\underline{r}')d^3\underline{r}'\ d^3\underline{k}'$$

or symbolically $\psi = \varphi_{\underline{k}} + \dfrac{1}{E_k - H_o + is}\, V\psi \qquad (3)$

The wave functions are now written as a linear combination of Wannier functions $a(\underline{r} - \underline{R}_j)$ which have the property of being localized around the lattice site $\underline{R}_j$ and are defined as $a(\underline{r}-\underline{R}_j)= \frac{1}{\sqrt{N}} \sum_{\underline{k}} e^{-i\underline{k}.\underline{R}_j} \psi_{\underline{k}}$, where N is the number of lattice sites in the crystal. The wave function is then $\psi(\underline{r}) = \sum_{\underline{R}_j} U(\underline{R}_j)\, a\,(\underline{r} - \underline{R}_j)$ (4). After substitution of (4) in (3) and with the help of the fact that $V(\underline{r})$ is localized at one lattice site $\underline{R}_o$ i.e. that $\int a^*(\underline{r} - \underline{R}_i)\, V(\underline{r})\, a(\underline{r} - \underline{R}_j)\, d^3\underline{r} = V_o\, \delta(\underline{R}_i - R_o)\, \delta(\underline{R}_j - \underline{R}_o)$, it is found that

$$U(\underline{R}_o) = \frac{e^{i\underline{k}.\,\underline{R}_o}}{[1 - V_o\, F(E)\,] + i\pi V_o\, \rho(E)} \qquad (5)$$

where $F(E) = P \int_o^\infty \frac{\rho(\varepsilon)}{E - \varepsilon}\, d\varepsilon \equiv \lim_{\delta \to o} \left[\int_o^{E-\delta} \frac{\rho(\varepsilon)}{E - \varepsilon}\, d\varepsilon + \int_{E+\delta}^{\infty} \frac{\rho(\varepsilon)}{E - \varepsilon}\, d\varepsilon \right]$

and $\rho(E)$ is the density of states in energy of the band. If $1-V_o\, F(E)= 0$ (6), $U(R_o)$ reaches a maximum and consequently the part of $\psi(\underline{r})$ localized at $\underline{R}_o$ also. The energy at which this occurs is the required resonance energy. If the resonance-energy E_o lies outside the band, then $\rho(E_o) = o$ and $U(\underline{R}_o) \to \infty$ as $E \to E_o$. This means that there exists a bound state with energy E_o. The question is now to find the energy E which satisfies equation 6.

If $\rho(E)$ has a parabolic form as is shown in Fig.8. F(E) is as indicated. For an attractive potential, E_o and E_1 are

FIG.8

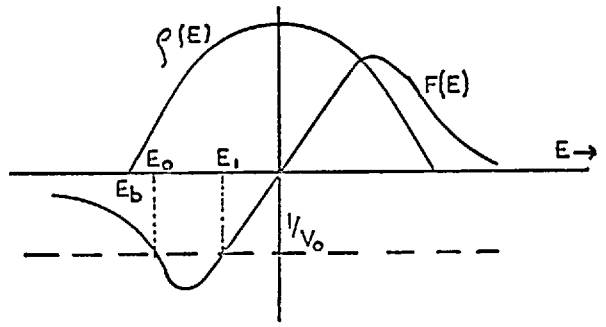

solutions of which E_1 represent an unstable state. If E_o lies to the left of E_b, this solution will be a bound state.

Clogston used the same model and came to the same result in a slightly different formulation as follows. If $V(\underline{r}) \equiv o$ then $U(\underline{R}_i) = e^{i\underline{k}.\underline{R}_i}$. If now again $V(\underline{r})$ is localized at the site $\underline{R}_o$, the perturbed $U(\underline{R}_o)$ is found to be $U(\underline{R}_i) = e^{i\underline{k}.\underline{R}_i} - \dfrac{V_o\ e^{i\underline{k}.\underline{R}_o}}{1 + V_o g_E\ (o)}\ g_E\ (\underline{R}_i - \underline{R}_o)$

$$\text{where } g_E(\underline{R}_i - \underline{R}_o) = \frac{1}{N} \sum_{\underline{k}} \frac{e^{i\underline{k}(\underline{R}_i - \underline{R}_o)}}{E_k - E}$$

So far the treatment is identical to that by Wolff. If this expression is expanded in spherical harmonics the l=o part is, taking $\underline{R}_o = \underline{o}$:

$$j_o(k.R_i) - \frac{V_o\ j_o(o)}{1 + V_o g_E(o)}\ g_E(\underline{R}_i - \underline{R}_o) \qquad (7).$$

The other terms ($l \neq o$) are not affected by V since $j_l(o) = o$ for $l \neq o$. (This does not imply that the wave function (eqn. 4) has s-character). For large values of R_i, (7) can be written as $\dfrac{e^{i\gamma}}{kR_i}\ \sin[\ kR_i + \gamma(E)]$ with $\gamma(E) = \text{arc tan}\ \dfrac{\pi\Omega\ \rho\ (E)}{F(e) - \dfrac{1}{V_o}}$. The condition for resonance is $\gamma = \dfrac{\pi}{2}$ which leads again to $F(E) = \dfrac{1}{V_o}$. If $\gamma(E)$ as found from the above mentioned function $\rho(E)$ is plotted vs E, (Fig.9) a relation similar to that found by Friedel emerges.

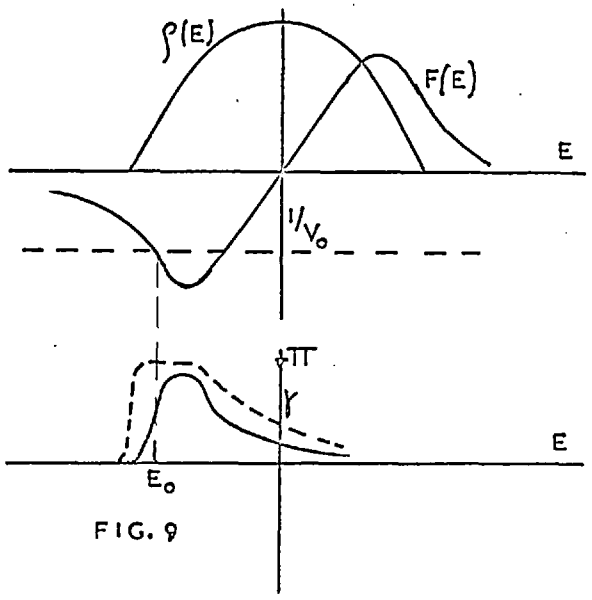

FIG. 9

From the sum rule the density of states of the extra state is found as $\frac{dz}{dE} = \frac{2}{\pi}\frac{d\gamma}{dE}$ this means that the level will be narrow if $\frac{d\gamma}{dE}$ is large. If the potential V_o is increased, E_o will move to the left, become sharper and to the left of E_b will be an energy level in the strict sense (in the case $U(R_o) \to \infty$ there is a finite value of U without an incoming wave, i.e. a bound state exists). This calculation also shows that the state is narrow if $\rho(E)$ is small for the function $\rho(E)$ as shown.

To investigate the conditions under which the virtual state can be magnetized Wolff then adds a spin dependent potential to V and considers the stability of this polarization in a HartreeFock model. The modified V for spin up and spin down electrons, $V+\delta V^{\uparrow}$ and $V+\delta V^{\downarrow}$ respectively, leads to different values of $U_{\uparrow}(R_o)$ and $U_{\downarrow}(R_o)$.

For energies near E_o it can be assumed that $\psi(r) \approx U(R_o)a(r-R_o)$

If this is substituted in the expression for the energy for the Hartree-Fock model the exchange energy is found to be cancelled by the Coulomb integral for states with parallel spin. The energy for the spin-up is found to be proportional to

$$J \times \sum_{\substack{\text{filled} \\ \text{states}}} \left| U_{\downarrow} (\underline{R}_o) \right|^2 \qquad (8)$$

$$\text{where } J = \iint \left| a(\underline{r}_1 - \underline{R}_o) \right|^2 \frac{e^2}{\underline{r}_1 - \underline{r}_2} \left| a(\underline{r}_2 - \underline{R}_o) \right|^2 d\underline{r}_1 \, d\underline{r}_2$$

The result is now that a change $\delta V^{\uparrow}$ will cause a change in $U^{\uparrow}(\underline{R}_o)$ (Eqn.5) which according to (8) causes a change in energy of the spin-down state, which is put equal to $\delta V^{\downarrow}$. The same argument holds if $\delta V^{\downarrow}$ and $\delta V^{\uparrow}$ are interchanged, so that two relations $\delta V^{\uparrow} = f(\delta V^{\downarrow})$ and $\delta V^{\downarrow} = f(\delta V^{\uparrow})$ are obtained which hold if $\delta V \ll V$. These equations can be solved numerically. It is found that these equations have either two solutions with $\delta V^{\uparrow} \neq \delta V_{\downarrow}$ and an unstable one with $\delta V^{\uparrow} = \delta V^{\downarrow}$ or one stable solution with $\delta V^{\uparrow} = \delta V^{\downarrow}$. Only in the first case is a magnetic state possible. The condition for the stability of this state is $\frac{\partial(\delta V^{\uparrow})}{\partial(\delta V^{\downarrow})} > 1$ which leads to

$$1 + \left(\frac{E_F - E_o}{\Delta} \right)^2 < \left| \frac{J}{\pi^2 V^4 \rho_o F'} \right|$$

where Δ, the width of the state, is defined as $\frac{\pi \rho_o}{F'(E)}$, $\rho_o \equiv \rho(E_o)$. It can be seen that a moment is possible if the virtual state lies close to the Fermi-energy and is relatively sharp.

The integral J is a Coulomb integral and no exchange energy appears in this theory. This is however due to the fact that the exchange integral is cancelled against part of the Coulomb integral. The magnetic splitting must be considered to be due to the total of Coulomb and exchange interactions.

d. The Theory by Anderson [16]

The nature of the virtual state was investigated by Anderson from the opposite approach. A localized d state with energy in the range of that of a band of Bloch states interacts with these states and is broadened in energy. The conditions were also investigated under which a stable magnetic state exists.

The theory is given for a single, nondegenerate level. One important parameter in the theory is the Coulomb integral between d-electrons $U = \int \left|\varphi_d(\underline{r}_1)\right|^2 \frac{e^2}{|\underline{r}_1 - \underline{r}_2|} \left|\varphi_d(\underline{r}_2)\right|^2 d^3\underline{r}_1\, d^3\underline{r}_2$ where $\varphi_d(r)$ is a localised d wave function. As in the treatment by Wolff the exchange integral is cancelled against the Coulomb integral for states with parallel spin and in the Hamiltonian for the problem only a term $H_c = U\, n_{d\uparrow}\, n_{d\downarrow}$ appears, representing a repulsion of opposite spins; n_d is the number of d states with spin up.

Another important quantity is the interaction of the d state with the Bloch states $H_{sd} = \sum_{k_1\sigma} V_{dk}\, (c^*_{k\sigma}\, c_{d\sigma} + c^*_{d\sigma}\, c_{k\sigma})$

the index k refers to Bloch states,

σ refers to the spin.

The total Hamiltonian of the system is written as $H = H_{of} + H_{od} + H_c + H_{sd}$, where H_{of} is the unperturbed free electron energy H_{od} the unperturbed energy of the d-level $= E_d(n_{d\uparrow} + n_{d\downarrow})$. Using Hartree-Fock theory it is shown that there is a state of the perturbed system having spin σ with energy $E_d + \Delta E_d + U\langle n_d, -\sigma\rangle - i\Delta$ where $\langle n_{d,-\sigma}\rangle$ is the average number of electrons in the d-state with spin $-\sigma$, $\Delta = \pi\langle V_{dk}^2\rangle \rho_k(E)$, $\rho_k(E)$ the density of Bloch states in energy and ΔE_d a shift in energy which is disregarded further. The wave function of this one-electron state is now $\psi(\underline{r},t) = \varphi(\underline{r})\, e^{-\frac{i\,Et}{\hbar}} = \varphi(\underline{r})\, e^{-\frac{iEt}{\hbar}} \cdot e^{-\frac{t\Delta}{\hbar}}$. The lifetime τ of an electron in this state is $\frac{\hbar}{\Delta}$, to this corresponds a width in energy $\frac{\hbar}{\tau} = \Delta$. This means that the perturbed system has a state with energy $E_\sigma = E_d + U\langle n_{d,-\sigma}\rangle$ and a width in energy Δ, i.e. the required virtual state.

For the density of perturbed d-state with spin σ is found

$$\rho_{d\sigma}(E) = \frac{1}{\pi}\,\frac{\Delta}{(E - E_\sigma)^2 + \Delta^2}$$

$\rho_{d\sigma}$ is plotted in Fig. 10. as function of E.

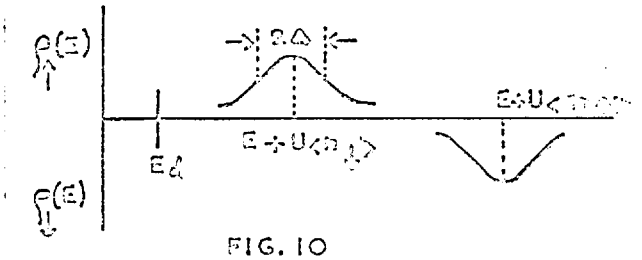

FIG. 10

The density of virtual states for up and down spins.

The occupation of the levels with different spin is now

$$n_+ \equiv \langle n_{d\uparrow} \rangle = \int_0^{\varepsilon_F} \rho_{d\sigma}(\varepsilon)\,d\varepsilon = \frac{1}{\pi}\cot^{-1}\frac{E_d - \varepsilon_F + U\langle n_{d\downarrow}\rangle}{\Delta} \qquad (9)$$

and a similar expression for $n_- \equiv \langle n_{d\downarrow} \rangle$ these two equations can be solved numerically. A solution with $n_+ \neq n_-$ represents a magnetic state. If two parameters x and y are defined as $x \equiv \frac{\varepsilon_F - E_d}{U}$ and $y \equiv \frac{U}{\Delta}$, the equation (9) becomes

$$\cot \pi n_+ = y(n_- - x)$$

$$\cot \pi n_- = y(n_+ - x)$$

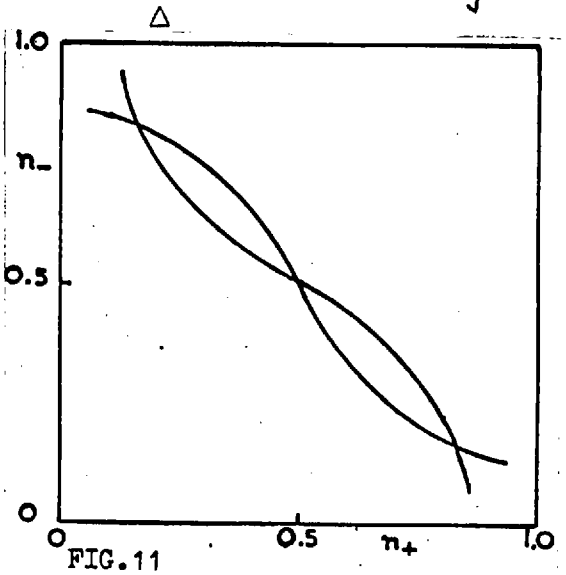

FIG. 11

The functions $n_- = f(n_+)$ and

The transition from magnetic to non-magnetic behaviour is determined by the condition that the two curves $n_+ = f(n_-)$ and $n_- = f(n_+)$ touch at $n_+ = n_- = n_c$. For the first curve $\frac{\partial n_-}{\partial n_+} = -\frac{\pi}{y \sin^2 \pi n_+}$, for the second $\frac{\partial n_-}{\partial n_+} = -\frac{y \sin^2 n_-}{\pi}$ so that the equations $\sin^2 \pi n_c = \frac{\pi}{y}$ and $\cot \pi n_c = y(n_c - x)$ define an area in the x-y plane, within which a magnetic solution is possible. i.e. the shaded area in Fig. 12. It is now seen that in this model the conditions for the existence of a moment are, an unperturbed d-level not too far from the Fermi-energy ($|x| < 1$) and a value of the Coulomb integral large compared with the width of the state.

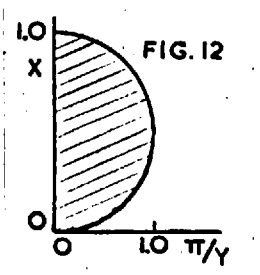

FIG. 12

The theory was extended to a twofold degenerate level, in that case the condition for the existence of a moment is $\frac{U}{\Delta} > \frac{\pi}{\sin^2 \pi n_c} - \frac{J}{2\Delta}$, where J is the exchange integral, which is favourable for the formation of a magnetic state. If U=o, the condition for splitting is $J > 2\pi\Delta$, so that the exchange energy (1 to 2 eV) only can not magnetize any level wider than $\frac{1}{3}$ eV.

In this treatment, the conditions for the stability of a magnetic virtual state are similar to those found in the scattering model. Both theories contain however parameters that are difficult to estimate (the function F(E) and the value of V_o in Wolff's and the matrix element V_{sd} in Anderson's treatment of the problem) and detailed comparison of either theory with experiment impossible. An estimate of the width of the state can however be made. In a free Mn atom the 3d-4s interaction is found from spectroscopic data to be of the order of 0.5eV. If a typical value for a transition metal, $\rho(E)$ = 2 state per atom per eV is taken, the width is $\Delta \approx 1$eV. For a transition metal dissolved in Cu where $\rho(E) \approx 1$ state per atom per eV the width is then of the order of 0.1 eV.

The variation of the atomic moment with temperature.

The theory of Anderson was extended to temperatures above zero by White and Clogston.[17]

For $T \neq o$, equation (9) becomes $n_{\mp}(T) = \int_{-\infty}^{+\infty} \rho_{d\mp}(E)\, f(E,T)dE$ where $f(E,T)$ is the Fermi-Dirac distribution function. This expression was

calculated numerically for several values of $\frac{kT}{\Delta}$. The results show that for a value of the Coulomb-integral of 10eV as for a free transition metal ion, a change in the atomic moment is either extremely small, or occurs at temperatures far above room temperature, so that this work does not predict any effects that can readily be checked by experiment.

SECTION B. INTERACTIONS BETWEEN MOMENTS ON SOLUTE ATOMS

§.1 Introduction

Experimental results for many dilute alloys suggest that interactions between magnetic moments on solute atoms must be assumed (e.g. in the systems Cu-Mn, Cu-Fe). In these alloys the distance between two nearest solute atoms will, for the most part be larger than the nearest neighbour distance of the lattice, e.g. face-centred cubic lattice containing 0.1 at % of impurity, 98% of the solute atoms have no nearest neighbours of the same kind. Under these circumstances the wave functions of the d-states of these atoms will not overlap, direct exchange and Coulomb interactions can not be held responsible for the apparent coupling, and a different mechanism of longer range must be operative.

Much attention has been given to the concept of a spin-polarization of the extended states of the crystal in a certain volume around a solute atom. If such spin-distributions, centered at different atoms, overlap, the solute spins will interact via this mechanism. This type of coupling was first suggest by Zener[18] for the interactions between atomic moments in pure transition metals. Kasuya[19] and Yosida[20] adapted the model given by Ruderman and Kittel for the polarization of conduction electrons by a nuclear spin to apply to the polarization of 4s-electrons in a dilute Cu-Mn alloy by the spin of a Mn atom. In this model the 3d-electrons which give rise to the moment of a solute atom were assumed to be in bound states.

For the same alloys Blandin and Friedel considered the case of a weaker impurity potential[10,21], i.e. the case that the 3d-state on a Mn atom

becomes a virtual bound state. The 3d-wave functions will then become mixed with the 4s-wave functions of the Bloch-states and extend to a large distance from the solute atom.

A completely different mechanism, a spin polarization of the electron gas extending over the whole volume of the metal and stabilized by the solute moments was proposed by Overhauser[22].

§.2 Polarization of conduction electrons (Yosida).

The model of Yosida[20] was developed for a dilute solution of Mn in Cu. The following assumptions were made :

1. The 3d electrons on the Mn atoms are in bound states and there is no overlap of wave functions of electrons on different atoms.
2. The orbital 3d moment vanishes.
3. The conduction electrons do not interact with each other and
4. have wave functions of the Bloch type.

The effect of exchange interactions between 4s conduction electrons and 3d electrons on the Mn atoms is considered. These interactions are represented by an interaction of the form $J_{in}\underline{s}_i \cdot \underline{S}_n$, where $\underline{s}_i$ is the spin of a 4s-electron $\underline{S}_n$ that of a Mn atom and H_{in} the 3d-4s exchange integral. This Hamiltonian, in the form given by Kasuya, is treated as a perturbation of the system. From the first order perturbation of the conduction electron wave functions the following expression for the volume density of 4s electrons is obtained:

$$\rho_{\pm}(r) = \frac{n}{V} \mp \frac{1}{V} \frac{4(3n)^2}{E_f} \frac{J(o)}{N} \sum_n 2k_F|\underline{r} - \underline{R}_n| F(2k_m|\underline{r} - \underline{R}_n|) S_n^z \qquad (10)$$

where 2n is the number of conduction electrons, N the number of lattice sites in the crystal, V the volume of the crystal, E_F the Fermi energy and k_F the corresponding wave vector. $J(\underline{k} - \underline{k}')$ is the exchange integral between a conduction electron and the d-core spin of a Mn ion and $\underline{R}_n$ the coordinate of a Mn atom with z-component of spin S_n^z. The subscript $\pm$ refers to the spin function of an electron, the function F(x) is defined as $F(x) \equiv \frac{1}{x^4}(x \cos x - \sin x)$. The energy of this system is calculated to second order and is found to contain a term representing the energy of the Mn spins as a result of this indirect interaction :

$$\left(\frac{3n}{N}\right)^2 \frac{2\pi}{E_f} J(o)^2 \sum_{\substack{n,m \\ \text{solute atoms}}} F\left\{2k_F |\underline{R}_n - \underline{R}_m|\right\} \underline{S}_n \cdot \underline{S}_m .$$

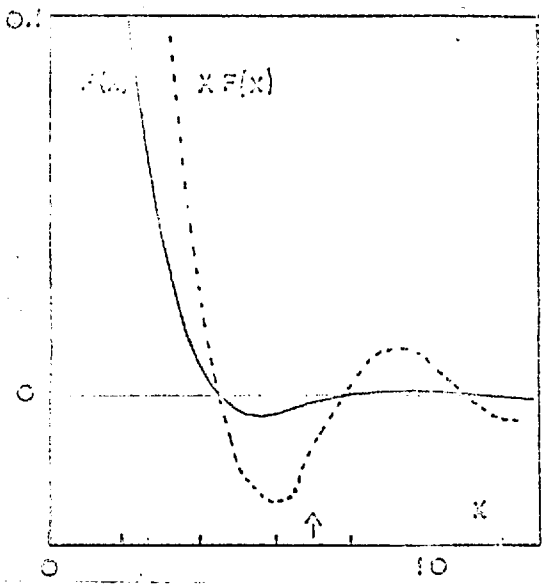

FIG. 13
The value $x = 2k_F r$ with k_F the Fermi-velocity and r the nearest neighbour distance in Cu is indicated by the arrow.

The functions F(x) and xF(x) are plotted in Fig. 13. It becomes clear that in a Cu-Mn alloy the spin polarization is concentrated near the Mn atoms. The absence of a shift in the nuclear resonance of the Cu and the electron

spin resonance of the Mn atoms which were expected by Owen et al. as the result of a homogeneous polarization seems to be explained by this result.

It has been put forward by Abrikosov and Gorkov[23] that the last stages in Yosida's calculation are not correct and that the correct expression for the charge densities is $\rho\pm = \frac{n}{V}\left(1 \pm c\ \frac{J(o)}{E_F}\ \overline{S^z}\right)$ instead of equ.(10). Here c is the impurity concentration and S^z the average z-component of the impurity spin. If the following values are substituted: $J(O) = 0.3eV$, $E_F = 7eV$, the Fermi energy of Cu, $c = 0.1$ at % and $\overline{S^z}$ is found with the help of the Curie-Weiss law for the susceptibility of a system of moments of $4.8\ \mu_B$, i.e. approximately the value for Mn in Cu and the system is in a field of 10^4 Oe, a spin polarization of the same order of magnitude as that due to the Pauli-paramagnetism in Cu in this field is found.

The critical temperature, below which the homogeneous polarization is possible, is $T_c = \frac{N_i S(S+1)\ a^2 \chi_o}{12\mu_B^2 \cdot k}$ where S is the spin of an impurity atom, χ_o the paramagnetic susceptibility of the electron gas in the absence of impurities and $a = \int J(\underline{r})\ d^3\underline{r}$ with $J(\underline{r})$ the function representing the interaction between an impurity and the conduction electrons. At T=o, the spin polarization per unit volume is $s = \frac{N_i a_1 S \chi_o}{4\mu_B^2}$. In a small external magnetic field H, the contributions to the magnetic moment considered here are

$$M = \frac{Ng\mu_B as\ S(S+1)}{3kT} + \frac{Ng^2\mu_B^2 S(S+1)H}{3kT} + 2\mu_B s$$

The first term can be written in the form $\frac{N\mu^2}{3kT}\ H'$ with $H' = \frac{as}{g\mu_B}$ and

$\mu = g\mu_B\sqrt{S(S+1)}$. H' represents the effective field acting on the impurity spins due to the spin polarization. The second term is the Curie-Weiss paramagnetic contribution of the solute moments and the third the conduction electron moment. For a solution of 0.1% impurity in Cu, for which the following magnitudes of the various quantities are taken :

$S=2$, $\chi_o = 10^{-6}$ cgs units, $J = 0.3$ eV and for the range of this interaction function the atomic radius, the above-mentioned formulae give : $T_c = \frac{1}{8}\,{}^{o}k$, the effective field $H' = 3500$ Oe, and the magnetic moment due to the spin polarization at T=o is about 0.03 $\frac{erg}{gauss}$ per cm^3. The normal Pauli paramagnetism in Cu in a field of 10^4 Oe is 0.01 $\frac{erg}{gauss}$ per cm^3.

§.3 Polarization of a virtual bound state.

If the impurity potential is not strong enough to hold a bound state, a spin polarization similar to that by Yosida will still be possible as was shown by Blandin and Friedel[10,21] and by Kohn and Vosko[21a].

In this case the system can be represented by a gas of free electrons, subjected to a localized potential. The wave function of an electron is written as

$$\psi_{\underline{k}}(\underline{r}) = \frac{1}{\sqrt{V}}\, e^{-i\underline{k}.\underline{r}} + \underline{f}_k(\vartheta)\, \frac{e^{ikr}}{r} \qquad (1)$$

at large distance from the origin.

The choice of this form for the wave function excludes the consideration of a bound state.

The change in charge density at a point $\underline{r}$ in space as a result of the introduction of the perturbing potential is

$$\Delta\rho\ (\underline{r}) = \int \frac{V}{4\pi^3}\left\{\ \psi^*(\underline{r})\ \psi(\underline{r}) - \frac{1}{V}\right\} d^3\underline{k} \qquad (2)\ ,$$

the integral is over the occupied volume in $\underline{k}$-space. Substitution of eqn.(1) into (2) and use of standard scattering theory leads to

$$\Delta\rho\ (\underline{r}) = -\ \frac{a_F}{2\pi^2\ r^3}\ \cos\ (2\underline{k}_F \cdot\ \underline{r} + \varphi_F) \qquad (3)$$

$$\text{with} \quad a \sin\varphi = \Sigma\,(-1)^l(2l+1)\sin^2\delta_l$$

$$\text{and} \quad a \cos\varphi = \Sigma\,(-1)^l(2l+1)\sin 2\delta_l\ .$$

$\underline{k}_F$ is the wave vector of an electron having the Fermi-energy, δ_l the phase shift of the l'th partial wave. This means that a virtual bound state gives rise to a charge distribution extending to large distances from the impurity potential, although rapidly decreasing in amplitude. If this charge distribution is different for electrons having different spin functions, a spin polarization similar to that found by Yosida will exist. If only the partial wave with l=2 is considered equ (3) gives

$$\Delta\rho_d = \frac{-5}{2\pi^2\ r^3}\ \cos\ (2k_F r + \delta_2)\ .$$

If the potential is spin-dependent $\Delta\rho$ can be separated into two parts, $\Delta\rho^+$ and $\Delta\rho^-$ for electrons in different spin states. In the case of strong spin decoupling it is possible that $\Delta\rho^- = 0$ and $\Delta\rho^+ = \frac{5}{4\pi^2\ r^3} \times \sin\delta_2^+ \cos\ (2\underline{k}_F \cdot \underline{r} + \delta_2^+)$. Here δ_2^+ is the phase shift of the l=2 partial

wave if only electrons with + spin are considered.

The interaction can now be investigated of a solute atom at position $\underline{R}_2$ having a spin $\underline{S}$ with the spin distribution $\Delta\rho_1^+ (\underline{r})$ which is centered around the impurity atom at position $\underline{R}_1$. If V_A is the volume of an impurity atom and ΔF the interaction energy of the spin $\underline{S}$ with that of a conduction electron, the interaction energy of $\underline{S}$ with the spin distribution $\Delta\rho_1^+ (\underline{r})$ is given by $\Delta E = \Delta\rho_1^+ (\underline{r})\, V_A\, \Delta F$.

This will now be applied to a Cu-Mn solution. For ΔF is taken half of the 4s-3d interaction energy in a free Mn atom, 0.3 eV, for V_A the atomic volume of Cu, $V_A \approx 1.2 \times 10^{-23}$ cm^3 and for δ_2^+ the resonance value $\frac{\pi}{2}$. The result is then $\Delta E \approx \frac{4.6 \times 10^{-25}\ \text{eVcm}^3}{r^3} \times \cos(2\underline{k}_F \cdot \underline{r})$, with $\underline{r} = \underline{R}_1 - \underline{R}_2$. For $r = 4\text{Å}$ this gives $\Delta E \approx 0.7 \times 10^{-2}$ eV. The expression given by Yosida for two spins only (eqn.10) is

$$\left(\frac{3n}{N}\right)^2 \frac{2\pi}{E_f} \quad J(o)^2 \quad \frac{\cos 2\,\underline{k}_F \cdot \underline{r}}{k_F^3\, r^3} \qquad \underline{S}_1 \cdot \underline{S}_2$$

For the case of Cu-Mn the following values are taken N=2n, $J(o) \approx 0.3$eV, $E_f = 7$eV, S=2, $k_F = 1.4 \times 10^8$ cm^{-1} the interaction energy of two spins in the Yosida model is $\frac{0.5 \times 10^{-25}\ \text{eV cm}^2}{r^3} \cos 2\,\underline{k}_F \cdot \underline{r}$, $r = 4\text{Å}$ gives for this energy about 0.08×10^{-2}eV.

§.4 Spin density waves.

A completely different approach was followed by Overhauser who argued that since Yosida's mechanism is in fact a short range interaction this will only lead to long range order of the system for high concentrations

of solute ($\gtrsim$10 at %) and consequently a different explanation of the observed coupling has to be given.

If was postulated by Overhauser[22] that in the gas of conduction electrons a spin polarization of the form $\underline{s}(\underline{r}) = bN\,\underline{\varepsilon}\cos \underline{q}.\underline{r}$ is possible. Here $\underline{s}(\underline{r})$ is the spin density at position $\underline{r}$, N the number of atoms per unit volume, $\underline{\varepsilon}$ a unit vector defining the direction of the polarization, $\underline{q}$ the wave vector of the polarization. This spin density wave can be seen as the sum of two charge density waves with spin parallel and antiparallel to $\underline{\varepsilon}$, equal in amplitude and opposite in phase so that the charge density remains uniform in space. Because this is a property of the electron gas and not of the alloy as a whole, the wave vector $\underline{q}$ will not be related directly to the lattice parameter of the crystal.

Within the Hartree-Fock theory a spin-density wave will be a stable state of the electron gas, however, if electron correlations are taken into account, it will have a higher energy than the unpolarized state.

If solute atoms carrying a magnetic moment are introduced in the lattice the interaction energy of these moments with the spin density wave can compensate the correlation energy and stabilize the polarization.

The effective field acting on an impurity atom at position $\underline{R}_j$ can then be written as $\underline{H}_j = Gb\,\underline{\varepsilon}\cos \underline{q}.\underline{R}_j$ where G is an interaction parameter. Since the wavelength of the spin density wave is not an integral multiple of the lattice parameter, the solute atoms can be assumed to be subjected to a random field with probability distribution $P(H) = \frac{2}{\pi}\frac{1}{\sqrt{G^2b^2 - H^2}}$.

With the help of this expression, the low-temperature specific heat of a dilute alloy was calculated, giving a good fit to the experimental data for Cu-Mn alloys. An expression for the paramagnetic susceptibility was not derived.

CHAPTER II

THE MAGNETIC SUSCEPTIBILITY OF METALS & ALLOYS

In this chapter a summary will be given of the mechanisms which contribute to the observed susceptibility of a metal or alloy.

§.1 Introduction

A solid, placed in a magnetic field will in general acquire a magnetic moment. If the magnetization (M) is proportional to the applied field (H) the magnetic susceptibility (χ) is defined as the magnetization per unit volume per unit field, otherwise as $\lim_{\Delta H \to 0} \frac{\Delta M}{\Delta H}$ if this limit exists. In a metal the observed susceptibility is the sum of several contributions due to the following mechanisms:

1. alignment of permanent magnetic moments localized on atoms or ions.
2. moments induced in atoms or ions.
3. alignment of moments carried by electrons in Bloch states.
4. diamagnetism of conduction electrons.
5. diamagnetism of electrons in closed orbits or core electrons.

§.2 The alignment of atomic moments and the Van Vleck paramagnetism.

Van Vleck[24] derived an expression for the effects 1 and 2, mentioned in §.1, for the following model. The atom has a permanent moment and the states in which it carries this moment can be divided into two groups: a) states which are likely to be occupied (normal states,) tho energy

intervals between these statos are small compared to kT, b) excited states which have a low probability of being occupied. The difference in energy between a normal and an excited state is large compared to kT.

If only that part of the magnetization is considered which is proportional to the applied field H, then the susceptibility χ is found to be $\chi = \frac{N\bar{\mu}^2}{3kT} + N\alpha(1)$ where N is the number of atoms which carry a moment, $\bar{\mu}^2$ the time average of the moment of a normal state, this again averaged over all normal states.

$N\alpha = \frac{2}{3} N \sum_{n' \neq n} \frac{|m^o(n';n)|^2}{h\nu(n';n)}$ where m^o is the magnetic moment operator and the index n' refers to an excited, n to a normal state. This term will in general be small, because $(n';n)$ is large. If the atom has Russell-Saunders coupling the first term can be written out simply in two cases. If the multiplet intervals are all small compared to kT, i.e. if all states are normal states, it is found using $\underline{\mu} = -\mu_B(\underline{L}+2\underline{S})$ that

$$\chi = \frac{N\mu_B^2}{3kT} \left\{ 4S(S+1)+L(L+1) \right\} \quad (2),$$

where μ_B is the Bohrmagneton.

If the multiplet intervals are all large compared with kT, only the lowest state is a normal state and $\chi = \frac{Ng^2 \mu_B^2 J(J+1)}{3kT} + N\alpha$ (3)

which can be written as

$$\chi = \frac{N\mu_{eff}^2}{3kT} + N\alpha \quad (4)$$

where the effective moment μ_{eff} is defined as $g\mu_B \sqrt{J(J+1)}$. If also multiplet intervals of the order of kT exist, transitions from the ground state with increase of temperature have to be taken into account and the temperature dependence of the susceptibility will be more complicated.

If not only the part of the magnetization proportional to the applied field is retained one finds instead of (3)

$$M = N\, Jg\mu_B\, B_J \left(\frac{Jg\mu_B H}{kT} \right) \qquad (5)$$

and a similar expression instead of (2). here B_J is the Brillouin function with argument J, Mthe magnetization.

It follows from this last equation that the saturation moment per atom is $Jg\mu_B$. This should not be confused with the effective moment $g\mu_B \sqrt{J(J+1)}$ found from the temperature dependence of the susceptibility. It has been found that the effective moments of atoms of transition elements of the first long period of the periodic system in salts are closer to $2\sqrt{S(S+1)}$ than to $g\sqrt{J(J+1)}$ as in salts of the rare earths. The absence of a contribution from the orbital moment to the susceptibility (quenching of the orbital moment) has been explained as follows : the 3d-state in the free atom is five-fold degenerate, these states having different charge distributions in space. In the lattice the atom will be subjected to a strong electrostatic field, especially the 3d-electrons which are in an outer shell of the atom. In such a field the charge clouds of different 3d-states will have different energy and the orbital degeneracy will be removed. Because it is necessary for a state to be at least two-fold degenerate to carry a moment, the only contribution of the orbital angular momentum to the susceptibility will be the term Na in eqn. (1) which is small if this crystal field splitting is much larger than kT. This mechanism was first proposed to explain the observed values of the

moment of transitionmetal ions in salts but should also apply to those in metal lattices. The spin degeneracy will not be removed by an electrostatic field.

In addition to the interaction of an atomic moment with an external field, interactions with other moments are possible, leading to increase paramagnetism, ferromagnetism or antiferromagnetism. These interactions can often be described formally by replacing H in eqn.5 by an effective field $H + \lambda M$, where λ is a constant.[25]

For ferromagnetic solids, the low-field susceptibility above the Curie-temperature Tc varies then with temperature as $\chi = \frac{C}{T-\vartheta}$ (7) with $\vartheta > o$. Experimentally χ is found to deviate from (7) near Tc. For lower temperatures χ is not a useful quantity and M varies with H at constant temperature as shown in Fig.I.

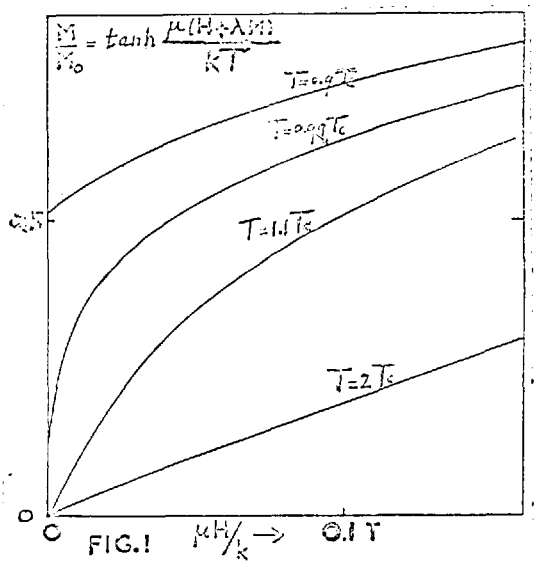

FIG.I

If the interactions are antiferromagnetic equ (7), holds with $\vartheta < o$, above the ordering temperature T_N.

The calculated variation of χ with T for lower temperatures depends strongly on the details of the model, but generally a sharp maximum at T_N is predicted. A very simple model developed by Dekker[26] for Cu-Mn alloys assuming antiferromagnetic coupling between nearest neighbour Mn atoms and ferromagnetic coupling between those at larger distance leads to a broad maximum as was observed in these alloys.

§.3 Alignment of moments carried by electrons in Bloch states

Pauli-paramagnetism

The paramagnetic susceptibility of a gas of electrons, obeying Fermi-Dirac statistics is $\chi = 2\mu_B^2 N(E_F) \left\{1+ \frac{\pi}{6}^2 (kT)^2 \frac{\partial^2 \ln N(E)}{\partial E^2}\right\}_{E=E_F}$ + higher order terms.[27] $N(E_F)$ is the density of states at the Fermi-energy. Usually only the first term is considered which is a good approximation for temperatures well below the degeneracy temperature $\frac{E_F}{k}$ which for most transition metals of the first long period os of the order of $1500^{\circ}k$.

Collective electron ferromagnetism

Also in this collective model, exchange interactions between the electrons can cause ferromagnetism or increased paramagnetism. The theory was developed by Stoner[28], who introduced a local field acting on the moment of an electron. As in the Weiss-model for ferromagnetism, this molecular field is introduced formally, its origin is not specified. Assuming that the local effective field is proportional to the macroscopic magnetisation of the crystal (i.e. the magnetic energy to the square of the

magnetization) it was found that in an external field H the energy of an electron can be written as $\mu_B H \pm k\vartheta' \zeta$, where μ is the moment of an electron, ζ the relative magnetization $\frac{M}{N\mu_B}$ with N the number of electrons, and ϑ' a constant characteristic of the molecular field. If a parabolic band-structure is assumed, the main results of this treatment are :

I. if no magnetic ordering takes place the interactions increase the paramagnetic susceptibility χ, such that $\frac{1}{\chi} = \frac{1}{\chi(\vartheta'=o)} - \frac{k\vartheta'}{N\mu_B^2}$

II. ferromagnetism is possible if $\frac{k\vartheta'}{\varepsilon_o} > \frac{2}{3}$

III. the relative magnetization at T=o, ζ_o can be calculated as a function of $\frac{k\vartheta'}{\varepsilon_o}$ and was found to be complete ($\zeta_o = 1$) if $\frac{k\vartheta'}{\varepsilon_o} > 2^{-1/3}$

IV. The magnetization at low temperatures varies with T as $M=1-ce^{-\alpha/T}$ where c and α are constants.

V. A peak in the specific heat at the Curie temperature is predicted.

VI. The reciprocal susceptibility above Tc although a fairly complicated function of T is, when plotted, found to be very nearly linear with temperature, as for the Curie-Weiss model for localized moments. The slope of this curve is determined by $\frac{k\vartheta'}{\varepsilon_o}$. For a rectangular band[29] similar results are found. Here, the condition for ferromagnetism is $\frac{k\vartheta'}{\varepsilon_o} > 1$ and if this condition is satisfied the magnetization at zero temperature is complete.

The theory was also developed[30] for a system of two overlapping bands which does not change the general features but leads to a number of corrections. Wohlfarth[31,32] and Gerstenberg[79] interpreted experimental results for a number of binary alloys in terms of this model.

The collective electron theory of antiferromagnetism

Lidiard [33] extended the collective electron theory to describe antiferromagnetism. This model assumes an antiferromagnetic order of localized moments at the lattice points of a metal, in particular a lattice divided into two interlocking sublattices A and B, containing atoms with + and - spins respectively. The Bloch like states will now be modified, the new wave functions can be divided into two groups, ψ_k, functions more concentrated near A, and φ_k, more concentrated near B sites.

The energy of an electron with wave function belonging to ψ_k is $\varepsilon(k) \pm (k\vartheta_1 \zeta_A + k\vartheta_{12} \zeta_B)$ depending on the spin of this electron. Here $\varepsilon(k)$ is the kinetic energy,

$\zeta_{A,B}$ the relative magnetization of the A(B) lattice

ϑ_1 and ϑ_{12} interaction constants

A similar expression holds for the φ_k set.

The treatment is similar to that given by Stoner for ferromagnetism and is given for a parabolic band of electrons. The main conclusions are:

1. antiferromagnetic order is possible if $\frac{k(\vartheta_1+\vartheta_{12})}{\varepsilon_o} > \frac{2}{3}$, otherwise the system is paramagnetic.

2. if $\frac{2}{3} < \frac{k(\vartheta_1+\vartheta_{12})}{\varepsilon_o} < 2^{-1/3}$, antiferromagnetic order is possible, the moment localized on an atom at T=o is smaller than the maximum possible.

3. if $\frac{k(\vartheta_1+\vartheta_{12})}{\varepsilon_o} > 2^{-1/3}$ there will be complete order at T=o i.e. the maximum moment at a lattice site.

4. In the absence of an external field, the relative magnetization of a sublattice $\zeta_A = \zeta_B = \zeta$ this varies at low temperatures as $\left(\frac{\zeta}{\zeta_o}\right)^2 = 1 - \left(\frac{T}{T_N}\right)^2$ where T_N is the magnetic ordering temperature.

5. the thermal properties can be taken over from Stoners treatment of ferromagnetism if ϑ' is replaced by $\vartheta_1 + \vartheta_{12}$.

6. For the magnetic susceptibility above the ordering temperature T_N the equation $\frac{1}{\chi} = \frac{1}{\chi\,(\vartheta_1=\vartheta_{12}=o)} - \frac{k(\vartheta_1-\vartheta_{12})}{N\mu_B^2}$ holds,

where N is the number of electrons

and μ_B the Bohrmagneton

Below T_N the susceptibility depends on the orientation of the applied field H with respect to the axis along which the moments are aligned. The susceptibility for H parallel to this axis, $\chi_{\parallel}$, will decrease with decreasing temperature from $T = T_N$ and that for H parallel to this axis, $\chi_{\perp}$, will be temperature independent below T_N.

For a powdered specimen with randomly distributed antiferromagnetic axes, the measured susceptibility will be $\chi = \frac{2}{3}\chi_{\perp} + \frac{1}{3}\chi_{\parallel}$.

The $\frac{1}{\chi}$ vs T curves, for $\frac{k(\vartheta_1+\vartheta_{12})}{\varepsilon_o} > \frac{2}{3}$ calculated numerically, show a discontinuity in the slope at $T = T_c$. If a susceptibility with this temperature-dependence would be measured, the points obtained would probably suggest a gradual change of slope.

These ideas were applied to Cr where neutron diffraction experiments[34] showed antiferromagnetic order but at the transition temperature no specific heat anomaly and only a very small effect in the magnetic susceptibility was observed. Lidiard showed that for this case the collective electron theory predicts only a very small anomaly in the thermal properties, so that this model is consistent with the observed properties of Cr. Overhauser[35] proposed for this metal the spin-density wave model, the main arguments being firstly that the parameter of the magnetic ordering is incommensurate with the lattice parameter which is not consistent with the above mentioned model and secondly that above the ordering temperature no paramagnetic scattering was observed, which rules out the possibility of atomic moments.

In Pd a maximum in the susceptibility was observed but no specific heat anomaly at any temperature near that of this maximum. Also for this case Lidiard showed that the absence of a measurable anomaly in the thermal properties is consistent with the model of collective electron antiferromagnetism, but no conclusive evidence of antiferromagnetism in Pd exists.

§3.4 Diamagnetism of conduction electrons.

The theory of diamagnetism was developed by Landau and Peierls[36]. More recently an exact theory, which is extremely complicated has been given

by Sondheimer et. al.[37] For free electrons, obeying Fermi-Dirac statistics, the diamagnetic susceptibility is one third of the Pauli paramagnetic susceptibility.

In a periodic lattice field such that the energy of an electron is $E = \frac{\hbar^2}{2m}\left\{ a_1 k_x^2 + a_2 k_y^2 + a_3 k_z^2 \right\}$, it can be found that for a field in the z-direction, $\chi_z = \chi_{free} \times \left\{ \frac{(a_1 a_2)^2}{a_3} \right\}^{1/3}$. Consequently, if the Fermi surface overlaps a Brillouin zone boundary this can strongly affect the diamagnetic susceptibility.

5. Diamagnetism of core electrons.

The diamagnetic susceptibility is given by

$$\chi = - \frac{e^2}{6mc^2} \Sigma \overline{r^2}$$

where r is the radius of the orbit of the electron and the sum is over the different electrons.

Calculations of this effect for actual solids are complicated, a review of theoretical work is given in Ref. 24. Experimentally ionic susceptibilities has been determined from the susceptibility of salts and solutions, under the assumption that different contributions to the total observed susceptibility are additive. For the alloys discussed in Chapter V and VI, this effect will be small. For the Mn^{7+} ion, the diamagnetic susceptibility is of the order of 0.1×10^{-6} emu per gram, so that in a solution of 0.1 at % Mn this part can be neglected.

CHAPTER III

PREVIOUS WORK ON DILUTE ALLOYS

In this chapter a short review will be given of the observed anomalies in the electrical and magnetic properties of dilute solutions of elements of the first transition group in other metals and a summary of the theories developed to explain these effects.

In section A the results for alloys of these elements with the noble metals will be summarized, in section B those for solutions in divalent and trivalent metals and in section C those where the solvent is a binary alloy. In section D a survey will be given of magnetic measurements on solutions of Fe in a transition metal of the second long period. In section E the models developed for dilute noble metal - transition metal alloys and the application to the experimental data will be reviewed and in section F the possible explanations of the behaviour of alloys of two transition metals.

PART I. SUMMARY OF THE EXPERIMENTAL WORK

SECTION A. DILUTE BINARY SOLUTIONS OF TRANSITION METALS OF THE FIRST LONG PERIOD IN A NOBLE METAL.

The alloys of this group can be divided into three groups, according to the observed behaviour of the magnetic susceptibility and the electrical resistivity.

The first group contains allcys for which the susceptibility of the solute system follows a Curie-Weiss law at high temperatures (above 100°k) and the susceptibility vs temperature curve shows a maximum at low temperatures. The curve of the resistivity vs temperature shows a maximum and a minimum for these alloys and for all the systems the transition metal dissolves easily up to high concentrations in the matrix. To this group belong the alloy systems Cu-Mn,Ag-Mn,Au-Mn,Au-Fe and Au-Cr.

The second group contains systems for which the susceptibility is paramagnetic and temperature-dependent but does not show a maximum at any temperature, and for which the electrical resistivity as function of temperature shows a minimum only. For the alloys of this group the solubility of the transition metal in the primary phase of the noble metal is low. To this group belong the systems Cu-Fe, Cu-Co and Au-Co.

The dilute alloys of the third group, Cu-Ni, Au-Ni and Au-V, do not show a significantly temperature-dependent susceptibility, the resistivity versus temperature curves do not show a maximum and only a shallow minimum, if any. For these systems the primary α-phase extends up to high solute concentrations.

Of the other possible combinations of one of the above-mentioned transition metals and a noble metal only in the systems Ag-Cr and Cu-Cr has some solid solubility been found, which is however small, and no magnetic measurements on these systems have been reported. In the remaining systems Ag-Ni, Ag-V, Ag-Fe, Cu-V and Ag-Co the solubility of the transition metal is too low to allow the preparation of a solid solution.

§.1 Group I. The systems Cu-Mn, Ag-Mn, Au-Mn, Au-Fe and Au-Cr

For all the alloy systems of this group a primary phase exists extending up to a transition metal concentration of at least 10 at %.[38]

a) Magnetic susceptibility.

Cu-Mn. Measurements have been made by Owen et. al[39] on alloys containing 0.03, 1.4, 5.6 and 11.1 at % Mn from 4 to 290°K. At high temperatures the susceptibility followed a Curie-Weiss law corresponding to an effective moment $\mu_{eff} = 5.0\mu_B$ and a positive Curie-Weiss constant ϑ (See Chapter II). Below 80°K the results showed a deviation from the Curie-Weiss law and for the alloys with 1.5 at % or more Mn a broad maximum in the susceptibility as function of temperature was observed. Even at the lowest temperature the susceptibility was found to be independent of the applied magnetic field.

Van Itterbeek et al.[40] measured specimens of Mn content c between 0.25 and 4.8 at % from 1.2 to 290°K. At high temperatures a Curie-Weiss law was found to apply with $\mu_{eff} = 4.5\mu_B$ and $\vartheta < o$ for $c \leqslant 1.6$ at % and $\vartheta > o$ for $c \geqslant 2.6$ at %.

For the alloys with $c \geqslant 1.4$ at % a maximum in the curve of susceptibility versus temperature was observed. The susceptibility was found to be field-dependent below and just above the temperature of the maximum T_N.

Measurements of the magnetization of a Cu-Mn alloy by Schmitt and Jacobs[41,46] at 4.2°K showed an extremely complex field dependence of the magnetization, this is in strong disagreement with the results found by Owen et. al.

Ag-Mn

Owen et. al[39] also made measurements on a Ag-4% Mn alloy down to 4.2°K. The susceptibility follows a Curie-Weiss law at high temperatures, $\mu eff = 5.5\mu_B$, $\vartheta > o$ and between 10 and 20°K the curve of susceptibility as function of temperature shows a broad maximum. No field-dependence was found at any temperature.

Van Itterbeek et. al[40] measured alloys with Mn concentration c from 0.5 to 5.3 at % down to 1.2°K. A Curie-Weiss law is followed at high temperatures, corresponding to $\mu eff = 5.7\mu_B$. For $c < 1.7\%$, ϑ is negative while for $c \geqslant 1.7\%$, ϑ is positive and a broad susceptibility-maximum is found. As for Cu-Mn the susceptibility was field-dependent below and just above T_N.

Au-Fe

Measurements on alloys containing from 0.6 to 15 at % Fe from 14 to 290°K were reported by Kaufmann et.al[42]. Above 77°K the results for Au-0.6 at % Fe show a Curie-Weiss behaviour with $\mu eff = 3.4\mu_B$ and $\vartheta = -25$°K. μeff increased with Fe content c to 5.7 μ_B at 12%, ϑ increased with c

and was positive for $c > 3.5\%$. Below $77^{\circ}K$ the results did not follow a Curie-Weiss law while for $c \geqslant 6.6$ at % the alloys show a remanent magnetization at $14^{\circ}K$.

Lutes and Schmit[43] measured alloys with 0.5 at 1 at % Fe from 0.5 to $30^{\circ}K$. At the higher temperatures a Curie-Weiss law was found to be applicable with $\mu eff = 3.6\ \mu_B$ and $3.3\ \mu_B$ respectively and $\vartheta < 0$. In disagreement with the results found by Kaufmann et al., ϑ increased in absolute value with increasing Fe concentration. At lower temperatures a remanent magnetization was found and the curve of the susceptibility in zero field showed a broad maximum at the temperature where the remanent magnetization disappeared.

Au-Cr and Au-Mn

Alloys containing from 0.5 to 2% of solute were investigated by Lutes and Schmit[43] between 0.5 and $30^{\circ}K$. A behaviour similar to that found for Au-Fe was observed. For the Au-1% Mn and Au-2% Mn alloys values of $\mu eff = 5.8$ and $6.6\ \mu_B$ respectively and positive values of ϑ were found. For the Au-0.5% Co and Au-1% Cr alloys μeff was 4.0 and $3.7\mu_B$ respectively and $\vartheta < o$. For both systems, ϑ increased in absolute value with increasing solute content. As for Au-Fe a remanent moment was observed at the lower temperatures and the zero-field susceptibility showed a broad maximum at the temperature where the remanence became zero.

b) Electrical Resistivity

The curves of the resistivity versus temperature for the alloys of this group shows a maximum above 1.2°K if the solute concentration is between 0.03 and 0.5 at %[44,45]. This composition range is somewhat narrower for the Au-Fe system and wider for Cu-Mn. At a temperature above that of the maximum a broad minimum is found. For alloys with lower solute content only a minimum is observed above 1.2°K, while for those with higher solute concentration the resistivity at low temperatures increased strongly with temperature without showing a maximum or a minimum. The temperatures of these maxima and minima vary with solute content.

c) Magnetoresistance.[45]

For all the alloys of this group the change of the resistivity in a magnetif field , $\Delta\rho$, does not follow Kohlers rule $\Delta\rho \alpha H^2$, the observed values of $\Delta\rho$ are smaller than for the pure metal and are in most cases negative. A detailed analysis of Cu-Mn alloys of Schmitt and Jacobs[46] showed that these results can be described by the relation $\Delta\rho = a(T)M^2$ where a (T) is a temperature-dependent parameter and M the magnetization of the alloy. For the other systems no such data are available.

d) Specific heat.

For those alloys of this group for which specific heat measurements have been reported the difference in the specific heat of the alloy and that of the pure solvent, ΔC, when plotted as a function of temperature,

shows a broad maximum at low temperatures. The shape of this curve is similar to that expected for a system of magnetic atoms in a field H, for which the magnetic contribution to the specific heat is given by

$$C_M = \frac{N\mu_B^2 H}{kT^2} \operatorname{sech}^2 \frac{\mu_B H}{kT} \quad (1)$$

if the atoms have a spin $S=\frac{1}{2}$[47] (see Fig.1). Here N is the number of atoms.

From the susceptibility and magnetization data mentioned at the beginning of this section it is obvious that in these alloys a magnetic ordering takes place and the observed extra specific heat Δc has been ascribed to this process. If the interactions between the atomic moments are represented by a molecular field H', the term Δ can be written as C_M in equ 1, with H=H'. If the atoms have a higher spin value a more complicated expression than 1,is found, a plot of C_M vs T will however have the same general shape as that in Fig. 1. In a dilute alloy the field H' will not have one well-defined value, but vary over the volume of the crystal, this will cause a broadening of the maximum in the curve of C vs T. From the integral of the function $\frac{\Delta C}{T}$ over T, the value of the spin of a solute atom can be found. As the temperature is raised the specific heat of the alloy increases and ΔC will become comparable to or smaller than the experimental error, so that no results can be obtained by subtracting the value found for the pure

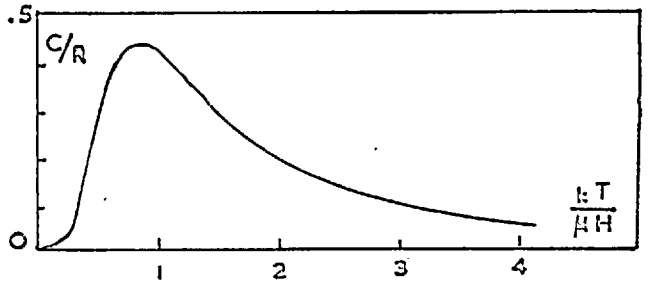

FIG.1 (AFTER REF. 47)

solvent from that found for the alloy. The absence of values of ΔC at very low temperatures and the large error on the values for high temperatures are the main sources of error on the experimental spin values.

Cu-Mn

The specific heat of Cu-Mn specimens containing from 0.1 to 10 at % Mn was measured from 1.6 to 15°K by Zimmerman and Hoare[48] and of a Cu-0.13 at % Mn specimen by De Nobel and Du Chatenier [49] in the same temperature range.

The first measurements showed that the difference in the results for alloys of different Mn content is very small below 4°K and can be described roughly by the relation $C + (aT + o.1T^3)$ $\frac{mJ}{mole\ deg^2}$, with a =3.5 for a Mn concentration c of 0.5 at 10%, a= 4.0 for c=1% and a=4.5 for c=2% and c=4%.

For the alloy Cu-0.5% Mn the value S=2 was derived as the most likely value for the spin of a Mn atom. The results by De Nobel and Du Chatenier agree well with those of Zimmerman and Hoare.

The difference in the specific heat of the Cu- 0.13 % Mn alloy and that of pure Cu, as measured by Franck et. al[50], shows a broad maximum between 3 and 4°K.

Ag-Mn

Three alloys, containing 0.09, 0.28 and 0.40 at % Mn were measured from 1.3 to 20°K by De Nobel and Du Chatenier. Also here the specific

heat at low temperatures is larger than that of pure Ag. Also for this system the results give a spin value between 2 and $\frac{5}{2}$. The C vs T curves for the 0.28 and 0.40% Mn alloys coincide below 1.9°K. The curve of ΔC vs. T for the Ag - 0.09 % Mn alloy shows a maximum at 1.8 ± 0.2°K. To fit the points for the 0.28% Mn alloy to a Schottky-curve an internal field of 25 to 30 K Oe had to be postulated, corresponding for $S = \frac{5}{2}$ to a critical temperature of about 9°K.

Au-Mn, Au-Cr.

For a preliminary report[51] on a series of measurements the presence of an anomaly in the specific heat of dilute Au-Mn and Au-Cr alloys was mentioned, but no more detailed results of these measurements have been published.

e) Thermoelectric power.

In all the alloys of this group large thermal powers have been observed at low temperatures. While at these temperatures the normal thermal power due to diffusion is estimated at less than 0.1 $\mu V/_{°K}$, in these alloys values of several μV per °K have been found in the temperature range from 1 to 20°K.[44,45] If the temperature is lowered the thermal power S decreases in absolute value and approaches zero as $T \rightarrow o$. Although the shape of the S vs T curves is very different for different alloy systems, there is no special property of these curves which is common to only the alloys of group I.

f) Summary

The results discussed in the previous paragraph show that in the alloys systems Cu-Mn, Ag-Mn, Au-Mn, Au-Cr and Au-Fe the transition metal atoms carry a magnetic moment and that a low temperature magnetic ordering takes place. The susceptibility, which because of the field dependence at low temperatures has to be seen as a quantity proportional to the magnetization in a constant field, reaches a maximum which indicates antiferromagnetic order. For the alloys with Mn as solute positive values of the Curie-Weiss constant have been found, indicating that also ferromagnetic interactions are operative.

The maximum in the resistivity can not be correlated directly with the susceptibility-maximum which has been found only in alloys of high solute concentration which do not show a resistivity maximum. For those systems for which specific heat measurements have been made, the specific heat of the solute system is independent of solute content at low temperatures and shows a maximum at a temperature T_c close to that of the resistivity maximum T_m. This is seen when both T_m and T_c are plotted as a function of solute concentration (Fig. 2). This indicates that both anomalies are connected with the same ordering process.

If the temperature of the susceptibility maximum as function of solute content is also plotted in Fig. 2, the points lie far below the extrapolation of the line drawn.

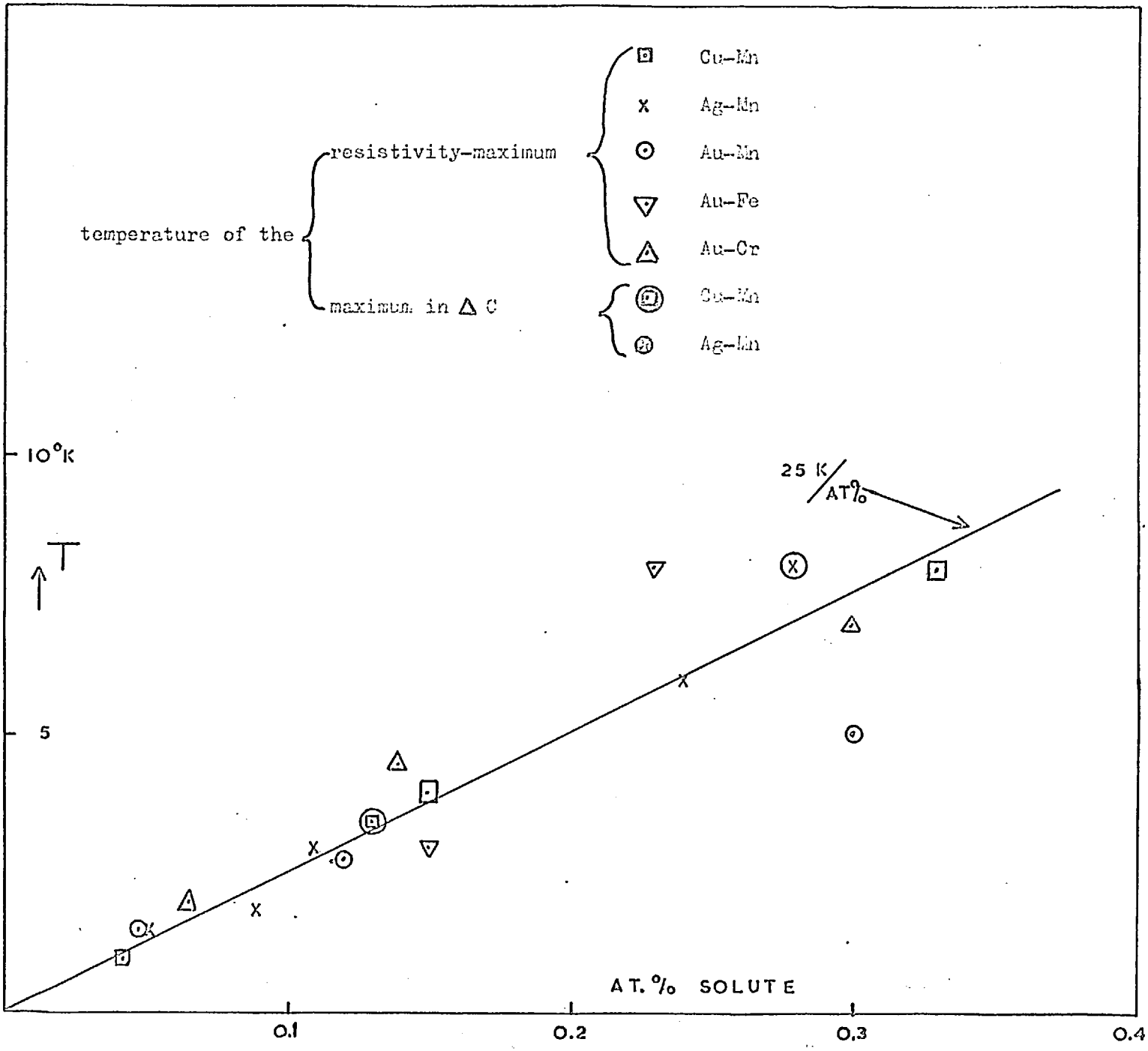
temperature of the
resistivity-maximum
Cu-Mn
Ag-Mn
Au-Mn
Au-Fe
Au-Cr
maximum in Δ C
Cu-Mn
Ag-Mn
10°K
T
5
25 K/AT%
AT. % SOLUTE
0.1
0.2
0.3
0.4

§.2 Group II. Dilute solutions of Fe in Cu, Co in Cu and Co in Au.

The alloys of this group are paramagnetic and the magnetic susceptibility does not show a maximum at any temperature. The resistivity as function of temperature does not show a maximum but a minimum is found in all cases.

The solid solubility[38] in the α-phase, which is several at % just below the metling point, falls off rapidly with decreasing temperature and is of the order of 0.2% at 400°C, is high enough to allow the preparation of a number of solutions, but is considerably lower than that for the alloys of Group I.

a) The magnetic susceptibility.

Cu-Fe

Measurements on alloys containing between 0.01 and 0.8 at % Fe from 14 to 300°K and from 1000 to 1300°K were reported by Bitter et al.[54] The alloys did not show ferromagnetism at room temperature and as the other phases of the Cu-Fe system contain at least 92% Fe any precipitate will be ferromagnetic. This shows that the Fe was in solution in the primary α-phase.

At 14°K the susceptibility of alloys with more than 0.1% Fe was field-dependent, but no remanent magnetization was observed. The susceptibility for zero field followed a Curie-Weiss law over the whole temperature range. The effective moment per Fe atom increased with Fe content of the sample from 2.0 μ_B for 0.01 at % to 4.9 μ_B for 0.8 at %, while ϑ increased from -16 to 0°K.

From the high-temperature measurements a value of $\mu eff = 4.7\ \mu_B$ was found for all the alloys.

Cu-Co.

The susceptibility of alloys containing from 0.1 to 0.5 at % C_o was measured by Hildebrand[53] from 90 to 300°K. The results were fitted to a Curie-Weiss law corresponding to values of ϑ between -800 and -1000°K. For the 0.5% Co alloy which showed a different behaviour, a value ϑ = -220 °K was found. These values are too large for dilute alloys to justify the assumption that the Curie-Weiss model is applicable.

Measurements by Schmitt and Jacobs[41] on alloys containing 0.5, 1 and 2 at % Co down to 2°K showed that a Curie-Weiss law is not obeyed. Down to 50°K, the susceptibility varies little with temperature, but is higher than that of Cu and increases on further cooling. At 4.2°K the magnetization is not proportional to the applied field. No remanence was observed. The results for the 0.5% Co alloy join up well with those of Hildebrand.

Au-Co

Specimens containing between 0.3 and 2% Co were measured by Hildebrand[53] from 90°K to room temperature. The reciprocal susceptibility of the system of solute atoms is linear with temperature. The characteristic temperature ϑ is between -250 and - 160°K, decreasing in absolute value with increasing Co concentration. As for the Cu-Co alloys these values are very large and the Curie-Weiss does not apply to this system.

Lutes and Schmit[43] measured the susceptibility of a Au-1 at % Co alloy from 0.5 to 10°K and found a small variation with temperature down to 6°K and a more rapid increase on further cooling. The results do not fit a Curie-Weiss law. No remanent magnetization was observed.

b) Electrical resistivity.

Cu-Fe

A resistivity minimum above 1.2°K was observed for solutions containing between 0.005 and 1 at % Fe[44,45,55]. For none of these alloys a maximum was found. The resistivity of a specimen containing 0.056 at % Fe was measured[56] down to 0.1°K and found to be constant below 1°K.

Cu-Co, Au-Co

For these systems no maximum has been found. A minimum was observed[45] but the value of the resistivity at the lowest temperature measured was not more than 2% above the minimum value.

c) Magnetoresistance.

The change in resistivity in a magnetic field, $\Delta\rho$, showed qualitatively the same behaviour of that found for the alloys of Group I.[44,45]

For Cu-Co alloys the relation $\Delta\rho = aM^2$ holds[54], where M is the magnetisation of the sample and a is a temperature independent constant. For Cu-Fe and Au-Co no analysis of results has been made to check this relation.

d) Specific heat.

Cu-Fe

Measurements on Cu-Fe alloys containing 0.05, 0.1 and 0.2 % Fe were made by Franck et al[50] from 0.4 to 30°K. All the alloys showed a specific heat anomaly.

The most important points of the results are :

1. At the low-temperature end of the range the slope of the ΔC vs T curves is appreciably different for the three alloys. However for the 0.1% and 0.2% Fe alloys the curves do not extrapolate to zero at T=o.

2. As the temperature is increased the slope of the ΔC vs T curves approaches zero as T is near 7°K, the results suggest a decrease in ΔC above this temperature, but because of the large error on ΔC in this region this is not shown conclusively.

3. For the spin of an Fe atom the value S = 0.5 was obtained, because of the large errors discussed in 1d this value is however uncertain.

Cu-Co and Au-Co

Measurements on Cu-Co and Au-Co alloys with solute concentration between 0.25 and 3.5 at % were made from 1.5 to 4.2°K by Crane and Zimmerman[57,58]. The specific heat of the alloys was larger than that of the pure solvent. At the high-temperature end of the range, $\frac{\Delta C}{T}$ was found to be independent of T, being proportional to the square of the Co concentration for the Cu-Co alloys and proportional to the $\frac{3}{2}$ power for the Au-Co alloys. At the low-temperature end of the range, $\frac{C}{T}$ increased

with decreasing temperature, this increase was stronger for a Cu-Co alloy than for the Au-Co alloy with the same solute content. The temperature range over which these measurements have been made is too narrow to allow a comparison with the results for other systems.

f) Summary.

The alloys discussed in paragraph 2 have in common firstly that the resistivity as function of temperature reaches a minimum but no maximum. Secondly, that at low temperatures the specimens are paramagnetic and a magnetic ordering takes place, which is of different type of that observed in the alloys of Group I, as no susceptibility maximum has been observed, and thirdly that the solid solubility of the Fe and the Co is low.

Further the specific heat shows an anomaly which for Cu-Fe is qualitatively different from that found for Cu-Mn and Ag-Mn. It is also clear that the specific heat results for Au-Co and Cu-Co are similar, although the available data do not allow a detailed comparison.

The Cu-Fe system shows however many differences from the Au-Co and Cu-Co systems; the susceptibility of Cu-Fe follows a Curie-Weiss law, while in the Co alloys a small temperature dependence at higher temperatures is found which can not be interpreted in the same way. (It must be noted that no susceptibility measurements on Cu-Fe alloys with 0.1% Fe or more have been done below 14°K).

Further the resistivity minimum is considerably more pronounced in Cu-Fe than in Cu-Co or Au-Co.

§.3 Group III. The systems Cu-Ni, Au-Ni and Au-V.

The above-mentioned alloys have in common that the susceptibility is temperature-independent at high temperatures, that the resistivity as function of temperature shows a shallow minimum only, and that the solubility is high[38].

a) Magnetic susceptibility

Cu-Ni

Measurements by Pugh et al[59] on Cu-Ni alloys containing 0.59, 1.16 and 2.48 at % Ni between 2.5 and 300°K showed at high temperatures a susceptibility different from that of Cu by a temperature-independent term, and a sharp increase with decreasing temperature below 20°K. In later measurements[60] on specimens of higher purity the increase at low temperatures was small for Ni concentrations lower than 5%. In none of the alloys a field dependence was observed. The difference between the susceptibility of the alloy and that of pure Cu was in the range $(0.021 \pm 0.002) \times 10^{-6}$ emu/g per at % Ni for all the alloys containing less than 5% Ni.

Au-Ni

No results on dilute Au-Ni alloys are available. Specimens of high Ni content (12.5 at % and more) were measured by Kaufmann et al[42]. For the Cu - 12.5 at % Ni alloy the susceptibility is constant above 100°K and from there increases with decreasing temperature. For this high solute concentration this increase must be due to the Ni. The difference between the constant high-temperature value and that for pure Au is 0.019×10^{-6} emu/g per at % Ni, close to the value for the Cu-Ni alloys.

Au-V

The susceptibility of a Au- 1% V specimen was measured from 0.5 to 10°K by Lutes and Schmit[43] and found to vary slightly with temperature below 1.3°K and to be almost constant at higher temperatures. No remanent moment was observed at any temperature.

b) Resistivity

Cu-Ni

A shallow resistivity minimum between 10 and 25°K was observed for alloys containing from 0.025 to 2.2 at % Ni[61]. However this minimum was also found in a specimen nominally free from Ni. No maximum was observed.

Au-Ni

A shallow minimum was found for specimens with Ni content between 0.7 and 1.2 at %, and no effect for concentrations of 0.05 at 0.19%[61]. The observed minimum could, according to the authors, will be due to Fe impurities.

c) Magnetoresistance.

For Au-Ni and Cu-Ni no anomalies were observed up to 0.5 at % Ni.[61]

For Au-V no resistivity or magnetoresistance data are available.

d) Specific heat.

No measurements on dilute alloys of these systems have been done. Cu-Ni alloys containing 10 at % or more Ni were measured by Guthrie et al.[62] The specific heat of the 10% Ni alloy showed, between 1.5 and 4.2°K no

anomaly of a Schottky type and obeyed the relation $c = \gamma T + \beta T^3$.

In the preliminary report by De Nobel and Du Chatenier[51] a measurement on a Cu-Ni alloy is also mentioned in which no anomaly was found.

For Au-Ni and Au-V no specific heat measurements have been done.

Thermoelectric power.

Data are available for Cu-Ni and Au-Ni.

In Cu-Ni, Gold et al[52a] found values of S between -1 and -2 $\mu V/^oK$ at 15^oK for solutions of small amounts of Ni. MacDonald et al[52] reported for Au-Ni alloys between 4 and 16^oK values of S which were of the same order of magnitude as those for Au-Mn and Au-Cr alloys of the same solute concentration.

Summary.

In the Au-V and Cu-Ni alloys the observed increase in susceptibility at low temperatures is very small and could well be due to Fe impurities. The temperature-independence of the susceptibility indicates then that Ni atoms dissolve in Cu and V atoms in Au without a magnetic moment. If the difference in susceptibility between Cu-Ni and Cu, $\Delta\chi$, which is found to be proportional to the Ni-concentration is assumed to be a Pauli-paramagnetic term, the increase in the density of states at the Fermi level as a result of the introduction of the Ni in the lattice is then 4 states per eV per Ni atom for Ni concentrations below 5%.

For Au-1% V, Δ = 0.49 x 10^{-6} emu/g and for the increase in density of states a very large value would be found, which shows that the situation is different from that in Cu-Ni.

The absence of a resistivity or magnetoresistance anomaly comparable in magnitude to that for the alloys discussed in 1 and 2 also shows that for these alloys the phenomena observed in those of Group I and II do not occur. It must however be noted that in Cu-Ni and Au-Ni large values for the thermoelectric power have been found.

SECTION B. SOLUTION OF TRANSITION METALS IN Mg, Zn and Al.

Investigations have been reported on the systems Mg-Mn, Mg-Fe, Zn-Mn Al-Mn, Al-Cr, Al-V. In paragraph 1 of this section the results for the alloys of Fe and Mn in the divalent metals Mg and Zn will be discussed, in paragraph 2 those for the Al-based alloys.

§.1 Solutions of Fe and Mn in Mg and Zn.

Solubility.

The solid solubility of Mn in Mg and Zn, which is of the order of 1 at % near the melting point is high enough to allow the preparation of the alloys.[38] Some solubility of Fe in Mg has been reported which was however so small that no numerical values could be given.

a) Magnetic Susceptibility

Mg-Mn

For a Mg - 1.34 at % Mn alloy the susceptibility was measured down to 1.3°K by Collings and Hedgcock[63] and found to obey a Curie-Weiss law at high temperatures, corresponding to an effective moment of $4.1\mu_B$ per Mn atom and a characteristic temperature $\vartheta = 0°K$. At low temperatures a

deviation from the Curie-Weiss law was found, similar to that reported for Cu-Mn, but no maximum was observed. In this report no mention is made of any field-dependence of the susceptibility.

Owen et al[39] made measurements on a sample containing 0.67 % Mn and found a similar behaviour, also here $\vartheta = 0^{\circ}K$. For the effective moment for Mn atom however a value 2.9 μ_B was found. The susceptibility was reported to be field-independent at all temperatures.

Zn-Mn

Collings et al[64] measured a specimen containing 0.43 at % Mn down to $1.2^{\circ}K$. The temperature variation is similar to that for Mg-Mn. The high temperature susceptibility followed a Curie-Weiss law corresponding to $\mu eff = 4.8\ \mu_B$ and $\vartheta = +\ 12^{\circ}K$. No mention is made in this report of a field-dependence of the susceptibility.

b) Electrical resistivity

Mg-Mn

For alloys with Mn content between 0.16 and 0.60 at % a maximum in the resistivity versus temperature curves and a minimum at a higher temperature was reported, for lower Mn concentrations only a minimum .

Mg-Fe

A resistivity minimum was observed by Spohr and Webber[65] in nominally pure Mg specimens which contained Fe and Mn contamination. The results showed that Fe enhanced the effect of Mn. Because of the low solubility of Fe no more systematic investigation has been done on this system.

Zn-Mn

For solute concentrations from 0.01 to 0.43 at % a minimum above 1.5°K was found[66], while none of the specimens showed a maximum.

c). Magnetoresistance.

For a Zn- 0.12 at % Mn alloy a negative magnetoresistance in fields below 30 KOe was reported[67]. For a Mg - 0.04 % Mn alloy Kohlers rule was found to apply[68]. The possibility must however not be excluded that for Mg-Mn alloys with higher Mn content an effect will be observed.

d) Specific heat.

Mg-Mn, Mg-Fe.

For two alloys, Mg - 0.043% Mn and Mg - 0.013% Fe which were measured by Logan et al.[69] the specific heat above 3°K did not show any deviation from that of pure Mg.

Measurements from 0.4 to 1.5°K by Martin[70] on specimens containing 0.025 and 0.15 at % Mn showed a specific heat larger than that of pure Mg. The temperature range over which the measurements were made was too small to obtain information about the detailed shape of the curve or to determine the spin value for the solute atoms.

Zn-Mn

For Zn-Mn an anomaly in the specific heat has been observed.[51] No details of this work have been published.

e) Summary.

The Mg-Mn alloys have many features in common with the Cu-Mn alloys. The resistivity vs temperature curves show a maximum and a minimum which disappear at high concentrations, the susceptibility deviates from a Curie-Weiss law at low temperatures suggesting antiferromagnetism, although no actual peak has been observed. If in any of the alloys of this system the susceptibility reaches a maximum at any temperature, the alloy of which the resistivity will show a maximum at the same temperature, will have a lower solute concentration.

For Zn-Mn and Zn-Fe the data available are not sufficient to make a comparison with other systems.

§.2 Dilute Alloys of Transition Metals in Al.

Some measurements have been made on solutions of Mn, Cr and V in Al.

The solid solubility of the transition metals is not high but enough to enable the preparation of a number of alloys.[38]

a) Magnetic susceptibility.

Taylor et. al. measured[71] the susceptibility of a number of Al-Cr, Al-V and Al-Mn alloys containing between 0.1 and 0.7 at % of solute from 100 to 290°K. In first approximation the difference between the susceptibility of the alloy and that of pure Al was temperature independent and proportional to the solute concentration, the values obtained were :

for Al-Mn $\Delta\chi = 13 \times 10^{-6}$ emu/gmol per at % of solute

Al-Cr $\Delta\chi = 4 \times 10^{-6}$ " " " " " "

Al-V $\Delta\chi = -5.2 \times 10^{-6}$ " " " " " "

Collings and Hedgcock[63] measured the susceptibility of an Al-1% Mn alloy at low temperatures and found that no Curie-Weiss law is obeyed. No more details of this work have been published.

b) Resistivity

Measurements by Hedgcock et al.[72] on Al-Mn and Al-Fe alloys of solute content from 0.01 to 0.1 at % showed no resistivity maximum or minimum.

c) Specific heat.

The specific heat of Al - 0.045 at % Mn was measured by Martin from 0.4 to 1.5 °K.[73] The effect of the addition of the Mn was to lower the superconducting transition temperature, which is 1.71°K for pure Al, to 0.84°K. Above these temperatures the specific heat was, within the experimental error, equal to that of Al.

SECTION C. SOLUTIONS OF Mn and Fe IN BINARY ALLOYS.

For a large number of solutions of Mn in the α-phase alloys of the system Ag-Sn, Cu-Zn, Cu-Al and Cu-Ge and in the ζ -phase of Ag-Sn and Cu-Sn, the magnetic susceptibility has been measured above 150°K.

In paragraph 1 of this section the results for the face-centered cubic α-phase alloys will be reviewed, in paragraph 2 those for the hexagonal ζ-phase alloys.

§.1 Solutions of Mn in face-centered cubic α-phase alloys.

The α-phase of the binary systems Ag-Sn, Cu-Zn, Cu-Al and Cu-Ge has a face-centered cubic structure and extends in composition from pure Ag or Cu up to 9 at % Sn, 30 at % Zn, 19 at % Al and 9% Ge respectively, No phase diagrams of the ternary systems considered here are available, but it was reported that metallographic examination of the alloys used showed no precipitate of a second phase.

Magnetic susceptibility.

a) The Au-Sn-Mn system

The susceptibility of a number of α-phase Ag-Sn-Mn alloys with Sn content varying from 0 to 10 at % and Mn content between 2 and 17 at % was measured from 300 to 700°K by Henderson and Raynor.[74]

The measurements were made at one field at all temperatures, no ordering effects could be detected. For the Cu-Mn alloys with high Mn content (10 at % and more) the magnetic properties are extremely complicated and also in those of the alloys discussed here which have a high Mn content the susceptibility might not be the adequate parameter to describe the magnetic behaviour even at high temperatures. All the alloys showed however Curie-Weiss behaviour in the temperature range investigated so that the effective moment per Mn atom, μ_{eff}, and the constant ϑ could be determined.

For Ag-Mn, μeff decreased with increasing Mn content from 5.7 μ_B for 2% Mn to 5.0 μ_B for 17% Mn. For constant Mn concentration, μeff increased with increasing Sn content from 0 to 4% Sn and decreased on further addition of Sn. This variation is of the order of $0.1\mu_B$ and must be small compared to the experimental error. It must however be noted that for all Mn concentrations a similar curve of μeff vs Sn-content is found, which suggests that this maximum is a genuine effect. The parameter ϑ did not vary within experimental error with Sn concentration and increased with increasing Mn content from 1°K for 2 at % Mn to 32°K for 16% Mn.

b) Solutions of Mn in α-phase Cu-Zn, Cu-Al and Cu-Ge alloys.

Myers and Westin measured the susceptibility of solutions of 1 or 2% Mn in α-phase Cu-Zn, Cu-Al and Cu-Ge alloys. The composition of the solvent was varied over the whole range of the binary α-phase. The measurements on the Cu-Zn based alloys were made from 150 to 500°K, those on the other systems from 150 to 700°K, the results showed that the susceptibility followed a Curie-Weiss law for all the alloys.

In the Cu-Au-Mn alloys the effective moment per Mn atom, μeff, decreased with increasing Zn content from $4.8\mu_B$ in pure Cu to $4.5\mu_B$ for the alloy at the Zn-rich end of the phase. In the Cu-Al-Mn system μeff was $4.9 \pm 0.1\ \mu_B$ for all the alloys measured and for Cu-Ge μeff decreased with increasing Ge content from 5.0 μ_B for Cu-Mn to 4.7 μ_B for 89% Cu - 9% Ge - 2% Mn.

The values of ϑ lie mainly in the range + 30 $\pm$ 10°K. As an extrapolation over a large temperature interval is necessary to obtain these values from high-temperature measurements, the reported variation of ϑ is not significant.

§.2 Solutions of Mn in Ag-Sn and Au-Sn ζ -phase alloys.

The susceptibility of solutions of Mn and Fe in binary alloys of the Ag-Sn and Au-Sn ζ phase systems was measured by Henderson and Raynor.[76]

The crystal structure of these binary alloys is close-packed hexagonal, the composition range is from 12 to 23 at % Sn for Ag-Sn and from 12 to 16 at % Sn for Au-Sn.

Solubility.

A metallographic investigation of the solubility of Mn and Fe over the whole composition range of the ζ -phase[77] indicated a maximum solid solubility of 20 at % Mn in the Ag-Sn ζ phase at 480°C and of 5 at % Mn in the Au - Sn ζ phase at 275°C. For solutions of Fe in the Au-Sn phase the same value as for Mn in this phase was found.

Magnetic susceptibility.

The susceptibility was measured from room temperature to 700°K of ternary alloys with varying Ag-Sn and Au-Sn ratio and a Mn concentration from 1% to the highest possible value as determined metallographically.

The susceptibility followed a Curie-Weiss law for all the alloys, from which the effective moment μeff and the parameter ϑ were determined.

Ag-Sn-Mn

For the alloys containing 2 or 5 % Mn, μeff decreased with increasing Sn content of the alloy from 5.8 μ_B for 13% Sn to 5.4μ_B for 20% Sn. For the alloys with higher Mn-concentration μeff decreased with increasing Sn content by 0.2 to 0.3 μ_B over the composition range of the ζ phase. It was also found that μ eff decreased with increasing Mn content, the lowest value observed was 5.1 μ_B for a Ag-20% Sn - 18% Mn alloy. Within the experimental error ϑ was independent of Sn concentration and increased with increasing Mn content from + 1°K for 2% Mn to + 35°K for 15% Mn.

Au-Sn-Mn and Au-Sn-Fe.

Also in these alloys μeff decreased by roughly 0.2μ_B with increase in Sn content from 12 to 15%. For Mn, μeff decreased with increase in Mn concentration from 5.7 μ_B for Au-12% Sn - 1% Mn to 5.6 μ_B for Au-12.5% Sn -4% Mn, and for Fe from 4.2μ_B for Au-12%Sn-1%Fe to 3.8μ_B for Au-13% Sn -4% Fe. For none of the two systems a significant variation of ϑ with Au-Sn ratio was found. For the alloys containing Mn, ϑ increased from 0°K for 1% Mn to 10°K for 4% Mn, i.e at the same rate as in the Ag-Sn-Mn system.

For the alloys containing Fe a strong variation of ϑ with solute content was found, here ϑ increased from 0°K for 1% Fe to 80°K for 4% Fe.

SECTION D. SOLUTIONS OF Fe AND Co IN TRANSITION METALS OF THE SECOND LONG PERIOD.

The susceptibility of solutions of 1% Fe in the elements between Nb and Pd in the periodic system and in binary alloys of these elements has been measured by Clogston et al. from 1.4 to 300°K in a field of 14.000 Oe.

For the alloys of Fe in Nb - Mo, Mo-Re, Ru-Rh and in the Rh-Pd alloys containing less than 30 at % Pd the susceptibility follows a Curie-Weiss law from which the moment per Fe atom, μ_{Fe} and the constant ϑ were determined. A plot of μ_{Fe} as function of the atomic number of the solvent is given in Fig. 3.

For the Rh-Pd-1% Fe alloys which contained more than 30% Pd the susceptibility did not follow a Curie-Weiss law. It was assumed that for these alloys the susceptibility can be written as

$$\chi = \chi_o + \frac{N\mu_{Fe}^2}{3k(T-\vartheta)} \qquad (1),$$

where χ_o is the susceptibility of the system of Rh-Pd atoms in the ternary alloy which is taken to be proportional to μ_{Fe} :

$$\chi_o = \frac{\chi_{or}}{\mu_{Fe}(T_r)} \cdot \mu_{Fe} \qquad (2)$$

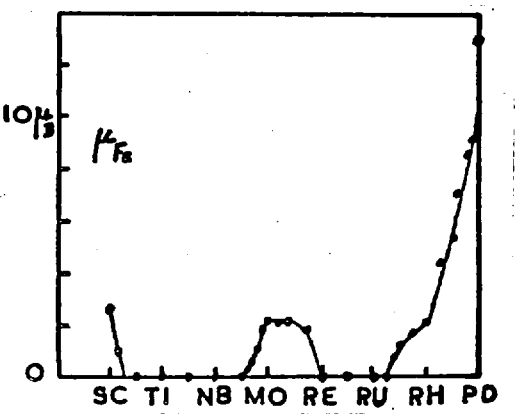

FIG.3 The magnetic moment of an Fe atom in solution in other transition metals and alloys. After ref. 78

where χ_{or} and $\mu_{Fe}(T_r)$ are the values at a temperature T_r. Equation (1) can then be written as

$$\frac{(\chi_o/\chi_{or})^2}{\chi - \chi_o} = \frac{3k(T-\vartheta)}{N[\mu_{Fe}(T_r)]^2} \qquad (3)$$

Experimental values of the expression on the left hand side of equ (3) were plotted as function of T, from which plot values of μ_{Fe} (100^oK) were obtained for the various alloys. It was however not indicated in the report how the necessary values of χ_o and χ_{or} were obtained.

The objections that can be made against this interpretation of the results are firstly that it is doubtful if a field-independent susceptibility is the adequate parameter to describe the magnetic behaviour of these alloys. The measurements were made in one field only, so this can not be checked, but the fact that ferromagnetism appears in some of the alloys of this system (see below) indicates a more complex situation. Secondly no argument for the assumption $\chi_o \propto \mu_{Fe}$ is given. It must be noted that in the binary Rh-Pd alloys with 30% or more Pd the susceptibility is temperature dependent and has been interpreted in terms of the collective electron theory. Fitting to this theory requires that in this system magnetic interactions in the 4d band take place which are not strong enough to cause magnetic order but cause enhanced paramagnetism. If in this system some of the Rh and Pd is replaced by Fe atoms which carry a moment, it can be expected that the susceptibility of the matrix will be affected. The relation (2) must be seen as a first approximation and although there is no doubt that in these alloys the moment per Fe atom is large (see below), the values of the moment as plotted in Fig. 3 can only be approximate.

§.2 Ferromagnetism in Pd-Fe, Rh-Pd-Co and Pd-Ag-Co

Measurements of the saturation magnetization and the magnetic susceptibility of Pd-Fe and Pd-Co alloys by Gerstenberg[79], Crangle[80] and Bozorth[81] et al showed that these alloys are ferromagnetic at low temperatures and that if it is assumed that only the solute atoms carry a moment, this moment per Fe atom is roughly $7\mu_B$ in Pd-1.25 at % Fe and that of a Co atom in Pd-0.1% Co roughly $10\mu_B$. A plot of $\frac{1}{\chi - \chi_{Pd}}$ vs T for Pd-0.1% Co (with the values

for Pd as found by Hoare for χ_{Pd}[83]) corresponds to a value of the effective moment per Co atom of $14\mu_B$. This value is only approximate but indicates that at high temperatures the moment retains a large value.

Bozorth et al[82] also investigated Rh-Pd-1% Co and Pd-Ag-1% Co alloys of different Rh/Pd and Pd/Ag ratio. In Pd-Ag-1% Co the saturation moment per Co atom n_A and the Curie-temperature T_c decreased with increasing Ag concentration, the ferromagnetism disappeared for 40% Ag. Also in Rh-Pd-1% Co a decrease of n_A and T_c with increasing Rh content was observed, which was however for low Rh content less rapid than for the corresponding Pd-Ag-Co alloys; here, T_c reached the value zero for 50% Rh.

§.3 Electrical resistivity

The resistivity of solutions of Fe in Nb, Mo, Rh and Pd was measured down to 1.8°K by Coles[84], who found in Nb-Fe, where Fe does not carry a moment, no anomaly in the variation of the resistivity with temperature, while the other systems in which the Fe atoms are magnetized do show anomalous behaviour. These anomalies are qualitatively different for the three different systems.

Mo-Fe.

In Mo-Fe the resistivity vs temperature curves are similar to those for Cu-Mn alloys. For a Mo-0.65 at % Fe alloy a maximum at 4°K and a minimum at 22°K were found which disappear when the Fe concentration is raised to 1.58%, in this last alloy the resistivity increases strongly with increase in temperature below 15°K.

Rh-Fe.

In Rh-Fe alloys with Rh content between 0.1 and 0.85 at % the difference in specific resistivity of an alloy and that of pure Rh is proportional to the concentration and increases strongly with temperature from 2 to 50°K. The magnetoresistance followed Kohlers rule and the thermoelectric power, which below 10°K is several microvolts per degree increased with decreasing temperature down to 1.8°K.

Pd-Fe.

In Pd-Fe alloys containing about 0.1 at % Fe the only anomaly observed is a decrease in resistivity with decreasing temperature below 2°K, no maximum or minimum have been observed for this system.

PART II. SUMMARY OF THE THEORETICAL WORK ON DILUTE ALLOYS

From the experimental results discussed in the previous sections it is seen that in those dilute alloys in which the solute atoms carry a magnetic moment the magnetic susceptibility, electrical resistivity, magnetoresistance, specific heat and thermoelectric power show anomalous behaviour. For the alloys in which no moment is observed, i.e. the Al based alloys and those in which Ni or V is the solute none of these effects have been found, with the exception that Au-Ni and Cu-Ni have a large thermoelectric power at low temperatures.

Recent experiments by Cape and Hake[85] on solutions of elements of the first transition group in Ti, Zr and Hf also indicated a one to one correspondence between the occurrence of an atomic moment and of a resistivity minimum.

In the following section the theories developed for dilute alloys will be discussed and the application of this work to the experimental results. The alloysfor which the solvent is a non-transition metal will be discussed in Section E, the solutions of Fe and Co in other transition metals in section F.

Section E. Theoretical models proposed for dilute alloys of a transition metal in a noble metal.

The alloys of a transition metal and a noble metal in which an atomic moment is observed can be divided into two groups showing different behaviour, firstly those alloys for which a maximum in the resistivity vs temperature curve is found for solute concentrations below 0.5 at % and a

maximum in the susceptibility at a higher concentration and secondly those in which none of these two maxima have been found. It must be noted however that the Cu-Fe system has not been investigated extensively at low temperatures.

The solid solubility of the solutions of the first group is considerably higher than that for those of the second group, a relation with the magnetic properties of these alloys is however not obvious.

For all these alloys an anomaly in the specific heat and a negative magnetoresistance have been observed.

No general theory has been given describing various properties of the alloys, but several models have been put forward, each of which deals with one aspect of the observed phenomena. This theoretical work can be classified according to the physical property treated and will be discussed with the application to the experimental results in the following paragraphs :

1. magnitude of the atomic moment
2. interactions between atomic moments
3. magnetoresistance
4. electrical resistivity
5. specific heat
6. thermoelectric power.

§.1 Magnitude of the atomic moment.

The existing theories an atomic moments and the qualitative explanation of some properties of Cu- and Al based alloys in terms of these theories have been discussed in Chapter I. It was shown that the 3d-states associated with a solute atom are broadened in energy by interactions with the Bloch states of the solvent. For the width of a state the expression $\Delta = \pi \langle V_{dk}^2 \rangle \rho(E)$ (1) was derived[16], where V_{dk} is a parameter describing the interaction of the 3d state with a Bloch state and $\rho(E)$ the density of the Bloch states in energy at the energy of the virtual state. Equation (1) shows that a low density of states at the Fermi-energy E_F, causing only a small broadening will be favourable for the existence of a moment. The electronic specific heat γ of the solvent which on a simple model is proportional to $\rho(E_F)$ will therefore be compared with the observed solute moments. For Cu, Ag, Au and Zn the values of γ lie close together and are all in the range 1.6 to 1.8 x 10^{-4} $\frac{\text{cal.}}{\text{mole deg}^2}$. This is consistont with the fact that the moment on a Mn atom is roughly the same in these solvents. For Fe the comparison can not be made as the moment per Fe atom in Cu in strongly dependent on the Fe concentration which indicates a more complex situation. In solutions of transition metals in Al (γ = 3.5 x 10^{-4} cal/mole deg^2) the solute does not carry a moment. This is consistent with the theory which then also predicts the absence of or a low value for the moment on a Mn atom, dissolved in Mg (γ= 3.25 x 10^{-4} cal/mole deg^2). For this moment values of 2.9 and 4.1μ_B have however been reported. This model then holds only if

$\langle V_{dk}^2 \rangle$ in equ (1) is larger for Mn in Al than for Mn in Mg. It is not unlikely that the interaction of the 3d-state on a Mn atom with a Bloch state with s-symmetry will be different from that with a Bloch state with p-symmetry. The average value of V_{dk}^2 will then vary with the ratio of the numbers of band states with s-character and with p-character. It might be possible that along these lines a difference in the values of $\langle V_{dk}^2 \rangle$ for Al and Mg can be explained, this problem is however too complicated than that any more detailed comparison with the experiments can be made.

For Cu-Zn α-phase alloys of different Cu-An ratio specific heat measurements have been reported.[86] This allows, for the α-Cu-Zn-1% Mn alloys a comparison of the electronic specific heat of the solvent with the moment of a Mn atom in solution. γ, plotted as a function of Zn concentration shows a maximum at 20 at % Zn, with a value of about 4% above that of pure Cu, while the effective moment per Mn atom, μeff decreases monotonically with increasing Zn content from $4.8\mu_B$ to $4.5\mu_B$ on the α-phase. The simplest explanation here is that the variation of $\rho(E_F)$ is not large enough to modify the width of the 3d state on a Mn atom and that the change in μeff is the result of a gradual filling of the spin up and the spin down part of the 3d-level. In these terms Henderson and Raynor[74] interpreted the results on the Ag-Sn-Mn alloys of low Mn content, taking also into account the possibility of transitions of electrons from the 3d state into the conduction band as a result of the change in lattice parameter over the phase. However the presence of a number of parameters which cano not be estimated and have to be treated as adjustable rules out any quantitative comparison of the

theory of the virtual bound state with the experimental values of atomic moments.

§.2 Interactions between atomic moments.

Experimental information about these interactions is the value of the Curie-Weiss constant ϑ and the temperature of the susceptibility maximum. In Cu-Mn, Ag-Mn and Au-Mn the value of ϑ derived from the high-temperature points, is positive, which indicates ferromagnetic interactions while at low temperatures a broad susceptibility maximum at temperature T_N is observed, indicating antiferromagnetic order. ϑ and T_N increase with increasing solute concentration.

No theoretical work has been applied to other alloys than these. The work by Yosida and Blandin (Ch.I) only shows that magnetic interactions in dilute alloys are possible but does not predict under which conditions these will be ferro- or antiferromagnetic.

The spin-density wave model (Ch.I) will lead to antiferromagnetism and was proposed as the explanation of the properties of Cu-Mn alloys. The consequences of this model for the shape of the susceptibility vs temperature curves were however not investigated.

The molecular field model for Cu-Mn.

The experimental result that in Cu-Mn the Curie-Weiss constant ϑ is positive while at low temperatures antiferromagnetic order is found was explained in terms of the following molecular field model by Owen et al[39]. Assume that the sites of the Mn atoms can be divided into two sublattices, A and B, assume further that the short range interactions between a Mn atom on

an A site and one on a B site is antiferromagnetic, those between two Mn atoms on the same sublattice ferromagnetic, and that both these interactions are independent of temperature. Then a straightforward molecular field argument shows that subject to conditions on the interaction parameters introduced, the above-mentioned experimental results are predicted qualitatively. The predicted maximum in the susceptibility is however a sharp peak, while the experiments show a broad transition. If it is now assumed that the actual structure of the alloy deviates from the ordered structure assumed above, the molecular field at the Mn sites will no longer have one well defined value. There will be instead a range of possible values and different Mn atoms will in general be in a different effective field which will broaden the transition region in temperature.

The pair-interaction model for Cu-Mn.

The same problem was discussed in different terms by Dekker[26], who considered the interactions between pairs of randomly distributed solute atoms. As in the previous model, these interactions are introduced formally.

Be λ_1 the distance between nearest neighbours in the Cu-Mn lattice and λ_2 that between next nearest neighbours, the Mn atoms can then for low concentrations be classified as follows :

1. single atoms which have no other Mn atoms at distance λ_1 or λ_2
2. nearest neighbour pairs, two Mn atoms at distance λ_1, none of which has another Mn atom at distance λ_1 or λ_2.
3. next nearest neighbour pairs, two Mn atoms at distance λ_2 none having another Mn atom at distance λ_1 or λ_2.

The interaction in a nearest neighbour pair is assumed to be anti-ferromagnetic, in a next nearest neighbour pair ferromagnetic and both interactions are taken to be temperature-independent. The susceptibility is then the sum of the contributions from the single atoms and the pairs. The detailed calculation of the magnetic behaviour in this model is extremely complicated, although this is possible in principle. It can however be shown simply that at high temperatures the susceptibility follows a Curie-Weiss law and that positive values of ϑ are possible, depending on the values of the interaction parameters. From this argument it can also be seen that ϑ is strongly concentration-dependent.

It was shown that for a very simplified model the desired broad maximum in the susceptibility is found.

§.3 Magnetoresistance.

It has generally been found that the resistivity of a pure metal increases as the result of the application of a magnetic field. If $\Delta\rho$ is the charge is resistivity, this is then positive and the relation $\Delta\rho \alpha H^2$ holds where H is the magnetic field.[27]

For the alloys discussed in Section A paragraph 1 and paragraph 2 , $\Delta\rho$ is smaller than the values for the pure solvent and is, except for very dilute solutions, negative. The fact that this behaviour is only found in alloys where the solute atoms are magnetized suggests a spin-dependent scattering of the conduction electrons by these solute atoms. If it is assumed that the cross-section for the elastic scattering of a conduction

electron by an impurity atom with spin parallel to that of the electron, σ_p, is different from that for the case of antiparallel spins σ_{ap} and only elastic scattering is considered, the resistivity in a magnetic field due to this scattering mechanism can be written as

$$\rho(H) = \rho(o) - \tfrac{1}{4} \frac{(N^+ - N^-)^2 (\sigma_p - \sigma_{ap})}{(N^+ + N^-)(\sigma_p + \sigma_{ap})} \qquad (3)$$

where $N^{\pm}$ is the number of impurity atoms with spin $\pm 4a$.

Equation (3) shows that $\Delta\rho$ is negative and proportional to $(N^+ - N^-)^2$ i.e. to the square of the magnetization of the alloy $\Delta\rho = aM^2$ (4). This relation has been found experimentally for the alloy systems for which this has been investigated, Cu-Mn and Cu-Co. A difference between these two systems is that a in (4) is temperature dependent for Cu-Mn and temperature-independent for Cu-Co.

§.4 Electrical resistivity.

It has been found in general that non-magnetic impurities increase the resistivity of a metal by a temperature-independent amount. The fact that a maximum and a minimum in the resistivity vs temperature curves have only been found in solutions of atoms, which carry a moment suggests that the mechanism responsible for these anomalies, as that for the magnetoresistance discussed in paragraph 3, is the interaction of the conduction electrons with the solute atoms. All theories given to explain these anomalies are based on this principle. A summary of these models is given below.

a) Korringa and Gerritsen[88,89] showed that formally a resistivity vs temperature curve having a minimum at low temperatures can be described by standard resistivity theory if the relaxation time τ is zero for electrons in a narrow energy range containing the Fermi-level (taken as E=o). The assumption that τ=o for electrons in an energy range Δ around energies $\pm E_1$ leads to a maximum and a minimum. By a proper choice of E_1 and Δ it was possible to find theoretical resistivity curves which fit the experimental data extremely well, for the systems Cu-Mn, Ag-Mn, Au-Mn and Au-Cr. The values needed for a good fit were E_1 from 2 to 10°K and Δ from 0.2 to 1°K. Physically this can be interpreted as a situation where states, not belonging to the conduction band, exist which have energy $\pm E_1$ and cause a resonance in the scattering of conduction electrons of these energies. In a one-electron model this assumption has no physical justification for the following reasons : firstly there is no reason why such energy levels should lie just at the Fermi-energy and secondly, a one-electron theory as discussed in Chapter I predicts a broadening of these states in energy to at least 0.1 eV ($\approx$1000°K). Therefore the authors proposed as a hypothesis that the introduction of the impurity causes some change in the system of conduction electrons as a whole and that, if the alloy is described by a one-electron model, this change can be represented by an increase of the density of states in one or two narrow energy ranges near the Fermi-energy. No theory, proving the possibility of the existence of these states has however been put forward.

b) Schmitt and Jacobs[90,46] suggested that magnetic ordering of the lattice is a condition for the appearance of the observed resistivity-anomalies. The relevant mechanism they assumed to be the scattering of conduction electrons by solute atoms, which is temperature-dependent for the following reasons. Below the magnetic ordering temperature the spin degeneracy of the impurity atoms is removed and inelastic scattering processes will take place, involving the reversal of the spin of the conduction electron and the transition of the atom into a different state. At zero temperature this part of the scattering vanishes because no empty states are available as final states for the electron and the magnetic atom. The inelastic scattering thus decreases with decreasing temperature.

If the cross-section for elastic scattering depends on the relative orientation of the two spins, a similar argument as given in paragraph 4 applies. Below the transition temperature, a change in temperature will cause a change in the occupation of the different states for the solute atoms. This will change the fraction of scattering events with a certain initial orientation of the spins concerned. If the cross-section for elastic scattering for lower lying states of the impurity atom is larger, the elastic scattering will increase with decreasing temperature.
A combination of these elastic and inelastic scattering mechanisms could explain the observed maximum and minimum. No more detailed theory was given by these authors but these ideas have been applied in subsequent work by others.

c) A more detailed treatment along the lines suggested by Schmitt and Jacobs was given by Yosida[91]. Here magnetic order of the Mn atoms is assumed and the resistivity due to s-d scattering of conduction electrons by these atoms worked out. The s-d interactions considered were those between the 4s-conduction electrons and the 3d-electrons on the Mn atoms and were taken to be of the form $H = \Sigma V(\underline{r}_i - \underline{R}_n) - 2 \sum_{i,n} J(\underline{r}_i - \underline{R}_n)\, \underline{s}_i \cdot \underline{S}_n$ (5) i.e. a spin-dependent and a spin-independent part here $\underline{r}_i$ and s_i are the position and the spin of a conduction electron, $\underline{R}_n$ and $\underline{S}_n$ those of a Mn atom, V represents the screened Coulomb potential of a Mn atom and J the 3d-4s exchange integral. The calculation is done in the following way : firstly it is shown that the resistance R is proportional to $(\Delta E_F^{+} + \Delta E_F^{-})^{-1}$ (6) where $\Delta E_F^{\pm}$ is the shift of the Fermi sphere for $\pm$ spins as a result of the application of an electric field. These $E_F^{\pm}$ must be found from the Boltzmann equation $\left(\frac{\partial f}{\partial t}\right)_{field} + \left(\frac{\partial f}{\partial t}\right)_{coll} = o$ (7). The contributions to (7) of elastic and inelastic collisions are written in terms of the potantials V and J and of $\Delta E_F^{\pm}$. These are then substituted into (7) after which $\Delta E_F^{\pm}$ are found and substituted into (6). This leads to a complicated expression for R which can be written as $R \propto \frac{W_o}{2} - \frac{w^2}{2W_o} M^2$ (8) where W_o is a transition probability which is equal for + and - spins, w a constant and M the magnetization of the Mn system. For a simple anti-ferromagnetic order of the Mn atoms M=o. The complete expression for (8) can then be simplified and is found to increase gradually with temperature from T=o to the Neel temperature and to remain constant from there, so that for this case the theory does not predict the anomalies. The condition m+o is however not likely to be fulfilled over the whole volume of an alloy and

for most alloys the second term in (8) will have to be considered. As Yosida pointed out the resistivity due to s-d interactions as discussed here will be large for high solute concentrations, and if these interactions would be responsible for the resistivity maximum and minimum, it would not be clear why these anomalies are not observed for higher concentrations.

For the change of resistivity in a magnetic field where $M \neq 0$ this theory predicts the relation $\Delta\rho \alpha M^2$ as is observed experimentally.

d) Brailsford and Overhauser[92] considered the scattering of conduction electrons by ferromagnetically coupled pairs of solute magnetic atoms. If the spin of a solute atom is $\underline{S}$ the total spin $\underline{I}$ of the pair can have values between 0 and 2S and the energy difference between states of different values of I depends on the interaction between the atomic spins. It is expected that the cross-section for the elastic scattering of a conduction electron by a pair is larger as the value of the total spin I of this pair is higher. If the coupling is ferromagnetic the occupation of states with high values of I will increase when the temperature is lowered and consequently the average elastic cross-section also. The temperature-dependent inelastic scattering which is the result of the s-d interactions between the conduction electrons and the impurity atoms will decrease as the temperature is lowered because less empty states into which transitions can be made become available. The total change of the scattering when the temperature is lowered is thus the difference between the increase in elastic and the decrease in inelastic scattering. A consideration of the interference of waves scattered by the two atoms of a pair led to the

conclusion that the elastic scattering predominates and thus this treatment explains the resistivity minimum.

Because this mechanism is due to pairs of solute atoms it is expected that for dilute solutions the size of the minimum will be proportional to the square of the solute concentration.

e) Dekker[93] gave a treatment of the elastic scattering of conduction electrons using a model similar to that applied to the magnetic properties. (paragraph 2).

The basic assumptions are : 1. The solute atoms can be divided into single atoms and nearest neighbour pairs, defined as in paragraph 2, this means that only very dilute alloys are considered, 2. there is a magnetic coupling between nearest neighbour solute atoms, which can be either ferro- or antiferromagnetic, 3. the scattering potential of a solute atom for a conduction electron can be written as the sum of a spin-independent and a spin-dependent term.

Expressions for the cross-section for elastic scattering by single atoms and by the above mentioned pairs were derived in terms of the scattering potential. The last part contained a term arising from the interference of the waves scattered by the two atoms of a pair. The total elastic scattering cross-section Q_{el} was found to vary with temperature T if the magnetic interaction between the nearest neighbour solute atoms is non-zero and, depending on the above-mentioned interference term, $\frac{dQ_{el}}{dT}$ was either positive or negative. It was assumed that the model leading to a negative value for

$\frac{dQ_{el}}{dT}$ is applicable to the actual alloys and that the appearance of a resistivity maximum is the result of the decrease of the inelastic scattering at low temperatures as suggested by Schmitt and Jacobs. This last effect was however not considered in more detail. It must be noted that here, as in the theory of Brailsford and Overhauser the interference of the waves scattered by nearest neighbour impurity atoms, is of major importance. It was also shown that this treatment leads to a decrease of the resistivity in a magnetic field.

§.5 Specific heat.

The specific heat anomalies observed in dilute alloys have in most cases been interpreted as broadened Schottky anomalies, as discussed in Sec. A paragraph 1, arising from the ordering of atomic moments in a molecular field. For few more detailed features of the experimental curves has it been possible to account in a theoretical model.

The fact that the specific heat of Cu-Mn alloys at low temperatures is independent of concentration was explained by Overhauser[22] on the spin density wave model (Ch.I) which also gave the correct order of magnitude of the specific heat at the temperatures considered.

Marshall[94] explained the same experimental result using a molecular field model. This has the advantage above the spin density wave theory that no new principle has to be introduced. In this work the concept of the molecular field in a dilute alloy is examined. Because this field will

vary over the volume of the alloy it is necessary to introduce the function p (H,T), the probability of finding at a lattice point a field H at a temperature T. For a lattice in which all the atoms carry a moment and in which there is perfect antiferromagnetic order, $|H|$ will have one well defined value h(T) at a given temperature so that $p(H,T) = \frac{1}{2}$ for $H = \pm h(T)$ and zero for all other values of H, while h(T) is zero above the ordering temperature. In a dilute alloy the solute atoms surrounding a given atom will not all have the same spin orientation and not all be at the same distance from that atom so that for $|H|$ a range of values is possible. The distribution function p(H,T) as function of H will have the shape as shown in Fig.4.

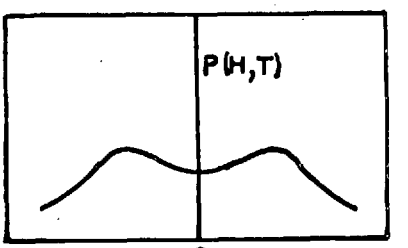

FIG.4 Probability-distribution of the molecular field in a dilute alloy. After ref. 94

The interaction between the atomic moments was taken to be of the form derived by Yosida (Ch.I). The energy of the system is

$$E(T) = -\tfrac{1}{2} Nc \int_{-}^{+} \left\{ p(H,T)\mu H \tanh \frac{\mu H}{kT} \right\} dH \quad (9),$$

where μ is the moment per solute atom, N the number of lattice points and c the impurity concentration. Differentiation of (9) gives the specific heat C_M. At low temperatures only small values of H are found to contribute to C_M, which means physically that only spins in small effective fields give rise to Schottky anomalies, while those in stronger fields remain rigidly aligned and do not contribute to the specific heat. Application of this result

then leads for low temperatures to a concentration-independent expression for C_M, in accordance with the experiments.

§.6 Thermoelectric power.

For a metal in which the scattering of the conduction electrons is purely elastic, the collision term in the Boltzmann equation can be written as $\left(\frac{\partial f}{\partial t}\right)_c = -\frac{f_k(E) - f_o(E)}{\tau}$ (10)[27] where $f_k(E)$ is the distribution function for wave vector k, E the energy, $f_o(E)$ the equilibrium value of the function, and τ the relaxation time. In this case the thermoelectric power arising from electron diffusion can be written as[52]

$$S \approx \frac{\pi^2 k^2 T}{3e} \left\{ \frac{d \ln N(E)}{dE} + \frac{d \ln v^2}{dE} + \frac{d \ln \tau}{dE} \right\}_{E=E_F} \qquad (11)$$

where N(E) is the density in energy of conduction electron states, v the velocity of an electron and E_F the Fermi-energy. At low temperatures this model predicts values of S of at most 0.1 $\mu V/^oK$. For several dilute alloys, mentioned in Sec.A paragraph 1, values of several $\mu V/^oK$ at temperature below 20^oK have been reported. Because these anomalously high values are found in alloys in which also the resistivity shows anomalies, the explanation of this behaviour has been sought in some anomalous scattering mechanism for the conduction electrons. The last term in equation (11) already indicates that if τ is strongly energy-dependent at $E=E_F$ large values of S are possible, but if inelastic scattering is taken into account, equation (10) and thus also (11) do not hold.

A simple model has been put forward by Guenault and MacDonald[95] in which the scattering of the electrons is partly elastic, partly inelastic. Within the limits of this model it was possible to derive a relation similar to (10), which contains a relaxation time τ' describing the total scattering of the electrons. This theory assumes two groups of conduction electron states, electrons can be scattered elastically into a state in the same group, while the scattering into the other group is an inelastic process. The elastic relaxation times of the two groups, τ_1 and τ_2 are taken to be different. It is now assumed that it is justified to work with a distribution function for each group and to write for these functions equations similar to (10). Then it is shown that the total scattering can be represented by one relaxation time τ'. In analogy with (11) the last term in the expression for S is then written as $S' \alpha \left(\frac{d \ln \tau'}{dE} \right)_{E_F}$ (12). From this relation it is seen that, if τ' is strongly energy-dependent and an asymmetrical function of E with respect to E_F, large values of S' are possible. If $\tau_1 = \tau_2$ the inelastic scattering does not affect τ', so that no anomaly is expected. The same applies if the inelastic scattering is either very large or very small compared to the elastic part.

This idea can be applied to the picture of alloys discussed in Sec. A paragraph 1 as a gas of conduction electrons scattering by magnetic impurities. The two groups of electrons mentioned above are those with $+$ and those with $-$ spin. The scattering of an electron in which the spin is not reversed, is elastic and the relaxation times for the elastic scattering must be different for the two groups. The transition of an electron from

one group to the other, i.e. the reversal of the spin, involves also a transition of the solute atom into a different state, since the total spin must be conserved. This part of the scattering is inelastic. The relation (12) is thus applicable to this system and if the elastic and inelastic relaxation times obey the conditions mentioned above, a large thermoelectric power is possible. The work by Guenault and MacDonald only indicates the principle of the method, De Vroomen and Potters[96] have treated this problem in more detail.

SECTION F. SOLUTIONS OF Fe and Co IN OTHER TRANSITION METALS.

For solutions of Fe in elements of the second transition group and alloys of those elements, the experiments show that the magnitude of the moment per Fe atom depends on the number of 4d-electrons per atom of the solvent. Further the saturation magnetization of solutions of Fe and Co in Pd and Pd-Rh indicates a large moment per solute atom and the resistivity of those alloys in which the solute carries a moment shows anomalies.

The theoretical work summarized in Section E can be expected to be applicable also to these alloys. Because of the large differences observed between the solutions, the following section will be divided according to alloy system, in the following paragraphs :

1. Nb-Mo-1% Fe alloys.
2. Rh-Fe alloys.
3. Fe and Co in Pd, Rh-Pd and Pd-Ag.

§.1 Nb-Mo-1% Fe alloys.

a. Magnitude of the atomic moment.

In this alloy system the Fe atoms do not carry a moment if the Mo content of the alloy is lower than 40%. In a $(Nb_{0.4}Mo_{0.6})1\%$ Fe alloy a moment of $0.3\mu_B$ is observed, which increases rapidly with Mo content to $2.1\mu_B$ in pure Mo. For the Nb-Mo alloys specific heat measurements are available so that the electronic specific heat γ can be compared with the atomic moment as in Sec.A paragraph 1. For these binary alloys γ decreases strongly

if the Mo-concentration is raised from zero to 40% and remains constant on further addition of Mo.

According to the theory given by Anderson[16], a low density of states of the solvent is favourable for the existence of a moment and the appearance of a moment at 40% Mo is in accordance with this model. As Anderson however pointed out the strong increase of the moment with increasing Mo content of the matrix can not be explained in these terms.

b. Electrical resistivity.

The variation of the resistivity with temperature for Mo-Fe alloys is similar to that for the noble metal-transition metal alloys discussed in Sec.A paragraph 1. This is the only evidence known of a resistivity maximum and minimum in an alloy of two transition metals. The theoretical work done to explain this phenomenon has been discussed in section E, paragraph 4.

§.2 Rh-Fe alloys.

a. Electrical resistivity.

In these alloys the increase in resistivity $\Delta\rho$ as a result of the addition of Fe is proportional to the Fe content c for Fe concentrations up to 0.85 at % at all temperatures observed. This suggests that $\Delta\rho$ is due to the scattering of conduction electrons by single Fe atoms. The strong increase in $\Delta\rho$ with temperature suggests the transition of the Fe into a state in which the atoms have a higher cross-section for the scattering of conduction electrons.

b. Thermoelectric power.

The thermoelectric power S is of the same order of magnitude as that for the alloys discussed in Sec.A paragraphs 1 and 2. The temperature dependence is however entirely different. For the noble metal based alloys S decreases below 4°K in absolute value with decreasing temperature while for the Rh-Fe solutions no such decrease has been observed down to 1.8°K.

§.3 Pd-Fe,Pd-Co,Rh-Pd-Co,Pd-Ag-Co.

In the Pd based alloys a very large moment (7 to 10μ_B) per solute atom is found. It was assumed by Gerstenberg, Crangle and Bozorth et al. that this is partly localized on the Pd atoms which are nearest neighbours to a solute atom. Recent neutron-diffraction experiments[97] on a Pd-1% Fe alloy showed the presence of a moment even on atoms which are next nearest neighbours to an Fe atom. This polarization of Pd atoms can be interpreted in terms of the model given by Clogston[78] which gives for the spin on a site which is a nearest neighbour to a solute atom the expression $\rho(E_F)\ S_o J'$ (13) where $\rho(E_F)$ is the density of 4d-states at the Fermi-energy, S_o the spin as the central Fe site and J' the exchange integral between the Fe and a nearest neighbour Pd atom, which Clogston estimated at 0.1 eV. Taking for the Fe atom $S_o=1$ and for $\rho(E_F)$ the value of 2 states per eV per atom as derived from the electronic specific heat of Pd one finds a value 0.2 for the spin on a Pd atom which is of the required order of magnitude to explain the experimental results. When in a Pd-Co alloy Pd atoms are

replaced by Ag or Rh the moment on a Co atom decreases. This decrease is more rapid in the case of Ag than for Rh as third component. This difference in the rate of fall-off with Rh or Ag-concentration might be explained in the following ways :

1. Ag nor Rh carry a moment but Ag reduces the Pd-Pd interactions stronger than Rh does.

2. The density of states in the Rh-Pd system is higher than that in the Pd-Ag system and Equ (13) predicts thus a higher moment on a Pd in Rh-Pd-1% Co than in Pd-Ag-1% Co.

3. The Rh atoms are polarized as Pd, though to a lesser degree.

CHAPTER IV

EXPERIMENTAL TECHNIQUES

In the present investigation the magnetic susceptibility has been measured of ternary solutions of 0.1% of a transition metal of the first long period in η, ε and γ phase Cu-Zn alloys. Also measured were some solutions of Fe in Mo, Rh and Ir, in which, as was mentioned in Chapter III, resistivity anomalies were found by others. The measurements were made in the temperature-range from 1.8 to 290°K.

In Part A of this chapter the preparation and treatment of the alloys used is given. In Part B the susceptibility-balance and the low-temperature apparatus used are described.

PART A. ALLOYS

Introduction

(a) The solubility of transition metals in Cu-Zn alloys

For ternary solutions of Cr, Mn, Fe or Co in γ and ε phase Cu-Zn alloys no phase diagrams are available. That single-phase alloys containing 0.1 at % of transition metal can be prepared is likely for the following reasons:

γ - phase: The systems Mn-Zn, Fe-Zn and Co-Zn also form a γ phase with $^{e}/_{a}$ between 1.54 and 1.70 assuming zero valency for the transition metal[98] Therefore it canbe expected that ternary Cu-Zn-X alloys containing small amounts of one of the above-mentioned transition metals will be stable. For Cr-Zn no data are available.

ε - phase: Henderson and Willcox[99] found that there is a complete range of solid solutions between the ε phases of the Mn-Zn and the Ag-Zn system. The phase diagram of Ag-Zn is very similar to that of Cu-Zn so that it can be expected that also a dilute solution of Mn in ε phase Cu-Zn will be stable. The systems Co-Zn and Fe-Zn do not form a hexagonal ε or ζ phase and for Cr-Zn no data is available.

Although thus no phase diagrams for these ternary systems have been published it is likely that single phase solutions (Cu-Zn) - 0.1 % X will exist. A number of these alloys was prepared and metallographic examination did not show the presence of a second phase in the specimens.

(b) Solutions of Fe in Mo, Rh and Ir

The solid solubility of Fe in Mo has been reported as 16.7 at % at 1480° C and 4.5 at % at 1100° C.[38] In the Rh-Fe system solid solutions exist up to 14 at % Fe[100]. For the solid solubility of Fe in Ir no data are available.

(c) The alloys of which the susceptibility was measured in this investigation were:

Zn - 0.1 at % Fe

Cu-Zn, Zn rich end of the ε phase (15% Cu) with 0.1% Mn added,

" " " " " " " " " " " " 0.1% Fe " ,

" " " " " " " " " " " " 0.1% Co " ,

Cu-Zn, Cu rich end of the ε phase (19% Cu) with 0.1% Cr added,

" " " " " " " " " " " " 0.1% Mn " ,

" " " " " " " " " " " " 0.1% Fe " ,

" " " " " " " " " " " " 0.1% Co " ,

Cu-Zn γ phase (62% Cu) with 0.1% Cr added,

" " " " " " " 0.1% Co " ,

Cu-Zn γ phase of three different Cu/Zn ratio's (41, 37 and 34% Cu), each with 0.1% Mn added, and the same three Cu-Zn alloys, each with 0.1% Fe added, Further Mo - 0.65 at % Fe, Rh - 0.8 at % Fe, and Ir - 0.8 at % Fe

In the paragraphs 1 to 7 the casting and treatment of the Cu-Zn - based alloys will be given. The preparation of the solutions of Fe in Mo, Rh and Ir requires different techniques and will be discussed in paragraph 8.

Cu-Zn based γ, ε and η phase alloys

§.1. General remarks.

The ε and η phase alloys have a hexagonal crystal structure and the possibility that the susceptibility will be anisotropic can not be excluded. To get meaningful susceptibility results it is therefore necessary to work either with single crystals or with polycrystalline material of small grain size. It is difficult in this case to produce single crystals without concentration gradients over the volume of the specimen, while a homogeneous polycrystalline sample can easily be prepared by quenching the melt and annealing the specimen for a not too long time, so that the last procedure was followed. For the cubic γ phase this problem does not arise and a larger grain size can be tolerated.

In all these alloys the danger exists that during the melting process Zn will evaporate from the melt and condense in colder parts of the tube which leads to a deviation from the intended Zn content of the alloy. For Zn-Fe alloys this only means a small increase in the relative Fe content, for the ε and γ phase alloys however this will cause a difference from the intended composition of the matrix, the consequences of which are discussed in Chapter V (introduction). On the other hand it is essential that all the transition metal goes into solution. To make sure that this will be the case without the necessity of having to keep the melt at a temperature much above that of the liquidus for a long time it was decided to cast first an alloy of a few percent of the transition metal in Cu and then to melt this with Cu and Zn to give the ternary alloy. If in the binary Cu-X master-alloys the components are thoroughly mixed the transition

metal will be well dissolved in the melt of the ternary alloy because Cu and Zn mix readily. The required shape of the specimens to be used in the susceptibility-balance was that of a cylinder of 2 mm diameter and a few mm length.

§ 2. Starting materials.

The sources of the pure elements used for the preparation of the Cu-Zn based alloys are given below. The indications in brackets will be used in Appendix A as a reference to the material.

Copper (a) a rod, supplied by Johnson, Matthey & Co. spectroscopically pure. (S).

(b) two other rods supplied by the same firm from a different batch. The impurity content was specified as 3 p.p.m. Ag, 1 p.p.m. Fe, 1 p.p.m. Pb. (JM).

Smaller pieces were cut from these rods and etched for 20 minutes in 1:3 HCl

Zinc (a) a bar supplied by L. Light & Co., the purity specified as 99.995 Zn - 0.004 Pb. (A)

Pieces were cut off with a hacksaw and etched in dilute HCl.

(b) Zinc shot, supplied by the same firm, 6N pure. Used as supplied. (L).

Chromium supplied by Johnson, Matthey & Co., Fe content specified as 0.3%, used as supplied.

Manganese supplied by the same firm, purity 99.98%, used as supplied.

Iron supplied by the same firm, in the form of a wire. Spectroscopically pure. Small pieces were cut off with

side-cutters and etched in dilute HCl

Cobalt — supplied by the Metallurgy Department of Imperial College. Spectroscopically pure. Used as supplied.

§ 3. Preparation of the Cu - X master alloys.

Four Cu-based alloys containing 2% Fe, 2% Co, 2% Cr and 13% Mn respectively were prepared. The elements were put in alumina crucibles and melted in an induction furnace at a temperature between 1100 and 1400°C for about 15 minutes in an Argon atmosphere. An advantage of this method is that the liquid Cu was stirred vigorously as a result of which the transition metal could dissolve quickly. The melt was then left to cool. After removal of the specimens from the crucibles some alumina was found to be stuck on the alloys, this was ground off on a grinding wheel and the alloys etched to remove possible contamination from the surface. The master alloys were then treated in the same way as the pure Cu mentioned above.

§ 4. Alloy preparation

Weighed quantities of Cu, Zn and the relevant master alloy of a total weight between 5 and 10 gram were put into a quartz tube as shown in Figure Ia, which was then evacuated while being heated at about 200°C and sealed off.

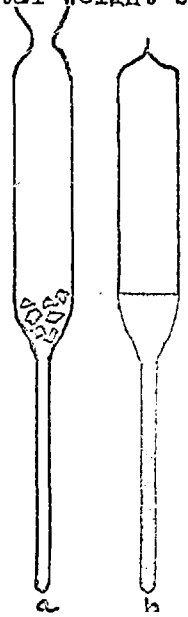

FIG. 1

The tube was then, with the thin end upwards, kept in a furnace at 50°C above the liquidus temperature and shaken every 5 or 10 minutes to mix the constituents. At the end of the melting

time, the furnace with the tube was turned upside down and the liquid cast in the thin end as shown in Figure 1b. The melt was then left for another 10 minutes, being shaken several times and quenched quickly, the thin end of the tube being lowered in water. During the quenching the tube was broken. If this procedure is followed the alloy solidifies gradually from the lower end of the tube and due to the weight of the liquid above, any empty volume caused by contraction of the melt on solidfying will be filled up. It was however found that the liquid ejected gas when solidfying which caused small spherical holes in the sample.

A Zn - 0.1% Fe specimen (referred to as Zn-Fe I), cast in the above-mentioned way was found to have a temperature-independent susceptibility equal to that of pure Zn. It was concluded that the specimen did not contain any Fe and a different alloy, hereafter referred to as Zn-Fe II prepared in the following way: Zn and Fe were kept molten at 300°C in a wide quartz tube for 5 hours, being shaken every 15 minutes and quenched rapidly in water. This sample was then remelted and cast as the alloy Zn-Fe I.

§ 5. Specimen treatment

After removal of the quartz from the sample the thin end was cut from the wider part with a hacksaw after which it was etched in 1:5 HCl to remove Fe contamination. The extremely brittle γ brass specimens could be broken easily. The 2 mm wide cylinders were then annealed to homogenize the alloys. The ε phase specimens were sealed in vacuo in separate pyrex tubes and annealed at a temperature just below that of the liquidus. The γ brass alloys were annealed in

vacuo at 700°C at which temperature the danger exists that Zn will evaporate from the specimens. These specimens were therefore all put into one close-fitting quartz tube, separated by small pieces of quartz to avoid diffusion from one specimen to another and a few mg of pure Zn were added to create a certain vapour pressure of Zn to avoid evaporation from the samples. At the end of the annealing time the ε and γ plane specimens were quenched in water.

The Zn-0.1% Fe alloys were supersaturated solutions and could therefore not be annealed. These specimens were kept in liquid nitrogen from the moment of casting till just before the low-temperature measurement. The total time the alloys were at room temperature was approximately 2 hours.

For a susceptibility measurement specimens of between 100 and 130 mg were cut from the cylinder with side cutters, the surface was then ground with emery paper to remove oxyde and, in case Zn had evaporated from the sample, the surface of low Zn content. These specimens were then etched in 1:5 HCl, rinsed in water, dried and put into the susceptibility balance. Details of the preparation and treatment of the alloys are given in Appendix A.

§ 6. Metallography and chemical analysis

To check on the pressure of precipitates of a different phase, the alloys were examined metallographically. Mounted specimens were ground with emery paper and polished, forst on a disc with diamond powder and next with alumina on a sylvet cloth. Also the brittle γ brass alloys could be polished satisfactorily in this way. The samples were etched with ferric chloride and

examined under an optical microscope. In two alloys, 0.1% solutions of Fe and Mn in a Zn rich ε phase Cu - Zn solvent with Cu - Zn ratio close to that of the phase boundary, (14% Cu), a precipitate in the grain boundaries was observed, which was assumed to be η phase. These alloys were therefore not used and replaced by the corresponding solutions in 15% Cu - 85% Zn. In none of the other specimens a precipitate was discovered.

Chemical analysis

Analyses were carried out by Daniel Griffith & Co. The results are shown in Appendix A.

The mass of a specimen used for a susceptibility measurement was not sufficient to enable an accurate analysis and the total amount of alloy cast (about 5 gram) had to be used. For the intended binary Cu - Zn alloys the Fe and the Cu content were analysed. In the ε phase specimens (no. 4 and 8) only a small amount of Fe was detected. In the γ phase alloy (no. 13) however, 0.18 wt% Fe was found. The Cu-Zn-Mn alloy (no. 18) which was cast immediately after No. 13 from the same batch of starting materials was therefore also analysed for Fe but contained only a trace. It must be noted that the susceptibility results in this γ brass alloy No. 13 did not show values very much above those reported by others for a binary alloy of this composition. It is thus not certain that the Fe detected during the chemical analysis was present in the susceptibility specimen.

Because the Cu/Zn ratio for the above-mentioned alloys as shown by the analysis, about 0.1% deviation in Cu - content, was close to the intended value this was not analysed for the other samples.

In the Zn-Fe and in all the ternary alloys only the transition metal content, needed for the determination of the effective moment of a solute atom from the susceptibility results, was analysed.

§ 7. Solutions of Fe in Cu - Zn γ phase alloys

Difficulties were met in the preparation of γ phase (Cu - Zn) - 0.1% Fe alloys. Because no significant susceptibility results could be obtained for these solutions and the problem is entirely metallurgical, the results will be discussed here.

Firstly, three alloys of different Cu/Zn ratio were cast as described in paragraph 4 and annealed for 5 days at 700°C. The susceptibility of two of these alloys as measured with the susceptibility-balance described below, showed a Curie-Weiss behaviour and a field-dependence at low temperatures. The values of the effective moment per Fe atom were 6.5 μ_B and 7.7 μ_B, while $|\theta| \leq 10°K$. These values of μ_{eff} were unexpectedly large. The susceptibility of the third alloy was found to vary considerably with time. Two alloys of higher Fe concentration, 0.25 and 0.50wt% which were prepared in the same way showed a large temperature-independent remanent magnetisation. In none of these five specimens did a metallographic examination reveal any precipitate. From the observed susceptibility results it is however clear that large Fe particles must have been present.
It was then tried to prepare the same alloys, using a Zn - 5% Fe master alloy. This master alloy was prepared in the following way: Fe filings and Zn were kept molten at 900°C for 9 hours, the melt being shaken every 15 minutes. After this the melt was left to cool to 750°C, kept for one hour at this temperature and quenched. With

this master-alloy solutions of 0.1% Fe in γ phase Cu-Zn were prepared and annealed as described in paragraphs 4 and 5. Also in these samples no precipitate was detected metallographically. A measurement on one of these alloys showed an almost zero susceptibility at 300°K and a large remanence at 77°K. This alloy was therefore remelted, kept at 850°C for 19 hours, quenched and annealed one week at 700°C, after which a susceptibility measurement showed a large remanent magnetization at 77° and 300°K. One of the alloys of this series (not remelted) was then powdered in an agate mortar and a small permanent magnet held close to the powder to remove strongly magnetic particles. This powder was put into the susceptibility balance and showed again a large remanence.

It was considered possible that torques were acting on the specimen in a magnetic as a result of the presence of ferromagnetic clusters. Such torques will in the susceptibility balance used be interpreted as vertical forces and an analysis of the apparent susceptibility with the help of a Honda-Owen plot (see Chapter V) will be impossible. Therefore one of the specimens of the first series (prepared with the Cu-Fe master alloy) was annealed for another 7 days at 600°C and the susceptibility measured in a Sartorius balance. For these measurements the apparatus of the Solid State Division, A.E.R.E. was used.*) The results are shown in Figure 2.

---

*) The author wishes to express his thanks to Dr. R. Anderson and Mr. J. Penfold for their kind permission for the use of the balance and help with the measurements.

FIG. 2

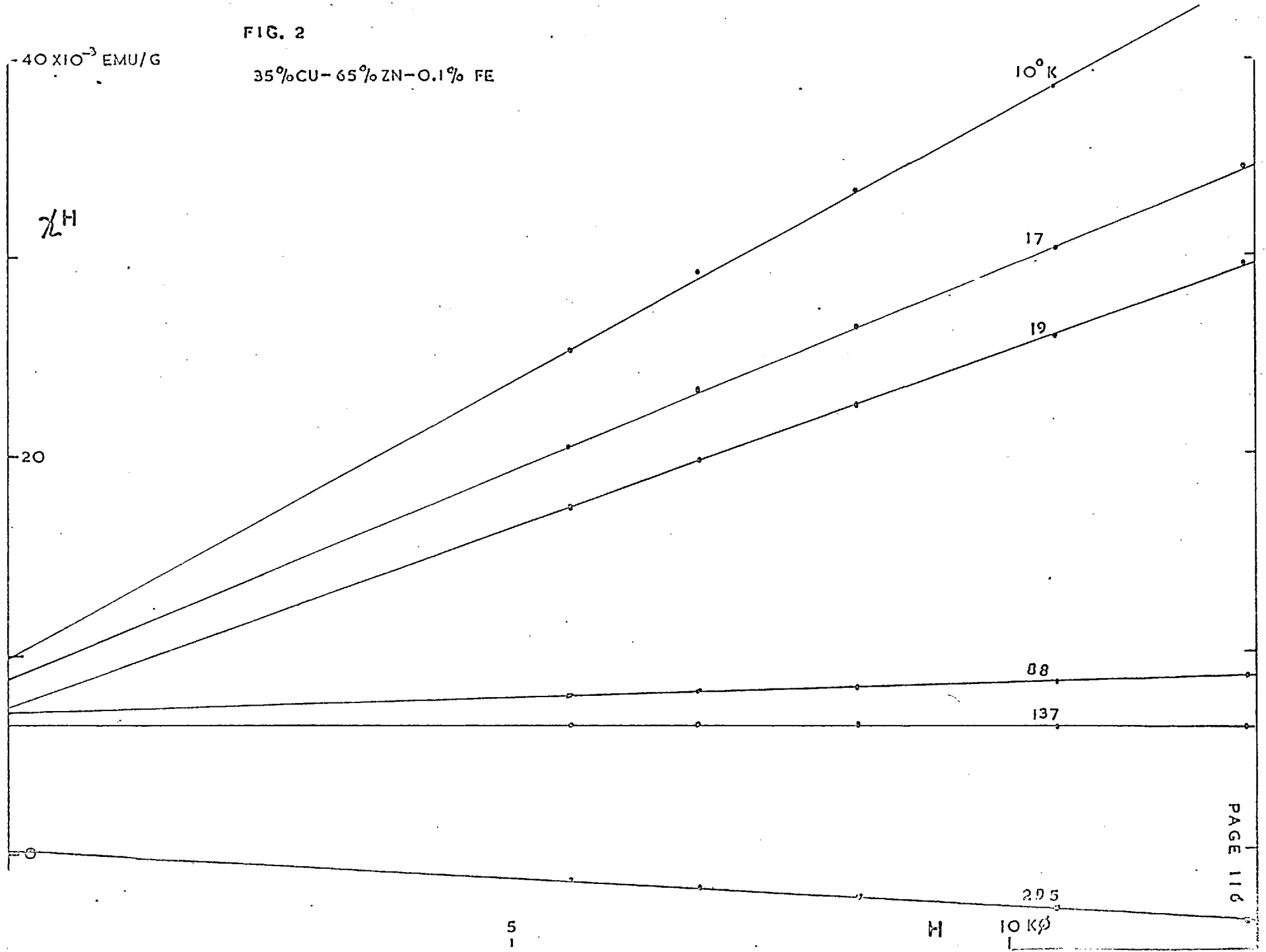

The fact that the remanence is temperature-dependent rules out a direct interpretation of these results.

It is thus clear that the γ phase Cu-Zn-0.1% Fe alloys prepared in the manner described above contained ferromagnetic or superparamagnetic clusters of Fe, which are too small to be seen under an optical microscope. It must be noted that solution of the other transition metals in this matrix could be prepared easily and as discussed above it is expected that also small amounts of Fe should dissolve readily. It seems thus necessary, before continuing this work to make a more thorough investigation of the metallurgy of the ternary Υ phase Cu-Zn-Fe system which is outside the scope of this work.

§ 8. The solutions of Fe in Mo, Rh and Ir.

The Mo-Fe and Rh-Fe alloys were cut from arc-melted buttons prepared at the University of California, La Jolla. The Ir-Fe specimen was kindly loaned by the International Nickel Company, Precious Metals Division.

PART B. MAGNETIC SUSCEPTIBILITY MEASUREMENTS

Section I Apparatus

§ 1. Introduction

The magnetic susceptibility is found from the force acting on a sample in an an inhomogeneous magnetic field. If the field H and the field-gradient $\frac{\partial H}{\partial z}$ do not change too much over the volume of the specimen, the force in the z-direction is $f_z = -m(\chi_m H + \frac{1}{2}\sigma_m)\frac{\partial H}{\partial z}$ (1) in c.g.s. units, if the magnetic moment per unit mass M of the specimen can be written as $\chi_m H + \frac{1}{2}\sigma_m$ and σ_m does not depend on the field H. Here χ_m is the susceptibility per unit mass, m the mass of the specimen and σ_m the remanent magnetisation per unit mass. If no assumptions are made about the relation between H and M and if

$H = H(z)$ and $M = M(z)$, the force $f_z = \frac{1}{2} m(M + H\frac{dM}{dH}) \cdot \frac{dH}{dz}$ (2)

(see appendix B.)

The force on the specimen in a field was measured with a balance which has been described in detail elsewhere.[101] A few changes have been made which will be mentioned in the course of a short description of the apparatus.

§ 2. The balance

In principle the balance is an elinvar spiral from which hangs a quartz rod, at the lower end of which is fixed a bucket holding the sample to be investigated. This sample is in an inhomogeneous part of the field of an electromagnet. If a magnetic field is applied the specimen, if paramagnetic, will be pulled towards the centre of the field, the spiral will be stretched and the small mirror attached to it will turn.

This turning of the mirror can be detected by measuring the output voltage of a Selenium photocell on which a light beam reflected by this mirror is focused. This effect of the force on the sample is then compensated by a current through the coil indicated in Figure 3., which hangs in the gap of a permanent magnet. The magnitude of this current is a measure of the force acting on the specimen. Calibration is done by lowering a 100 mg weight to a plate on top of the coil and measuring the restoring current necessary to compensate for this extra force. The current necessary to compensate a force of one dyne is about 30μA.

The bucket holding the specimen is a new feature and is shown in Figure 4. It can be connected to the quartz rod by sliding it upwards around the rod, a "pip" on this rod fits in the J-shaped slit in the bucket, when the bucket is in the highest position it is turned and is then fixed to the rod. The advantages of this specimen holder are firstly that the outer diameter (3.5 mm) allows a reasonable clearance between the bucket and the surrounding oopper cap (inside diameter 4.8 mm.). The danger that the bucket will touch the cap after the dewars have been put on is smaller than with the bucket used previously. Secondly the force on the balance without specimen is small (1.2 dyne in a field of 8000 Oe). The quartz rod to which the bucket is connected is surrounded by a German silver tube ending in a joint to which the copper cap mentioned above can be sealed. For this seal Edwards silicone grease was used which gave a satisfactory seal at low temperatures. To the copper cap are connected the thermocouple and the carbon resistance thermometer discussed in Paragraph 4. For a

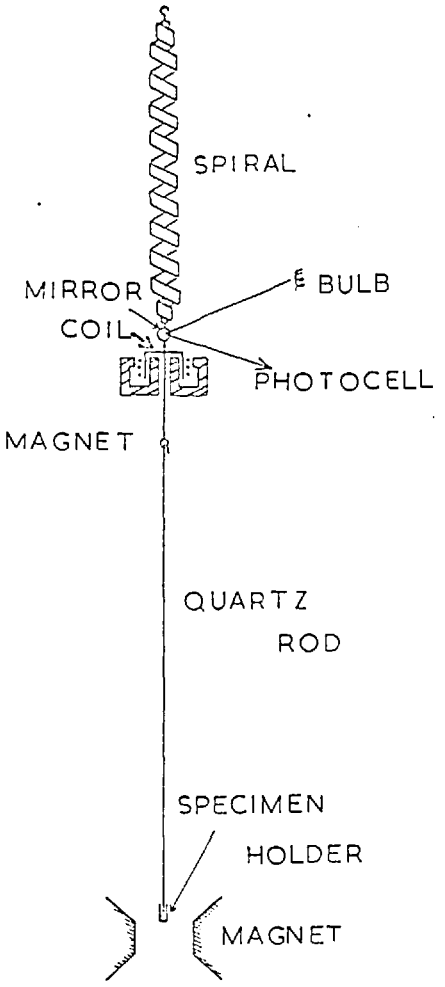

FIG. 3

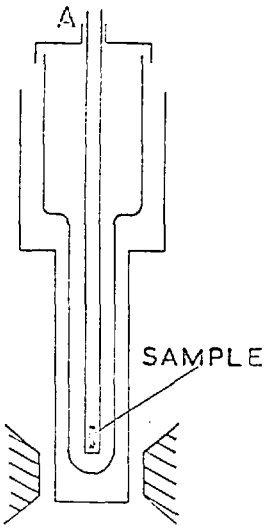

FIG. 5

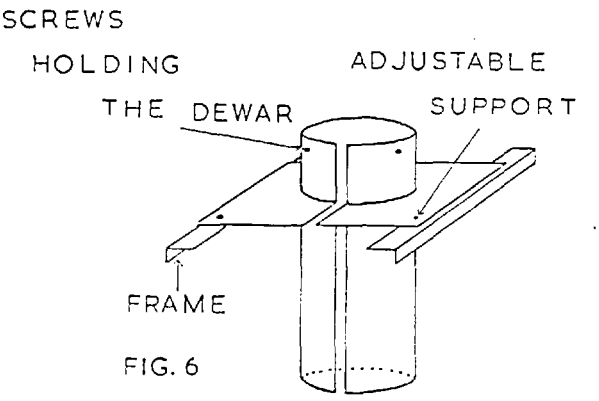

FIG. 6

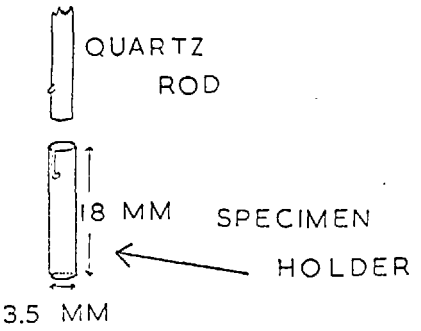

FIG. 4

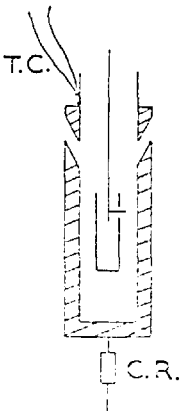

FIG. 7

change of specimen only this cap has to be removed. Over the upper end of the balance is a glass jar, so that the space in which the balance is standing can be evacuated.

§ 3. Dewar location

A pyrex helium dewar and a brass nitrogen dewar are suspended as shown in Figure 5 in such a way that the German silver tube and the copper cap surrounding the lower end of the quartz rod and the specimen holder, are in the narrow tail of the helium dewar. The tail of the nitrogen vessel fits in the 31 mm pole gap of the magnet. A brass cap slides round the tube at A and can be sealed to the pyrex dewar as shown in Figure 5. Due to the small clearance between the quartz assembly and the surrounding tube and between this tube and the inside of the dewar careful alignment of the dewar system is necessary. To avoid the need of a laborious adjustment of the system after every change of specimen, a wide tube in which the outer dewar can be suspended was permanently fixed to the frame on which the apparatus is standing (Figure 6.). This tube, in which the dewar fits closely was soldered to the plate. The plate is fixed to the frame of the apparatus with three adjustable screws which allow some movement in a horizontal plane and slight tilting of the tube. The dewars are brought into position by sliding them into the tube from underneath, then three screws are screwed in through the tube under a rim at the top of the outer dewar. The slit allows the pumping line of the helium vessel to pass through. The lower end of the wide tube is well above the joint of the copper cap so that this arrangement does not interfere with the removal of the cap. Once the dewar-support has been fixed in the

correct position, the dewars can be put on without further adjustment after a change of specimen.

All further low-temperature equipment used has been described in detail in Reference 101.

§ 4. Temperature measurement

With the balance measurements were done between 1.8 and 290°K Because it is not possible to fix a thermometer directly to the specimen, the temperature measured is that of the copper cap (see Paragraph 2) to which are soldered an Allan-Bradley carbon resistance thermometer (42 Ω at room temperature) and a Au-2% Co versus normal silver thermocouple. The carbon resistor is soldered with one of the leads to the copper. In this way the carbon and the copper are in direct thermal contact. To each of the leads is soldered a copper wire (40 swg), these wires are twisted together, wound with four turns round the cap and stuck to this with G.E. low-temperature varnish to avoid temperature gradients in the carbon by heat leaking down the wires. The two wires of the thermocouple were melted together and the joint soldered to the copper tube to which the cap is sealed as shown in Figure 7. The wires were wound with three turns over about one inch length around the German silver tube for the same reason as mentioned above.

§ 5. Control of the magnet current

For the measurements a Newport type A magnet was used with conical pole pieces. The highest current normally used was 6.5 amp. which gives for the gap of 31 mm a field of 8000 ∅ at the position of the specimen. The magent current was supplied by a Newport stabilized

15 amp. D.C. power supply. This unit could not be placed near the apparatus and a remote-control panel was built with which it is possible to vary the magnet current either in steps or continuously, to put a resistor of low value in parallel with the magent and to reverse the direction of the magnet current. An alarm system becomes operative if an attempt is made to open circuit or shunt the magnet when a current of more than 1.5 amp. is flowing, or to reverse the current direction when the magnet is not shunted.

Details of the magnet circuit and the control unit are given in Appendix C.

§ 6. Recording of data

The data to be recorded during a measurement are:

(1) The restoring current through the coil in Figure 3, compensating the paramagnetic force on the specimen.

(2) The voltage from the thermocouple.

(3) The magnet current.

(4) The resistance of the carbon thermometer.

1. It was found that, when no current flows through the coil and no magnetic field is applied, the position of the mirror (Figure 3) changes with time. The procedure adopted therefore is to put the photocell in such a position that, if no field is applied, a small restoring current is needed to obtain a zero voltage from the photocell. The corresponding position of the balance is taken as zero position. For a susceptibility measurement the restoring current necessary to bring the balance in the zero position is measured with field off, with field on and again with field off.

The average of the two zero-field values, if not too different, is taken as zero-field reading. The principle of the circuit is shown in Figure 8.

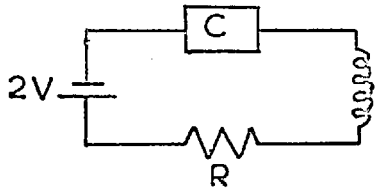

FIG. 8

The restoring current can be varied with the circuit C (see Reference 101) and is measured as the voltage across the resistor R which, if a measurement at constant temperature is made, is measured with a Tinsley potentiometer. If the apparatus is warming up and a certain speed in taking the readings is required, this voltage is read by three channels of a six-channel Honeywell chart recorder having a maximum deflection of 10 mV. The resistor R can be varied stepwise between 3 and 150 Ω, this to allow for a given current as large a voltage as possible below 10 mV.

2. The voltage from the thermocouple, which is used mainly during warming up of the apparatus is also printed om the recorder. As the readings at the end of the scale, below 0.5 and above 9.5 mV are somewhat doubtful, a constant voltage of 1.38 mV derived from a Mallory-cell was added to that from the thermocouple. From the same Mallory-cell were also derived constant voltages of 2.8 and 7.1 mV which were read by two channels as a check on the recorder.

3. The magnet current could not be read by the recorder because of ground loops between the recorder and the magnet power

supply and was read on a Crompton-Parkinson moving coil meter.

4. The resistance of the carbon resistance thermometer was measured with the circuit described in Reference 101.

Section II Experimental procedure.

§ 1. The specimens were in the form of cylinders a few mm long and 2 mm in diameter. The position of the quartz bucket is shown in Figure 9. This position was chosen because the specimen has to be in the same part of the field in every run and in this case the alignment could be done easily with a microscope, the edges of the pole pieces being used as a reference.

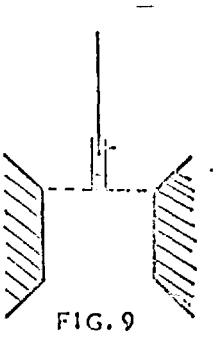

FIG. 9

After the specimen had been put into the bucket the apparatus was assembled as described in the previous paragraphs, the case of the balance was evacuated and one mm of helium gas let in to obtain a thermal link between the specimen and the copper cap of which the temperature is measured. The susceptibility of the specimen was measured at room temperature in four fields to check on the presence of ferromagnetic impurity. The outer dewar was then filled with nitrogen to precool the apparatus to 77°K. A measurement of the susceptibility at 77°K was made after which liquid helium was transferred into the inner dewar. The susceptibility was measured in four fields at 4.2°K after which the temperature was lowered by reducing the pressure above the helium bath. The lowest temperature

that could be obtained was 1.7°K, when this was reached the vapour pressure was kept constant with a manostat of conventional design and again the susceptibility measured in four fields. After this the balance was left to warm up while the force was measured continuously in one field (8000 Oe) till the temperature reached 77°K, when again measurements in different fields were taken. Points between 77° and 290° were obtained by putting a small amount of nitrogen into the inner dewar and from the moment the temperature started to rise, measuring the force in one field at intervals of about 5°K. Taking readings in this temperature range when the apparatus is being precooled to 77°K was found to be less satisfactory. In this case the temperature decreased rapidly at the beginning and the results suggested a difference in temperature between the specimen and the thermocouple of about 5°K in the range from 290° to 150°K.

During a few experiments it was found that above 30°K the paramagnetic force on the specimen increased rapidly with temperature, showed a maximum between 50° and 60°K and decreased on further increase of temperature. When this had been observed the inner dewar was filled with nitrogen, the vapour pressure reduced and readings down to 53°K taken which always gave lower values of the susceptibility, which followed the Curie-Weiss curve through the points below 30 and above 77°K. The only explanation that can be given of this effect is that the extra paramagnetic force is due to oxygen which evaporates from higher parts of the German silver tube when the apparatus is warming up, condenses on the bucket and evaporates on further increase of temperature. As oxygen is strongly paramagnetic an extra force will be measured if this is present on the bucket. However no

significant increase in the pressure in the inner space was detected after this effect had been observed. The presence of oxygen has thus not been shown and the possibility exists that a different mechanism is responsible.

§§ 2a. Calibration data (force measurement)

The quantity $H\frac{\partial H}{\partial X}$ at the position of the specimen needed to determine the susceptibility from the measured force, was found from the force as a sample of Vanadium (at room temperature $\chi_m = 5.86 \times 10^{-6}$ emu/g) for different values of the magent current. As a check this was also done with a piece of pure Pd (room temperature susceptibility 5.23×10^{-6}). The difference between these results was well below the error in the force measurement discussed in Paragraph 3.

The fields used and the force on the empty balance are given in the table below

amps magnet	$H\frac{\partial H}{\partial X} \times 10^{-6}$ e.m.u. units	H Oe	$\frac{\partial H}{\partial X}$ Oe cm^{-1}	force on the balance in dyne (room temp.)
1.70	1.22	2800	435	-0.02
2.70	3.31	4300	770	-0.19
4.00	6.84	6200	1105	-0.53
6.30	11.75	8000	1470	-0.96

A negative force means that the bucket is pushed out of the field, i.e. is diamagnetic. The force on the empty balance does not vary with temperature down to 15°K and then decreases in absolute value to about -0.80 dyne at 1.7°K. This background force changed with use of the balance. From time to time it was measured at 290 and 77°K

and if a change was found from the previously measured values also at helium temperatures. Before such a run on the empty balance the bucket and the end of the quartz rod were cleaned with dilute HCl to dissolve any metallic contamination. As no powdered specimens were used, the bucket was not cleaned again before a new specimen was put in, since etching might change the force on the quartz assembly in a magnetic field.

§ 2b. The balance is sensitive to forces of about 4×10^{-3} dyne. In practice the accuracy is limited by other factors which are:

1. drifts in the zero field position of the balance, which are especially large when the balance is warming up fast. For a normal warm-up this drift is between 0.01 and 0.05 dyne during the time needed for a measurement ($\frac{1}{2}$ to 1 minute), and in the worst case 0.4 dyne.

2. changes in the force on the quartz bucket and rod which have been found to be as large as 0.05 dyne at 8000 Oe. As said above, this was checked regularly.

3. errors in the reading of the magnet current of 0.01 to 0.02 amp. which lead to an error in the susceptibility of 0.2% at high and 1% at low fields.

4. different position of the bucket with respect to the magnet after a change of specimen. The magnitude of this error can be seen from the measurements on the V and Pd specimens mentioned above in Paragraph 2, and from the measurements on the solution of Mn in brass (Chapter IV, Sec. 1, 8). This last specimen was measured, taken out of the balance, put back in again and measured. These last two series of measurements gave at high temperatures values different by

0.02 to 0.03×10^{-6} emu/g. This difference is larger than that between the Pd and V points in Paragraph 2, so that in this last case the agreement was probably fortuitous. If the effect 4 is not considered the error on the force measurement is about 0.01 to 0.02×10^{-6} emu/g in the highest field used. The absolute error mentioned under 4 will depend on the weight and the susceptibility of the specimen, but as the sample of the Mn solution mentioned had a mass and a susceptibility close to those of the other specimens this error can for the present work be estimated at 0.02 to 0.03×10^{-6} emu/g.

§ 3a. Temperature measurement

Up to 20°K the temperature is measured with the carbon resistance thermometer, above 20°K with the Au-2% Co versus normal silver thermocouple. As has already been mentioned the carbon-resistor is soldered to the copper cap and the thermocouple joint to the tube above the joint of the cap (see Figure 7). The heat link between the cap and the specimen is helium gas at 1 mm so that at a constant temperature the temperature-difference will be negligible. When the apparatus is warming up however, this difference becomes noticeable and is the main error on the measurement. The carbon-resistor was calibrated against vapour pressure of helium gas in equilibrium with the liquid at six temperatures. The resistance-temperature relation was assumed to be of the form

$\log R + \frac{A}{\log R} = B + \frac{C}{T}$ (3) where R is the resistance and A, B and C constants. The values of A, B and C giving the best fit to the experimental points were determined and the relation (3) with these

values was used as calibration. The thermocouple was used with liquid oxygen as a reference temperature bath. The thermoelectric voltage was measured with the variable junction at 4.2°K and at room temperature. The difference between these values and those reported by others [102] was 0.04 and 0.19 mV respectively. The change in the thermoelectric voltage with temperature for this thermocouple is about 0.03 mV per degree K below 30°K and 0.04 $mV/^{o}K$ above 50°K. Because of the difference in temperature between the specimen and the thermocouple it is meaningless to measure the temperature more accurately than to 0.5°K above 20°K, so that it is justified to use as a calibration the values given in the tables mentioned above to which a correction is added, this correction being the linear interpolation with respect to temperature of the difference between the tabulated values and those measured here.

§ 3b. Accuracy of the temperature measurement.

As a check on the accuracy the force on a few mg of Manganous Ammonium Sulphate ($Mn(NH_4)_2(SO_4)_2 . 6H_2O, \chi = \frac{11.0}{T} \times 10^{-3}$ emu/g) was measured from 4.2 to 7.7°K. The results between 4.2 and 14°K were not reliable as the susceptibility varies strongly with temperature in this interval and the force on the specimen changed noticeably within the time needed for a measurement. The results from 14 to 77°K are given in Appendix D. The fact that the apparatus warms up fairly rapidly from 14 to 20°K explains the larger error in this region than at the higher temperature where it is of the order of 1°K. At temperatures below 4.2° the error is small (0.02°K), if the balance warms up slowly from 2°K with the copper cap well immersed in liquid

helium. If however only a small amount of helium is left, the temperature will rise more rapidly and larger errors are likely. The results in Chapter V show that the errors in the interval from 4 to 14°K can be as large as 3°K. All in all the error in the temperature measurement is normally less than 0.05°K below 4.2°K, large (1 to 3°K) between 4 and 14°K and of the order of one degree K at higher temperatures.

CHAPTER V

DILUTE SOLUTIONS OF A TRANSITION METAL IN BINARY Cu-Zn ALLOYS.

Section I. Results

Introduction

The magnetic susceptibility of the Cu-Zn based ternary alloys mentioned in Chapter IV was measured at 1.8°, 4.2°, 77° and 290°K in fields of 2800, 4500, 6500 and 8000 Oe at constant temperature and at intermediate temperatures while the apparatus was warming up, in a field of 8000 Oe.

The accuracy of the measurements was discussed in Chapter IV, Sec.II, 2b. The relative error in the susceptibility measurements for one specimen is 0.01to 0.02 x 10^{-6} emu/g and the error in the actual values up to 0.04 x 10^{-6} emu/g The error in temperature (Chapter IV, Sec.II, 3b) is about 1°K above 20°K and varies with temperature at lower temperatures.

In addition to errors in the measurements, errors in the interpretation will arise if the metallurgical state of the alloy is not as was intended. Possible differences between actual and ideal state of a sample which can have an effect on the susceptibility are:

1. A well dissolved impurity, the atoms of which carry a magnetic moment (Fe most likely). This will give rise to an additional term in the susceptibility, which follows a Curie-Weiss law and can not be separated from the obtained results if the impurity content is not known.

2. The presence of ferromagnetic particles, consisting of atoms of the intended or a different impurity. These particles, if saturated domains can cause an additional temperature-independent magnetization σ of the sample. If the total magnetization of the sample can be written as $M=\chi H+\sigma$, where χ is the susceptibility of the alloy, the apparent susceptibility measured with the balance used here will be $\chi_{app} = \chi + \frac{\sigma}{2H}$ (1). If this is the case it can be verified with the help of a Honda-Owen plot, i.e. a plot of χ_{app} at a given temperature versus $\frac{1}{H}$. If it is found that the relation (1) holds at several temperatures, including 300°K, that χ is temperature-independent and that the first term in (1) is large compared to the second, it will in general be justified to assume the presence of undissolved ferromagnetic particles and to find the true value χ from a plot as mentioned. Further the possibility must not be excluded that as a result of the presence of these particles, a torque will act on the sample in a magnetic field, which will in the balance used here, cause a rotation of the spiral and thus be a source of error on the force measurement. No conclusive evidence of this effect has however been found.

3. Superparamagnetic particles. These are large clusters of transition metal atoms which have a large moment and can behave in a manner analogous to the Curie-Weiss paramagnetism for atomic moments. If the magnetic properties of these particles are not isotropic, the susceptibility of this type of system will deviate from a Curie-Weiss law and be a complicated function of temperature. No typical behaviour for these systems can be given which makes it possible to recognise

easily a superparamagnetic contribution to the susceptibility.

4. The Cu-Zn ratio of a ternary Cu-Zn - X alloy where X is a transition metal, can be different from the intended value. If the ternary alloy is made by melting together pieces of the binary solvent and the impurity X, this error can be expected to be equal for the binary solvent and the ternary solution. The difference of the susceptibility of the two alloys should then give the correct change due to the introduction of the third component. If however, as is done in this work, the alloys are prepared from the elements and a Cu-X master alloy, the deviation in the Cu-Zn ratio from the intended value for the ternary alloy will be independent from that for the corresponding binary alloy, i.e. the alloy with the same nominal Cu-Zn ratio. If the susceptibility of the matrix varies strongly with composition, as is the case for Cu-Zn γ phase alloys, the difference in susceptibility between the ternary and the corresponding binary alloy is then not necessarily entirely due to the presence of the transition metal.

In this section the experimental results for the magnetic susceptibility of the Cu-Zn based ternary alloys mentioned above will be given. Graphs are presented of the susceptibility in a field of 8000 Oe as a function of temperature. Where it was found that the apparent susceptibility was field-dependent at a given temperature the observed values in different fields are quoted and either a plot of χ vs $\frac{I}{H}$ or of χH vs H is given. The compositions of the alloys are in atomic per cent, the number corresponds to that in Appendix A.

χ as given is the mass susceptibility in electromagnetic units, emu/g. To convert this into MKS units the values quoted here

have to be multiplied by $4\pi \times 10^{-3}$.

§ 1. Pure Zn and binary Cu-Zn ε phase alloys.

Measured were a pure Zn specimen and two binary Cu-Zn ε phase alloys with composition near the Cu and Zn-rich ends of the phase. The results are shown below. Also included is the average susceptibility $\bar{\chi} = \frac{2}{3}\chi_{\perp} + \frac{1}{3}\chi_{\parallel}$ derived from the measurements of Marcus.[103] χ is the susceptibility of a single crystal measured with the field perpendicular to the hexagonal axis, χ that measured with the field parallel to this axis.

T	pure Zn	Pure Zn	ε phase	ε phase
°K	No. (1)	Marcus	15.4% Cu	19.4% Cu
	this work		(No.4)	(No. 8)
295	-0.11	-0.14	-0.26	-0.27
77	-0.14	-0.16	-0.28	-0.32
4.2	-0.08	-0.16 (14°K)	-0.31	-0.28
1.7	-	-	-0.30	-

§ 2. Zn-Fe

Two Zn-0.1% Fe specimens were measured because it was concluded from the results for the first alloy that no Fe had dissolved (See Chapter IV, Sec.I,4).

The results were:

T	$\chi \times 10^6$ emu/g	
°K	Zn-Fe I (No. 2)	Zn-Fe II (No. 3)
295	-0.17	-0.12
77	-0.14	-0.15
4.2	-0.14	-0.12

§ 3. Solutions of Fe in ε phase Cu-Zn

εphase (Zn-rich) with 0.1% Fe.

Composition 84.5%Zn - 15.4% Cu-0.1% Fe (No.6).

T	χ x 10^6	H
°K	emu/g	Oe
295	-0.33	
77	-0.36	
4.2	-0.35	
1.7	-0.20 ± 0.07	2800
	-0.27 ± 0.03	4560
	-0.29 ± 0.02	6560
	-0.33 ± 0.01	8025

Because of the small variation with temperature no points were taken at intermediate temperatures.

ε phase (Cu-rich) with 0.1% Fe

Composition 80.5% Zn - 19.4% Cu - 0.1% Fe (No. 11)

T	χ x 10^6
°K	emu/g
295	-0.22[5]
80	-0.18
4.2	+0.67
1.8	+1.36

The points taken between 1.8 and 77°K at 8000 Oe are shown in Figure 1.

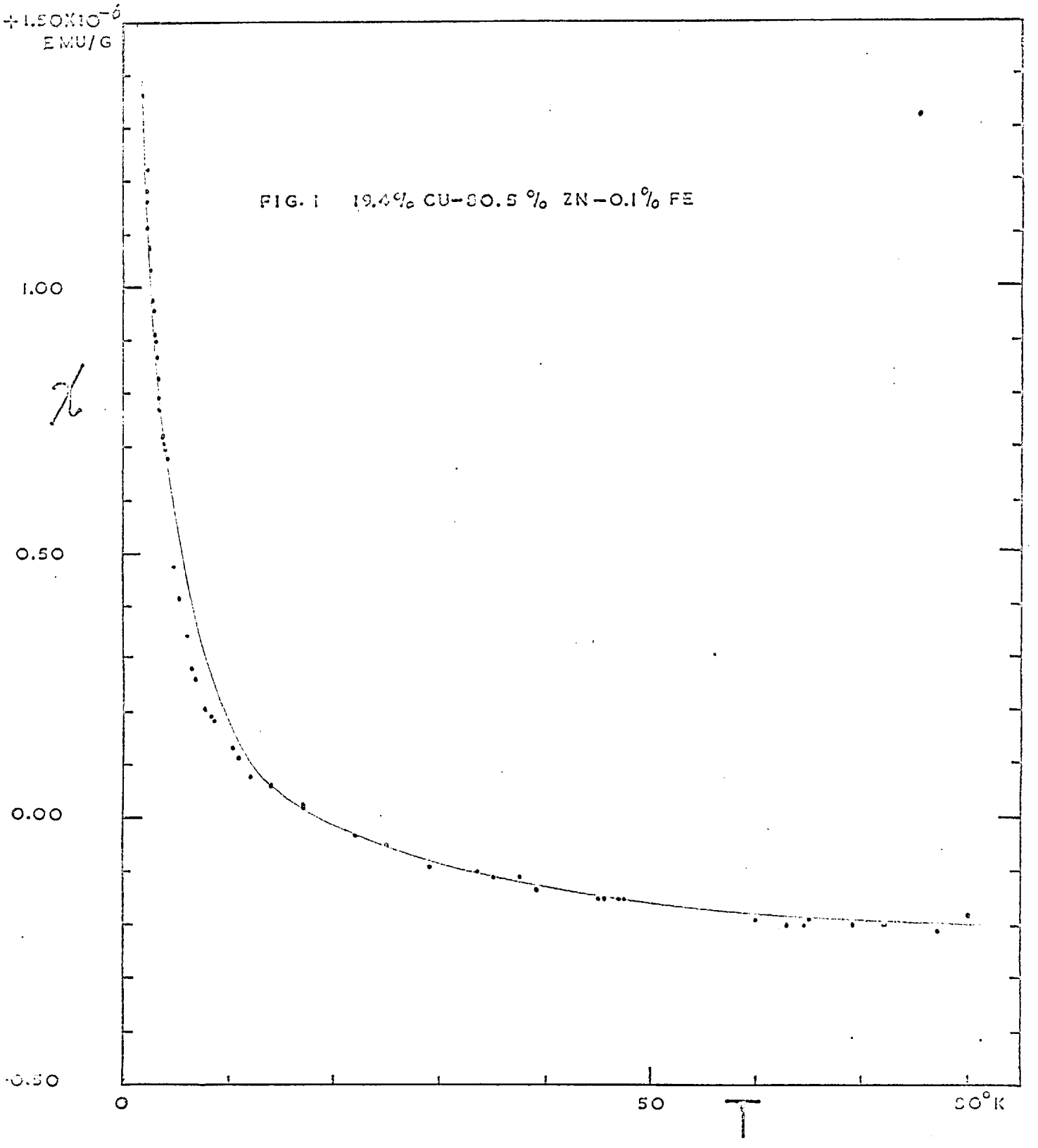

FIG. 1 19.4% CU-80.5 % ZN-0.1% FE

§ 4 Solutions of Mn in ε phase Cu-Zn.

ε phase (Zn rich) with 0.15% Mn

Composition 84.5% Zn - 15.4% Cu - 0.15% Mn (No. 5.)

T	$\chi \times 10^6$	H
^oK	emu/g	Oe
295	-0.15	
77	+0.26	
4.2	+10.40	2800
	+ 8.90	4550
	+ 7.66	6460
	+ 6.91	8025
1.70	+ 20.67	2800
	+ 18.13	4550
	+ 15.77	6560
	+ 14.24	8070

Points between 1.7^oK and room temperature were taken in a field of 8000 Oe. The apparent susceptibility in this field as a function of temperature and the magnetization of the sample as a function of field at 1.7^o and 4.2^oK are given in Figure 2a and 2b.

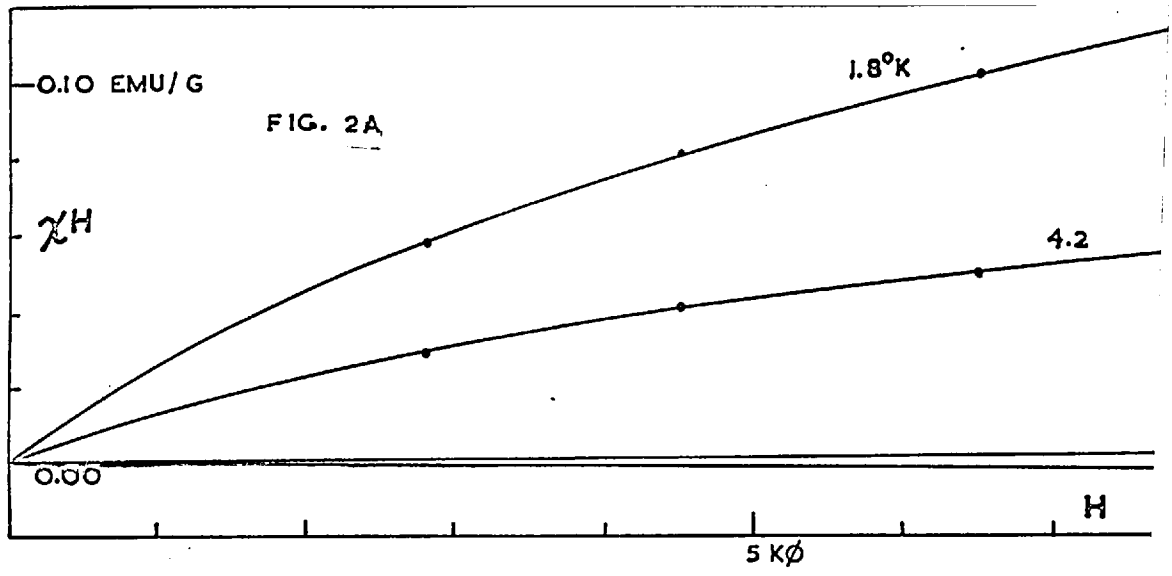

FIG. 2A

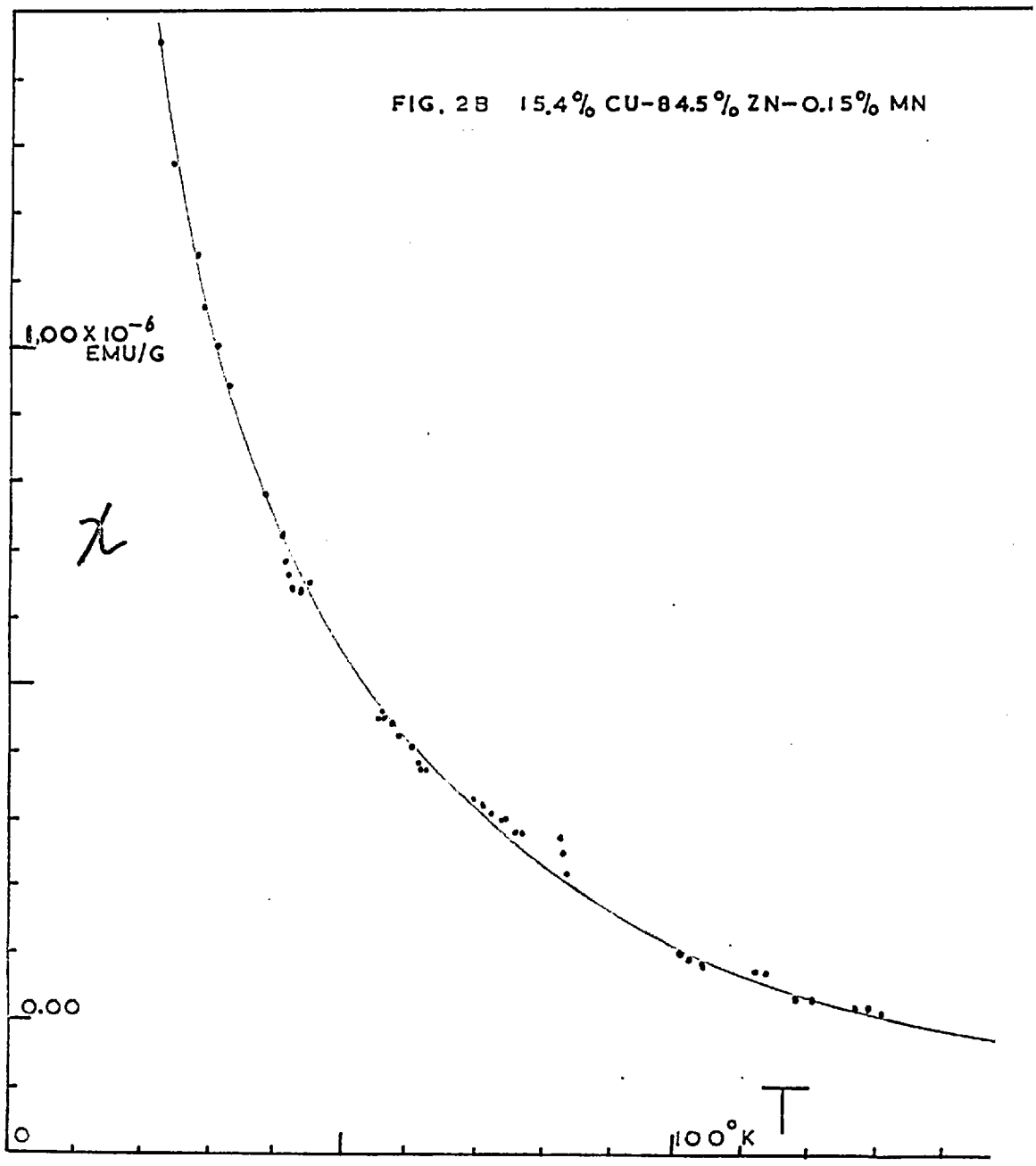

FIG. 2B 15.4% CU-84.5% ZN-0.15% MN

ε phase (Cu-rich) with 0.1% Mn

Composition 80.6% Zn-19.3% Cu - 0.1% Mn (No. 10).

T	$\chi \times 10^6$	H
°K	emu/g	Oe
295	-0.19	
77	-0.05	
4.2	+2.43	2800
	+2.43	4470
	+2.36	
	+2.28	
1.79	+5.49	6440
	+5.17	7960
1.50	+6.32	2790

The susceptibility in a field of 8000 Oe as function of temperature is given in Figure 3.

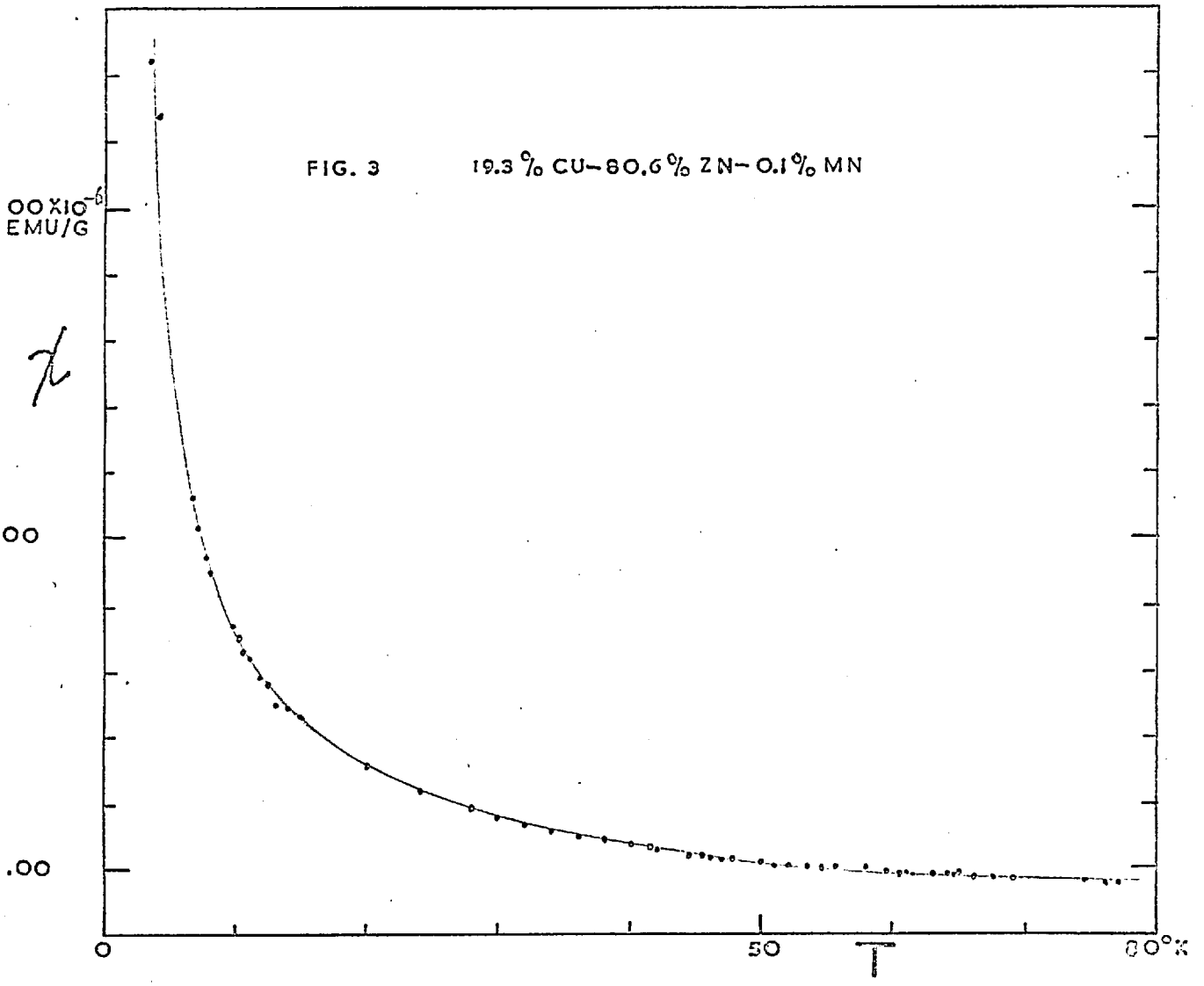

FIG. 3 19.3 % CU–80.6 % ZN–0.1 % MN

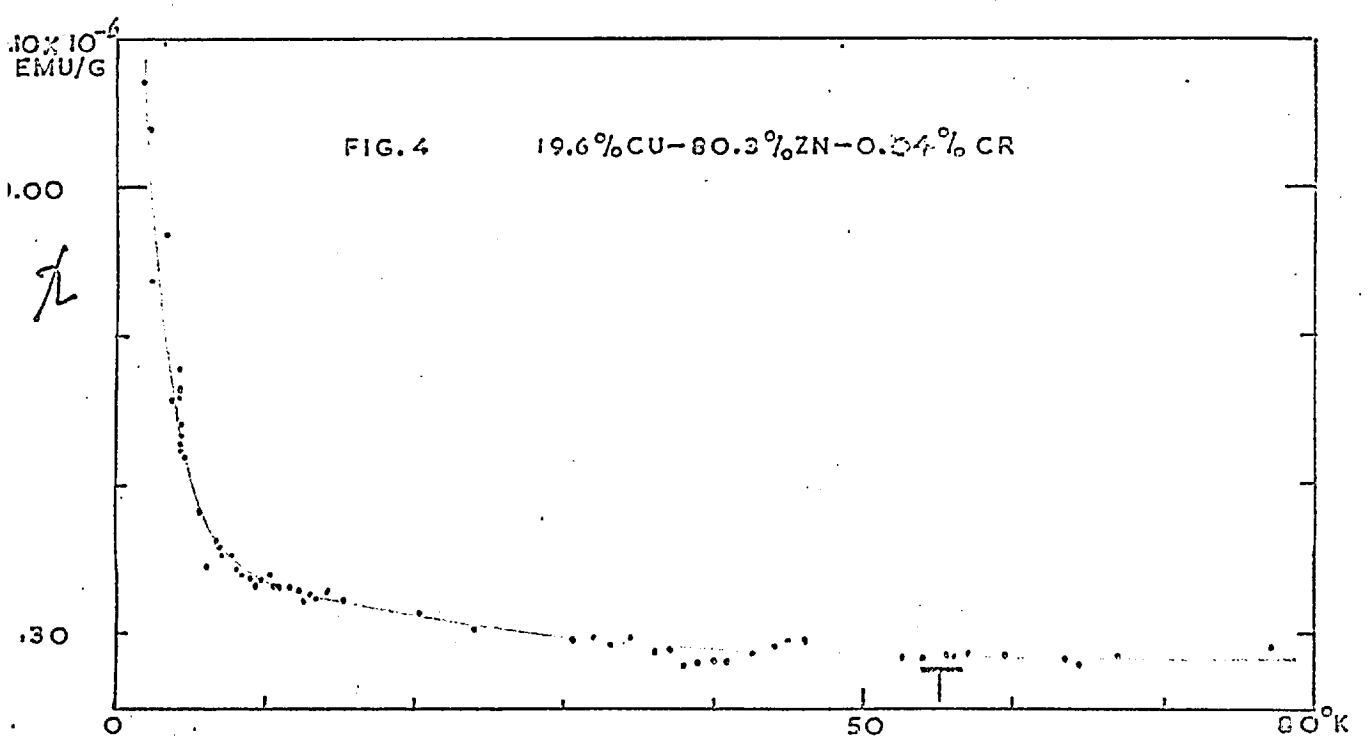

FIG. 4 19.6 % CU–80.3 % ZN–0.04 % CR

§ 5. Solutions of Co in ε phase Cu - Zn

ε phase (Zn-rich) with 0.1% Co.

Composition 8 0.5% Zn - 15.4% Cu - 0.1% Co (No. 7.)

T	$\chi \times 10^6$	H
°K	emu/g	Oe
295	-0.21	
77	-0.20	
4.2	-0.03	2820
	-0.15	4500
	-0.22	6500
	-0.25	8050
1.7	+0.21	2800
	-0.03	4480
	-0.10	6560
	-0.16	8060

ε phase (Cu-rich) with 0.1% Co.

Composition 8 0.7% Zn - 19.2% Cu - 0.1% Co. (No. 12)

T	$\chi \times 10^6$
°K	emu/g
295	-0.28
77	-0.30
4.2	-0.32
1.6	-0.24 at H = 8000 Oe, no readings at other fields

were taken because the apparatus started warming up after this point.

§§ 6. ε phase (Cu-rich) -0.04% Cr.

Composition 8 0.3% Zn - 19.6% Cu - 0.04 Cr (No. 9)

T	$\chi \times 10^6$	H
295	-0.32	Oe
	-0.31	
4.2	-0.04	3350
	-0.10	4460
	-0.10	6440
	-0.12	8000
1.8	+0.14	4450
	+0.10	6420
	+0.07	8000

The change with field at 4.2°K is within the normal error, that at 1.8° is however significant. Points taken in a field of 8000 Oe at temperatures between 1.8° and 77°K are shown in Figure 4.

§ 7. Binary γ phase Cu - Zn

Composition intended 61.6% Zn - 38.4% Cu (No. 13)

T	$\chi \times 10^6$
°K	emu/g
295	-0.39
77	-0.34
4.2	-0.29
1.8	-0,27

The chemical analysis on this alloy showed the presence of a large amount of Fe (0.18 wt%). This is more than the intended Fe content of the specimens discussed in Chapter IV, A7. The variation

of χ with temperature is only slight here, in contrast with the other results. Because of this inconsistency the results on the intended binary Cu - Zn alloy will not be used.

§ 8. χ phase with Mn

Composition 60.4% Zn-39.6% Cu - 0.04% Mn (No. 15).

T	$\chi \times 10^6$	H
^oK	emu/g	Oe
295	-0.39	
77	-0.38	
4.2	-0.19	
1.76	+0.15	2800
	+0.13	4560
	+0.07	6560
	+0.05	8080

The susceptibility in a field of 8000 Oe at temperature between 1.8 and 4.2^oK is shown in Figure 5.

During this run no points between 4.2^o and 53^oK could be taken. From the results obtained it seemed desirable to check this alloy also at these remperatures. The sample was again put into the balance, the second time the results were

T	$\chi \times 10^6$
^oK	emu/g
295	-0.36
77	-0.36
4.2	-0.14

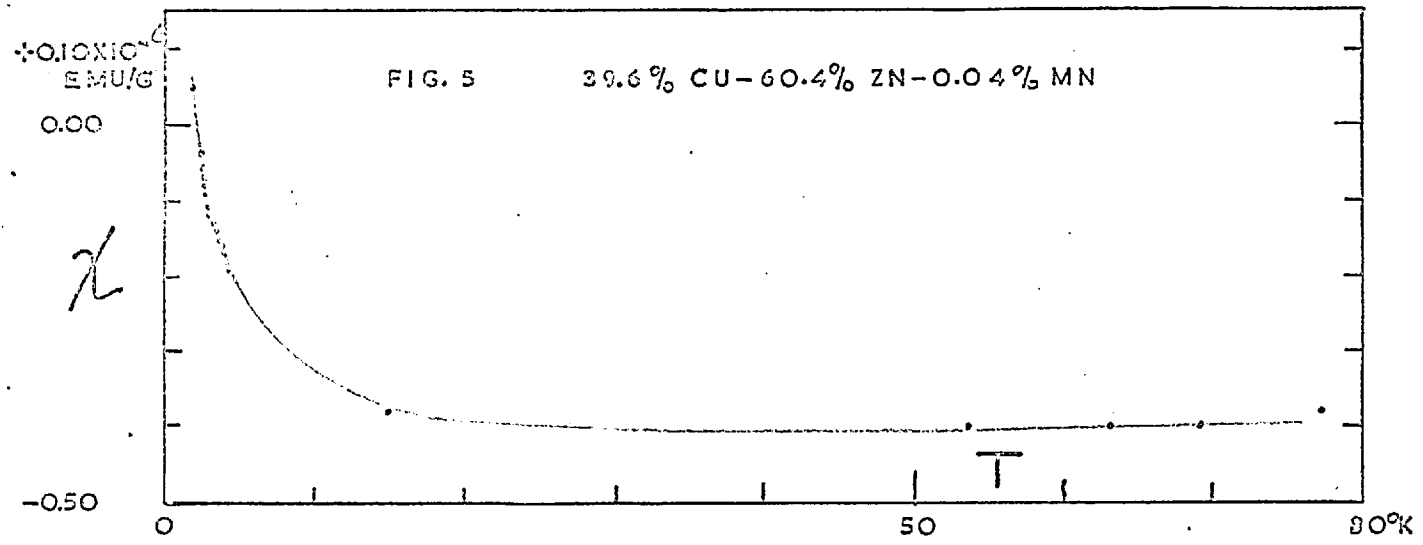

FIG. 5 39.6% CU – 60.4% ZN – 0.04% MN

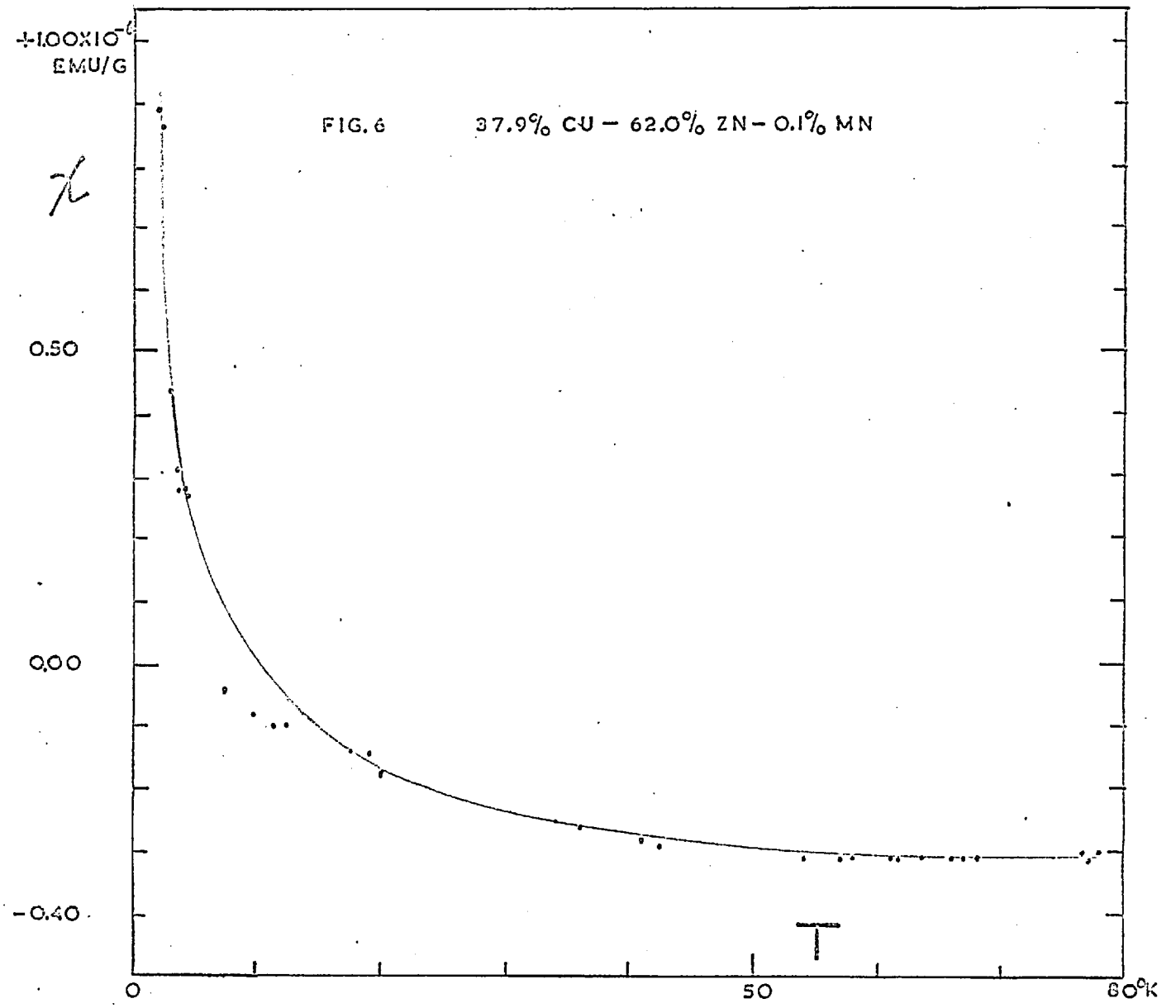

FIG. 6 37.9% CU – 62.0% ZN – 0.1% MN

The zero drift (Chapter IV, Ssc.II, 2b) during the warming up from 4.2 to 77°K was extremely large and the points are not accurate. The general shape of the curve χ vs T is however similar to that for the other solutions of Mn in γ brass. These points will not be used in the analysis of the results.

These results also show the error in the measurements due to the variation of the specimen position from run to run.

γ phase (middle of the phase) with 0.1% Mn

Composition 62.0% Zn - 37.9% Cu - 0.09% Mn (No. 16)

T	$\chi \times 10^6$	H
°K	emu/g	Oe
295	-0.32	
77	-0.31	
4.2	+0.33	4400
	+0.31	6350
	+0.29	8000
1.8	+0.92	2800
	+1.02	4400
	+0.94	6340
	+0.89	8025

Points were taken for H = 8000 Oe between 1.8° and 77°K. The curve χ vs T is given in Figure 6. During this run the carbon-resistance thermometer circuit went out of order. All temperatures above 15°K have therefore been measured with the thermocouple, which is not accurate below 20°K.

Υ phase (Zn-rich) with 0.1% Mn

Composition 64.7% Zn - 35.2% Cu - 0.09% Mn (No. 17)

T	$\chi \times 10^6$	H
^oK	emu/g	Oe
295	-0.42	
77	-0.42	
4.2	-0.24	
1.8^oK	+0.10	2800
	+0.04	4550
	0.00	6560
	-0.03	8080

The susceptibility in a field of 8000 Oe at temperatures between 1.8 and 77^oK is shown in Figure 7.

§§ 9. Υ phase with 0.1% Co.

Composition 61.4% Zn - 38.5% Cu - 0.10% Co (No. 18.)

T	$\chi \times 10^6$	H
^oK	emu/g	Oe
295	-0.22	
77	-0.18	
4.2	+0.35	
1.78	+1.14	2800
	+1.09	4550
	+1.01	6460
	+0.96	8020

The curve χ vs T for H = 8000 Oe is given in Figure 8.

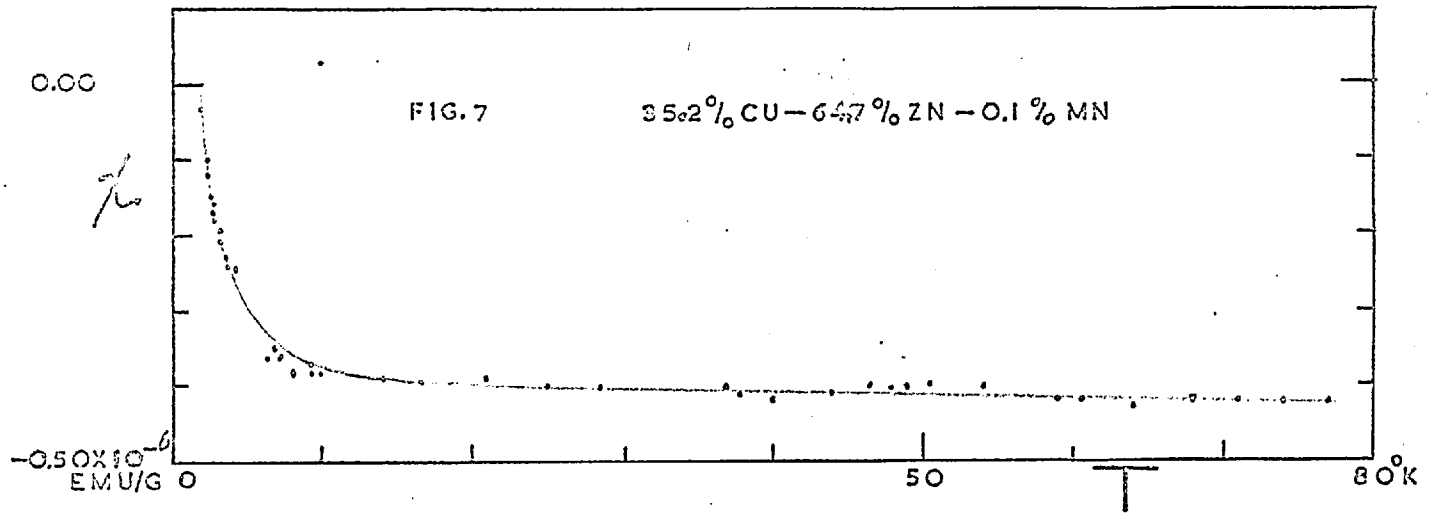

FIG. 7 35.2% CU—64.7% ZN—0.1 % MN

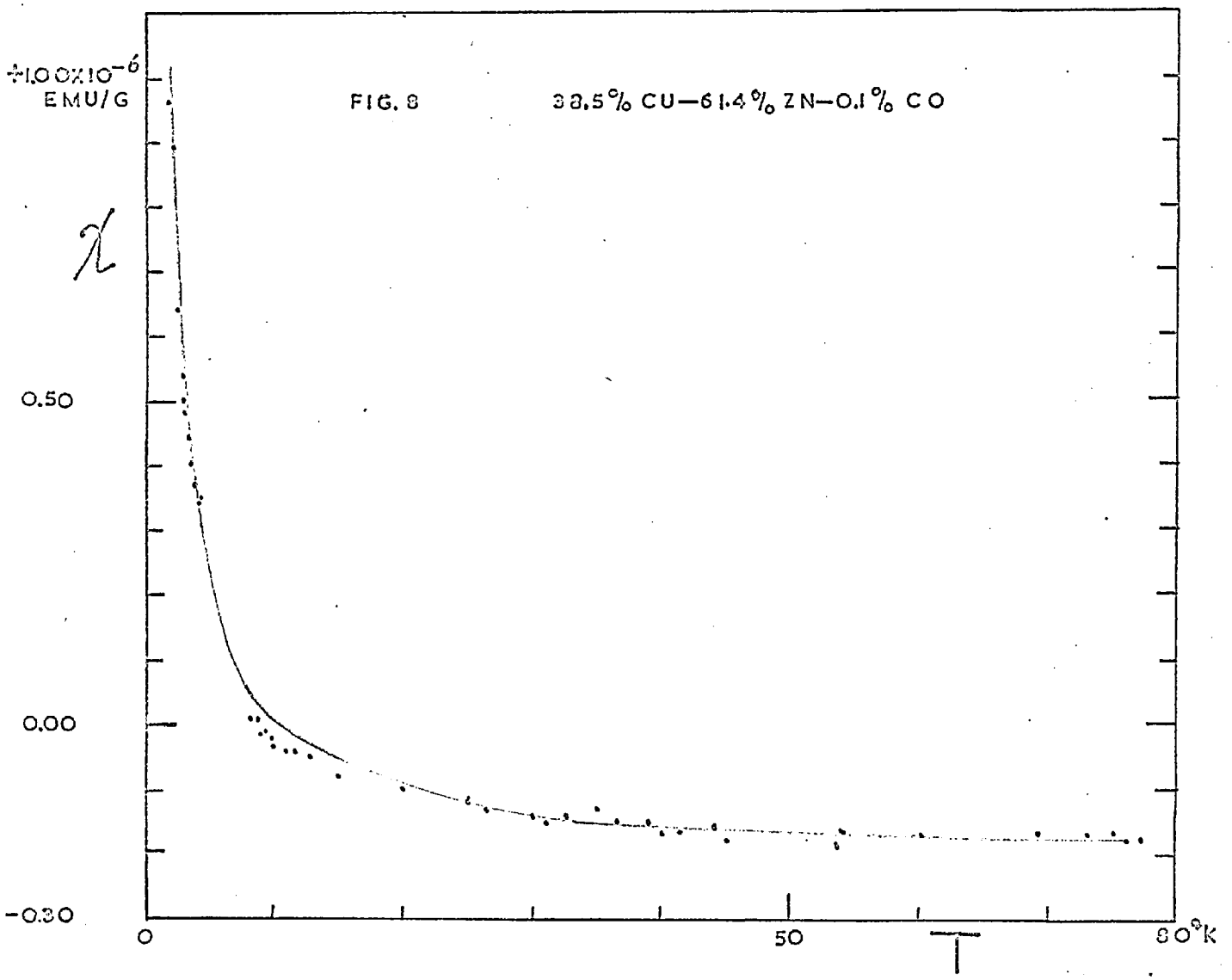

FIG. 8 38.5% CU—61.4% ZN—0.1 % CO

§ 10. γ phase with 0.1% Cr.

Composition 60.8% Zn - 39.1% Cu - 0.09% Cr (No.14)

T	χ x 10^6	H
^oK	emu/g	Oe
295	-0.31	
77	-0.27	
4.2	-0.35	
1.68	+1.24	2900
	+1.26	4550
	+1.16	6500
	+1.09	8050

The curve χ vs T for H = 8000 Oe is given in Figure 9.

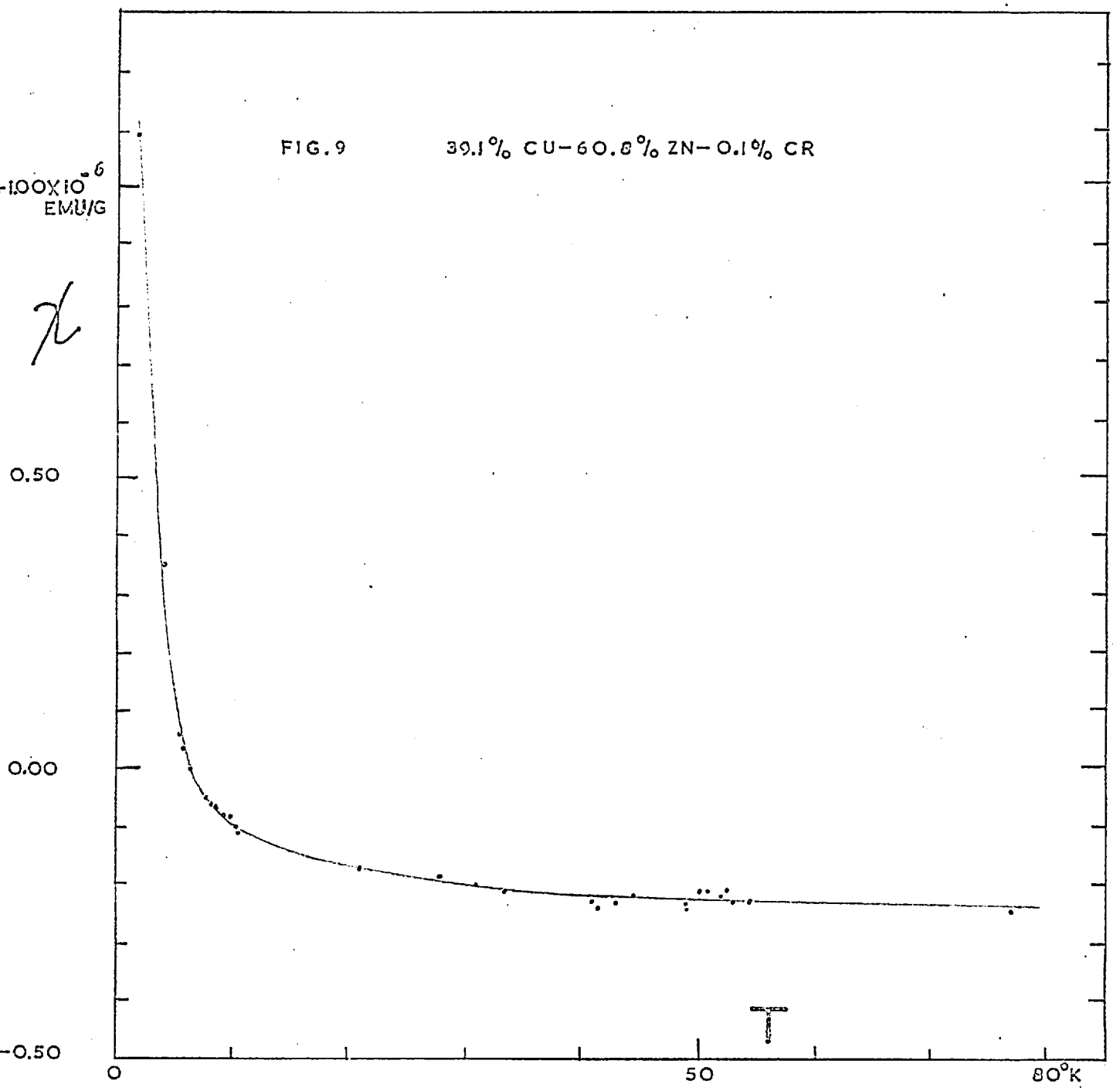
FIG. 9
39.1% CU-60.8% ZN-0.1% CR
-1.00X10^-6 EMU/G
χ
0.50
0.00
-0.50
0
50
80°K
T

Section II. Discussion

Introduction.

For the interpretation of experimental susceptibility data for dilute solutions of a transition metal two lines of approach are possible. One possibility is to assume that the d-electrons, responsible for a paramagnetic term in the susceptibility, are in bound or virtual bound states localised near a lattice site, the alternative is to assume a collective band model for the alloy. As discussed in Chapter I, for an alloy of two transition metals the band model can be applicable, while for solutions in a noble metal and thus also for the alloys discussed here the first model is a better approximation. The susceptibility can then be written as

$$\chi = \chi_o + \frac{N\mu_{eff}^2}{3k(T-\theta)} \qquad (2)$$

The second term in (2) is the paramagnetic susceptibility of the system of moments on the solute atoms as discussed in Chapter II. The first term χ_o is a temperature-independent term representing the diamagnetism and Pauli-paramagnetism of the conduction electrons and the Van Vleck term due to the transition metal (see Chapter II). For this χ_o is usually taken the susceptibility of the solvent, χ_m. This is correct if the Van Vleck paramagnetism is negligible and the introduction of the solute in the host lattice does not perturb the conduction electrons system to such an extent that the diamagnetism and Pauli-paramagnetism are modified. If a plot of $\frac{1}{\chi - \chi_m}$ vs T is found to be linear, μ_{eff} and θ can be determined easily. There is however no reason to assume a priori that the presence of the impurity will not affect the

susceptibility of the electron gas or that the temperature-independent Van Vleck paramagnetism will always be negligible.

It is thus possible that the susceptibility of an alloy follows equ. (2) with $\chi_o \neq \chi_m$ and it can in cases be more justified to take for χ_o a value such that a plot of $\frac{1}{\chi - \chi_o}$ vs T is linear, i.e. to fit the experimental points to (2) by varying χ_o. The difference between χ_o and χ_m will then have to be explained. The effect of varying χ_o on a plot as mentioned is shown in Figure 10. In the molecular field theory θ (equ.2) is related to the interactions between atomic moments. In the alloys considered in this work, which contain 0.1 at % of solute, these interactions are not likely to be strong so that θ is expected to be small.

In the following paragraphs the results for the hexagonal η and ε phase alloys will be discussed. In paragraph 1 an explanation of the variation of the susceptibility of the solvents with temperature will be given and in paragraph 2 a discussion of the Zn-Fe alloys, which will be compared with results obtained by others for Zn - based solutions. In paragraph 3 the derivation of the effective atomic moment and the Curie-Weiss constant for the ternary ε -phase alloys will be discussed. In paragraph 4 a tentative explanation of these results will be given. In paragraph 5 the effective atomic moment will be derived for the solutions of a transition metal in γ-phase Cu-Zn and in paragraph 6 these results will be discussed.

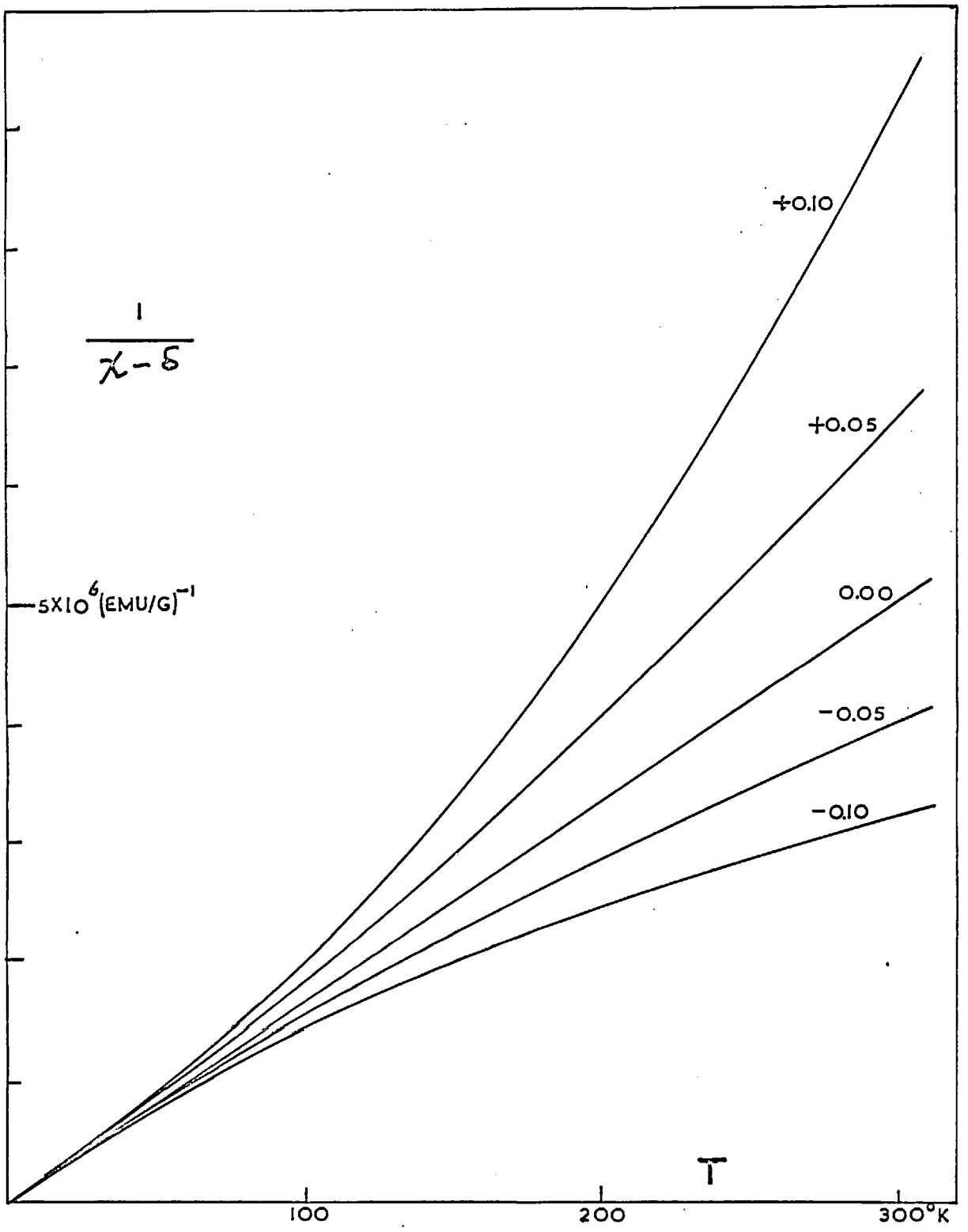

FIG. 10. χ is the susceptibility of an alloy of average atomic weight 60 in which 0.1 % of the atoms carry a moment of $5\mu_B$ and the remaining atoms none. Values of $\delta \times 10^6$ are indicated on the curves.

§ 1. Pure Zn and binary Cu - Zn ε phase alloys.

The observed variation of the susceptibility of these alloys is not consistent with the model of a temperature-independent diamagnetism and superimposed on this a paramagnetic impurity contribution. An explanation can be found from a consideration of measurements by Marcus [103] on a Zn single crystal which are shown in Figure 11.

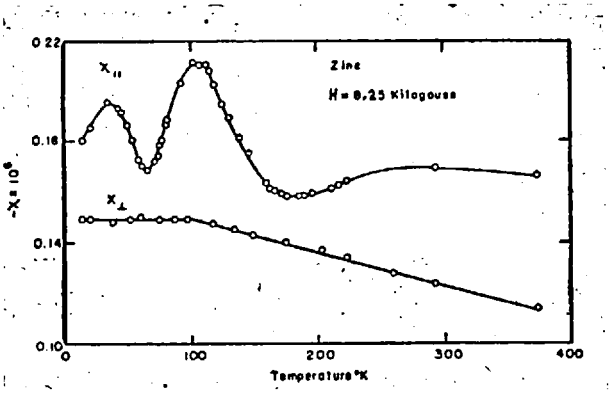

FIG.11 The susceptibility of a Zn single crystal. After ref. 103.

The difference between the maximum and minimum value of the susceptibility, measured with the field parallel to the hexagonal axis of the crystal, $\chi_{\parallel}$, is 0.07×10^{-6} emu/g. The decrease of the susceptibility with field parallel to this axis, $\chi_{\perp}$, between 77 and 300°K is 0.03×10^{-6} emu/g. For a polycrystalline specimen the average susceptibility $\overline{\chi} = \frac{2}{3}\chi_{\perp} + \frac{1}{3}\chi_{\parallel}$ will be measured. If impurities or strains in the crystal cause a shift of the extrema in $\chi_{\parallel}$ the value of $\overline{\chi}$ at a given temperature will change as well. On this basis a difference of 0.03×10^{-6} emu/g between the values for one specimen at different temperatures or between the values for different specimens at a given temperature is not surprising if polycrystalline specimens are used.

For the ε phase alloys which also have a hexagonal close packed structure no data on single crystals are available but the results might well be explained in the same way. The only point of which the deviation seems too large for this explanation is the value found for the pure Zn at 4.2°K, -0.08×10^{-6} emu/g. Because contamination by transition metals other than Fe is unlikely and Fe does not carry a moment in Zn (see paragraph 2) the observed deviation must be due to a different Zn-Fe phase or to undissolved Fe.

§ 2. Zn - Fe

If the explanation of the susceptibility results for pure Zn given in paragraph 1 is correct, this argument also applies to the results for the Zn-Fe alloys. It follows then firstly that the Fe is well dissolved in the matrix because the presence of Fe in some form is shown by chemical analysis and large clusters of Fe atoms or regions of a different Fe-rich phase would have caused an appreciable magnetization in a magnetic field. Secondly it follows that an Fe atom in solution in Zn does not carry a magnetic moment. This is consistent with the results of specific heat measurements by De Nobel and Du Chatenier [51] who found for a Zn-Fe alloy no deviation from the values for pure Zn. Further available experimental information about this system is that the presence of Fe in Zn causes a depression of the superconducting transition temperature T_c. This change is -10.5°K per at % Fe.

If the theoretical model given by Anderson [16] is valid the absence of a moment can be due to a high density of states of the conduction band at the Fermi level, which causes a strong broadening in

energy of the 3-d levels associated with an Fe atom. It is therefore of interest to consider the electronic specific heat γ of pure Zn. Measurements by Daunt and Silvidi [104] give a value for $\gamma = 1.5 \times 10^{-4} \frac{\text{cal}}{\text{mole deg}^2}$, leading for a free-electron model to a density of states of 0.13 states per atom per eV, which is not very high. Also if the absence of a moment in Zn-Fe is ascribed to a high density of Bloch states in the solvent a small moment is expected in a dilute solution of Mn in Zn as well. Collings and Hedgcock found however that Mn dissolves in Zn with a large moment ($4.8 \mu_B$). Further a specific heat anomaly for dilute Zn - Mn alloys has been reported by De Nobel and Du Chatenier.[51] The depression of T_c which has generally been found to be associated with the presence of atomic moments, is an order of magnitude larger in this system than in Zn - Fe and has a value of $-170^{\circ}K$ per at % Mn. Further an anomaly has been found in the specific heat of a Zn - Cr solution. This evidence rules out the possibility that the absence of a moment in Zn - 0.1% Fe is due to a property of the matrix only.

A different cause of a large width of the 3d-state on a transition-metal atom can be that the interactions of this state with the 4s conduction electron states are strong. Why the strength of these interactions should be an order of magnitude larger for an Fe atom than for a Mn atom in solution is not obvious.

The last parameters available are the exchange and Coulomb interaction within a solute atom. The hypothesis that these are not sufficient to cause a splitting of the 3d-state on an Fe atom dissolved in Zn can be rejected as Fe carries a moment in many other solvents.

§ 3. Ternary ε phase alloys. Interpretation of the results.

In this paragraph the experimental susceptibility curves given in Section 1 are fitted to equ (2) with N equal to the number of transition metal atoms per gram alloy as found from the results of the chemical analysis. A value of μ_{eff} is the effective moment on a solute transition metal atom in Bohr magnetons (0.927×10^{-20} erg/gauss).

ε phase (Zn-rich) with 0.1% Fe.

The difference between the values found at 4°, 77° and 295°K which is at most 0.03×10^{-6} emu/g can be ascribed to the mechanism discussed in paragraph 2. It then follows that above 4.2°K, Fe atoms dissolved in this matrix do not carry a moment. Further it must be noted that this alloy is more strongly diamagnetic than the solvent. This could be due to a systematic error (see Chapter IV) although the difference, 0.04×10^{-6} emu/g seems somewhat large for this explanation. Also the variation of with applied field at 1.7°K is small but just too large to be entirely due to experimental errors.

ε phase (Cu-rich) with 0.1% Fe.

In this alloy the susceptibility varies with temperature, the effect of the solute is a paramagnetic contribution. If the reciprocal of the difference of the measured susceptibility χ and that of the pure solvent χ_m is plotted versus temperature, this relation is not linear over the whole temperature range (Figure 12a). In this plot a straight line can be drawn through the points between 15° and 77°K which corresponds to $\mu_{eff} = 2.1\ \mu_B$, $\theta = 13°K$. That this value χ_m for the temperature-independent term might be wrong is shown by the fact that at 295°K the value of χ is 0.05×10^{-6} emu/g higher than χ_m. The

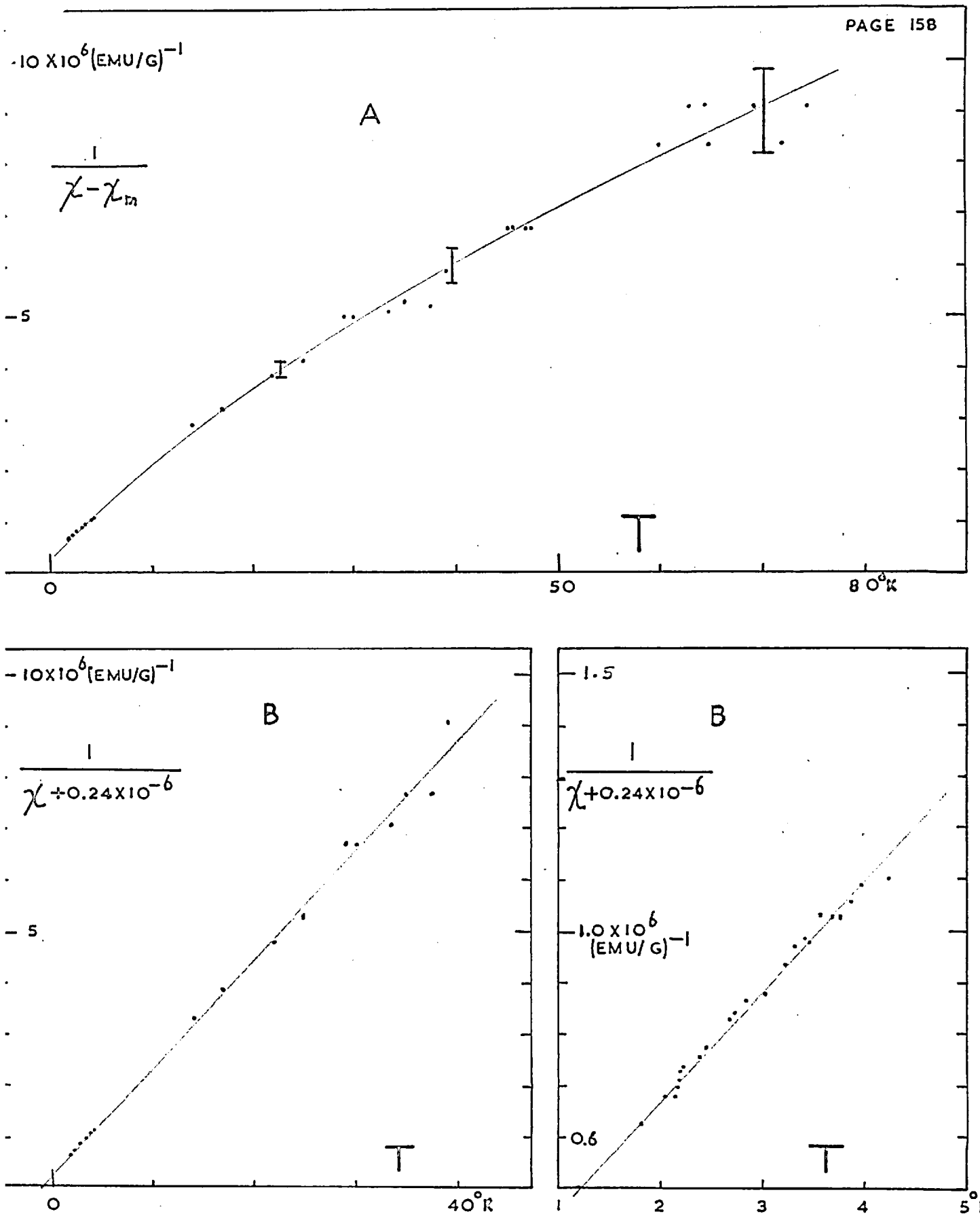

FIG.12. 19.4%Cu-80.5%Zn-0.1%Fe. The error bars correspond to a spread in susceptibility of 0.02×10^{-6} emu/g.

value of the paramagnetic term at 4.2°K is about 0.95×10^{-6}. If this term follows a Curie law ($\theta = o$) its value at 300°K will be $\frac{0.95}{75} \approx 0.1 \times 10^{-6}$. Observed was $\chi = -0.22^5 \times 10^{-6}$ at 295°K, so that the most likely value of the term χ_o in equ (2) is -0.24×10^{-6}. The quantity $\frac{1}{\chi - \chi_o}$ was plotted as a function of T for values of of -0.22, -0.24 and -0.25×10^{-6} emu/g. On all these graphs the points taken above 14°K join up reasonably well with those below 4.2°K, while those at temperatures in between deviate from this Curie-Weiss relation. This deviation is so large that it is impossible to obtain a curve through these points and those below 4.2°K by varying χ_o within reasonable limits. It was also found that during this run the temperature of the carbon-resistance thermometer and that of the thermocouple were about 3°K different below 20°K which is more than normal. This suggests that from 4.2°K the apparatus warmed up fast and that the deviation of the points between 4.2 and 14°K is due to a difference in temperature between the carbon-resistor and the specimen.

If the points between 5° and 14°K are not considered the best fit to a Curie-Weiss law is obtained from a plot of $\frac{1}{\chi - \chi_o}$ vs T with $\chi_o = -0.24 \times 10^{-6}$ emu/g (Figure 12b). Allowance might have to be made for a variation of χ_o with temperature. It is however not possible to decide independently from this data how this variation will be.

The plot in Figure 12b gives $\mu_{eff} = 1.5\mu_B$, $\theta = -1.2$°K.

ε phase (Zn-rich) with 0.15% Mn

Also here a plot of $\frac{1}{\chi - \chi_m}$ vs T does not follow a Curie-Weiss law over the whole temperature-range measured (Figure 13a) and it is

not justified to derive values of μ_{eff} and θ from this curve. The solution of Fe in the same solvent has a temperature-independent susceptibility which is in absolute value larger than χ_m, so that it is justified to investigage the possibility of values $\chi \neq \chi_m$. For $\chi_o = -0.34 \times 10^{-6}$ a good fit to equ (2) could be obtained for the points between 14 and 250°k (Figure 13b). The slope of the curve $\frac{1}{\chi - \chi_o}$ vs T with χ_o as above is 2.03×10^4 emu units. Above 250°K the points in Figure 13b show a deviation from the Curie-Weiss law, a value of χ_o smaller in absolute value would give a better fit here. This is consistent with the results for the pure solvent and the solution of Fe in this solvent. Because the value of χ_o used is close to the value of χ for this last alloy, these values were also substituted for χ_o, leading to a good fit on the whole temperature range from 14 to 295°K. The slope of the curve $\frac{1}{\chi - \chi_o}$ vs T is in this case 1.96×10^4 emu units. If this analysis is correct, the term representing the diamagnetism and Pauli-paramagnetism in this alloy and the solution of Fe in the same matrix are equal and 0.04×10^{-6} emu/g larger in absolute value than the susceptibility of the solvent. This difference could be the result of errors although the value is somewhat large.

The Curie-Weiss curve as drawn in Figure 13b corresponds to $\mu_{eff} = 4.1\mu_B$ and $\theta = -6$°K, which indicates antiferromagnetic interactions. The points at temperatures below 14°K deviate from the Curie-Weiss law. This is consistent with the fact that the susceptibility is field-dependent at 1.8 and 4.2°K. That the points below 14°K lie below the Curie-Weiss curve drawn suggests a ferromagnetic interaction.

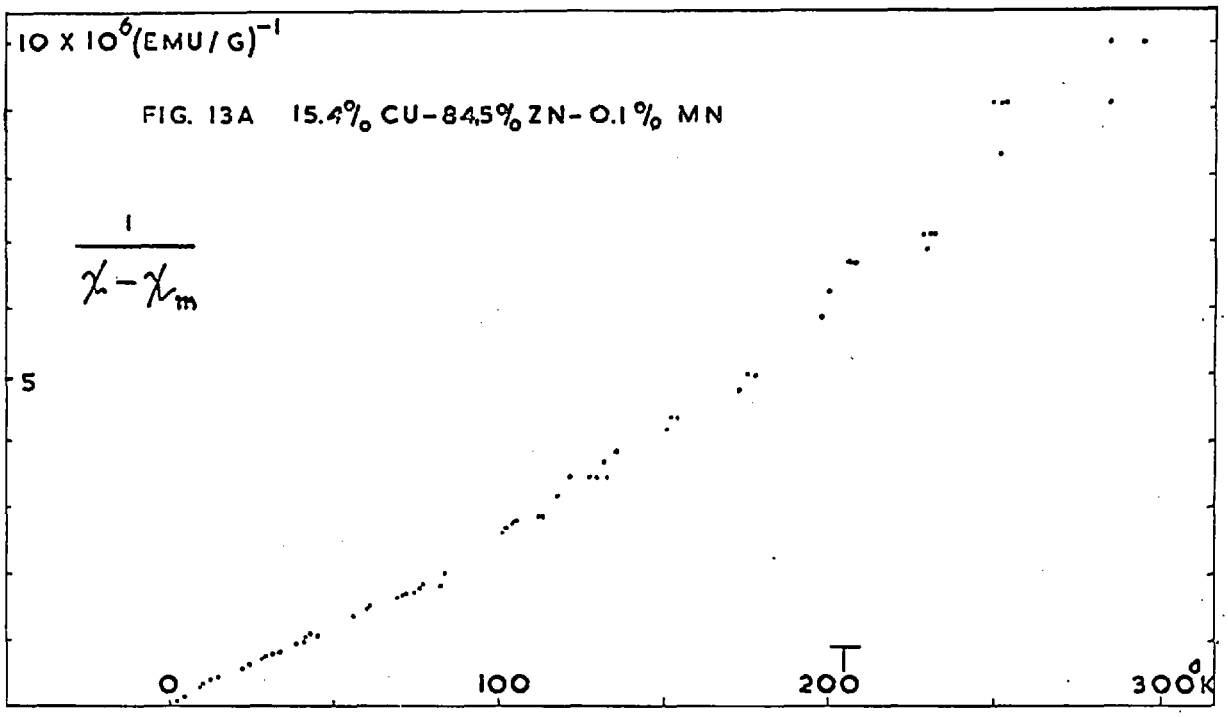

FIG. 13A 15.4% CU-84.5% ZN-0.1% MN

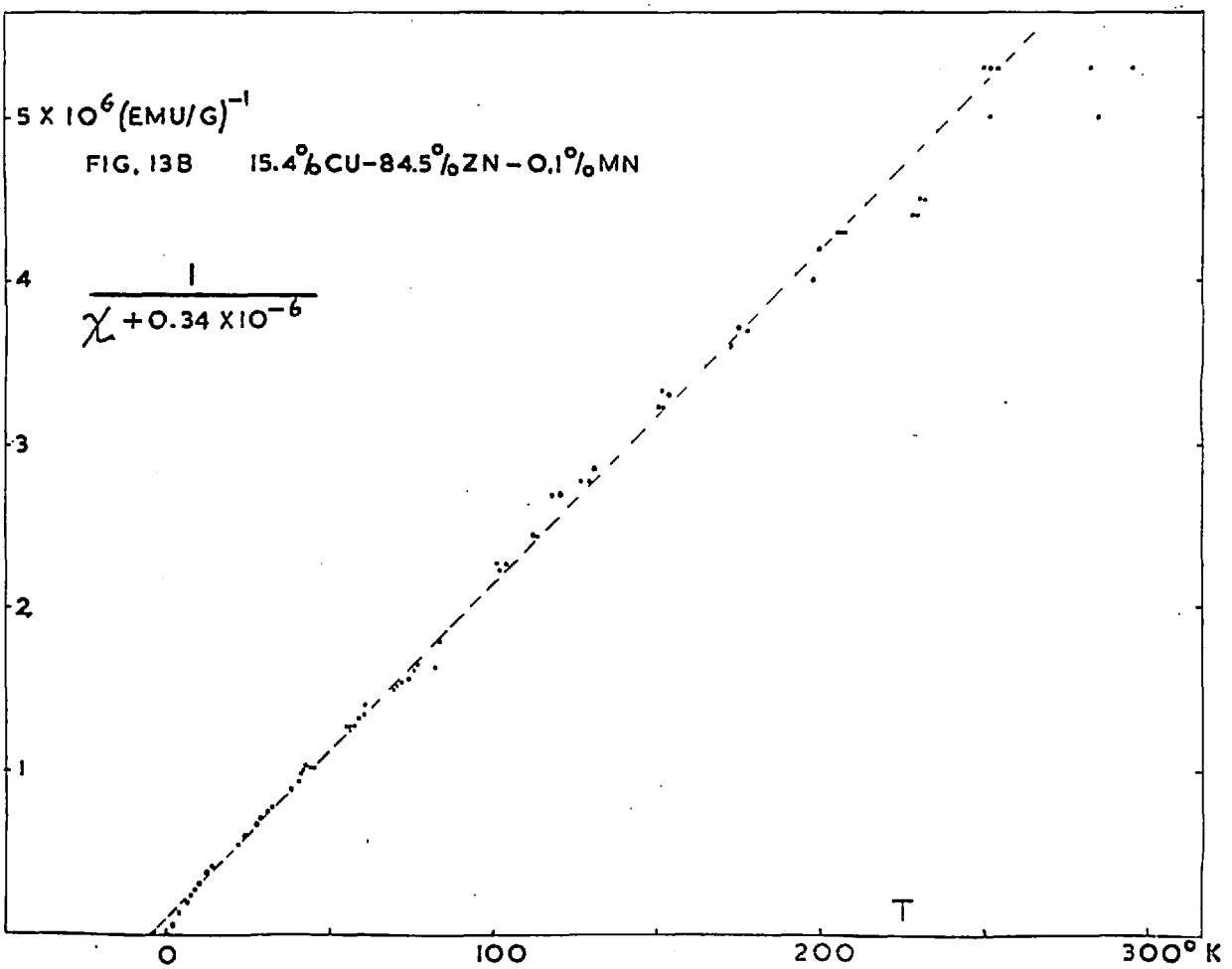

FIG. 13B 15.4% CU-84.5% ZN-0.1% MN

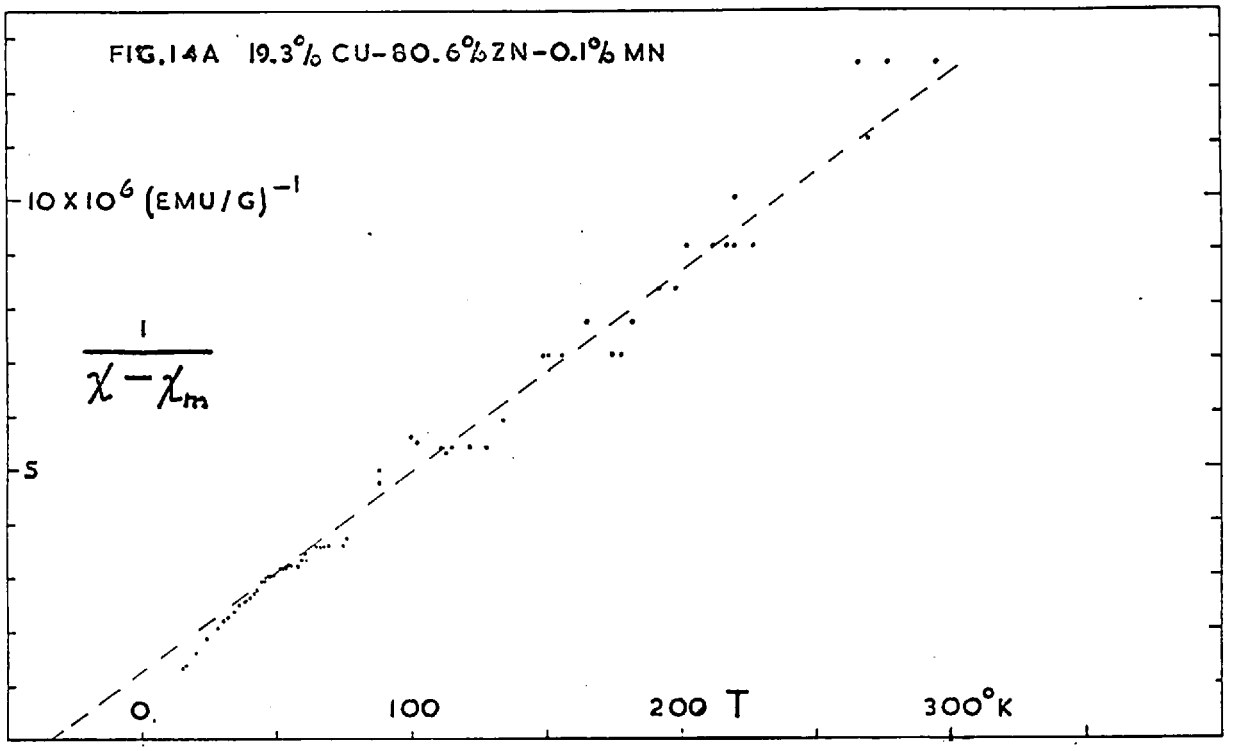
FIG. 14A 19.3% CU-80.6% ZN-0.1% MN
10 X 10^6 (EMU/G)^-1
1/(χ − χm)
5
0
100
200 T
300°K

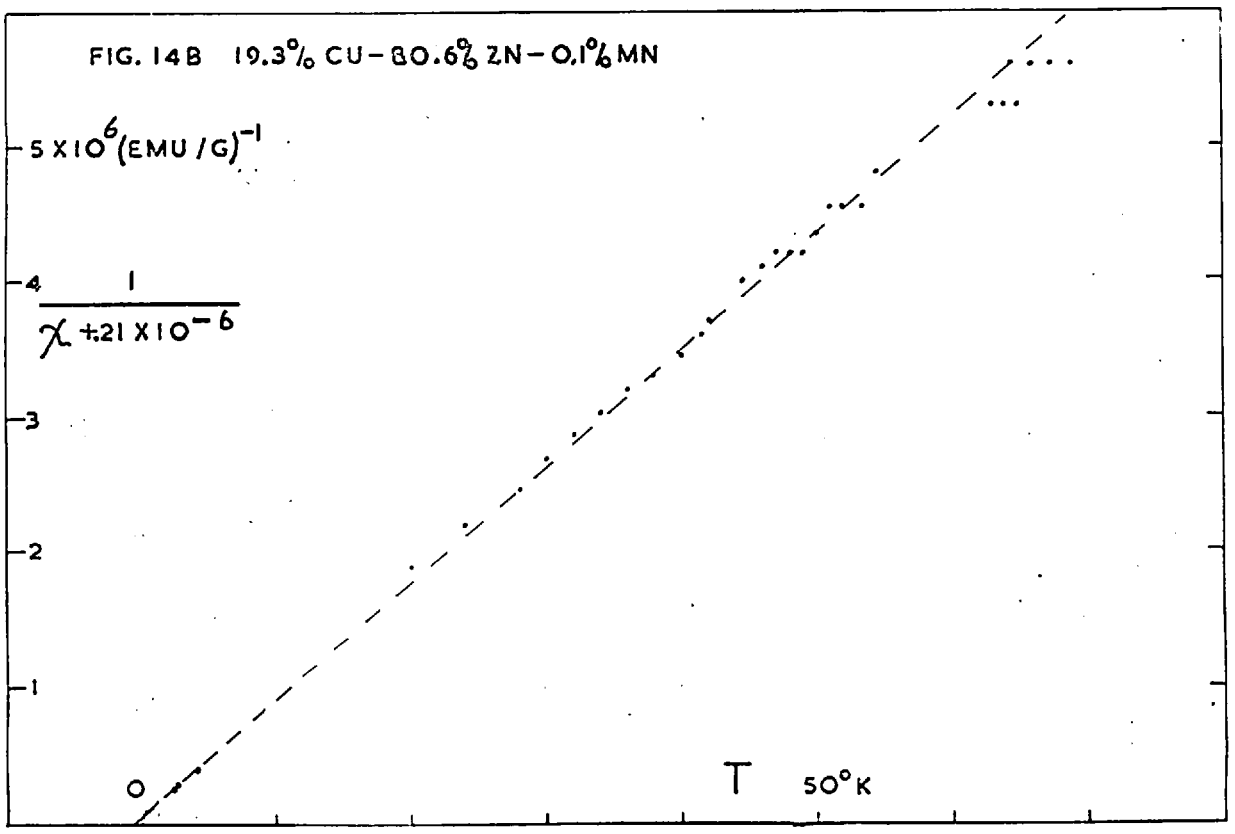
FIG. 14B 19.3% CU-80.6% ZN-0.1% MN
5 X 10^6 (EMU/G)^-1
1/(χ + .21 X 10^-6)
4
3
2
1
0
T
50°K

ε phase (Cu-rich) with 0.1% Mn

For this alloy the difference $\chi - \chi_m$ does not obey a Curie-Weiss relation. The plot of $\frac{1}{\chi - \chi_m}$ is shown in Figure 14a. The line drawn through the points corresponds to $\mu_{eff} = 3.5\,\mu_B$ and $\theta = -35^{\circ}K$. The absolute value of θ is very large for a dilute alloy and raises doubts as to the validity of this interpretation. Proceeding as for the previously mentioned alloys one finds that a value of $\chi_o = -0.21 \times 10^{-6}$ emu/g leads to the best fit of the relation (2) to the experimental points. This Curie-Weiss relation gives $\mu_{eff} = 2.3\,\mu_B$ and $\theta = -0.6^{\circ}K$. (FIG. 14b)

The value of $\chi_o = -0.24 \times 10^{-6}$ emu/g which gave the best fit for the solution of Fe in the same solvent, leads to a lesser fit in this case and gives $\mu_{eff} = 2.4\,\mu_B$ and $\theta = -1.0^{\circ}K$.

ε phase (Zn-rich) with 0.1% Co.

The susceptibility of this alloy in a field of 8000 Oe varies only slightly with temperature. This suggests that Co dissolves without carrying a moment. At 1.7° and $4.2^{\circ}K$ however the susceptibility is field-dependent and increases with decreasing field strength, the effect being too large to be due to the experimental error. This can not be ascribed to a contamination because Fe, the most likely impurity, does not carry a moment in this matrix and Mn is not likely to be present in this sample. If a small moment appeared on Co at low temperatures the susceptibility in the high fields would be larger at $4.2^{\circ}K$ than at $77^{\circ}K$, which is not the case. The same objection can be made against the assumption that this effect is due to clusters of Fe, so that no complete interpretation of these data can be given.

ε phase (Cu-rich) with 0.1% Co.

For this alloy the susceptibility at 4.2°K and at higher temperatures is close to that of the pure solvent. In this case no field-dependence was observed at 4.2°K, while at 1.7°K this could not be checked. It is seen however that the change of the susceptibility in the highest field on cooling from 4.2 to 1.7°K is of the same order of magnitude as that found for the previous alloy. In this solvent Fe carries a moment and could be the cause of this increase.

The points at 4.2°K and above indicate that the introduction of Co has no effect on the susceptibility of the alloy so that the moment per Co atom is zero.

ε phase (Cu-rich) with 0.03% Cr.

The field-dependence of the susceptibility at 1.7°K suggests an interaction between the solute atoms. The values at 77° and 295°K are close to those for the solvent. A plot of $\frac{1}{\chi - \chi_o}$ vs T with χ_o equal to the value at 295°K, is given in Figure 15. Because the effect of the solute is small, the error on the points in this graph are large. The line drawn in Figure 15 corresponds to $\mu_{eff} = 0.7\mu_B$, $\theta = +2°K$. If for χ_o the values of the solvent are taken the result is $\mu_{eff} = 0.5\mu_B$, $\theta = +3°K$.

These values of θ are consistent with the fact that the susceptibility is field-dependent at 1.8°K. The fact that the points at this temperature lie above the line drawn in Figure 15 suggests anti-ferromagnetic interactions, while the fact that θ is positive indicates ferromagnetic interactions at the higher temperatures.

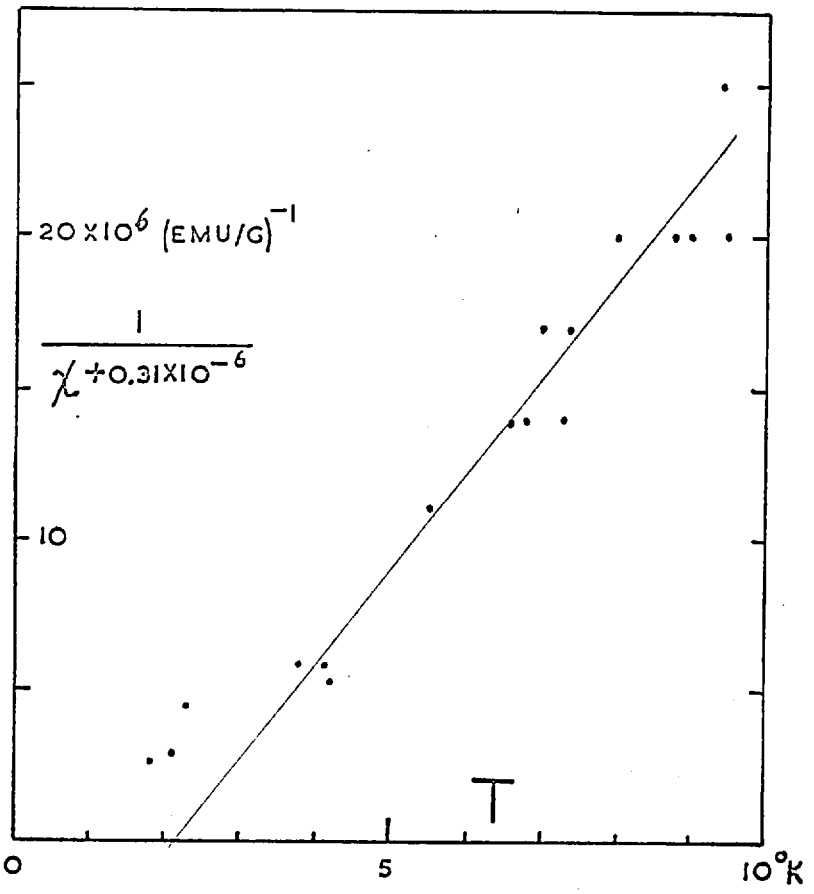

FIG. 15 19.6% CU–80.3% ZN–0.04% CR

§ 4. Ternary ε phase alloys. Discussion.

The binary Cu-Zn ε phase has a close-packed hexagonal structure with an axial ratio $\frac{c}{a}$ of approximately 1.56 which is smaller than the ideal value, 1.63. The number of conduction electrons per atom $\frac{e}{a}$ varies from 1.79 at the Cu-rich end of the phase (20 at % Cu) to 1.87 at the Zn-rich end (14 at % Cu). The smallest region in k-space bounded by planes of energy discontinuity is the Jones zone, shown in Figure 16.[27] This zone contains the first and part of the second Brillouin zone and can hold somewhat less than 2 electrons per atom and is thus for these ε phase alloys nearly full. If $\frac{c}{a} < 1.63$, the point A in Figure 16 is closer to the origin than either B or C. No experimental data have been reported on the electric and magnetic properties of these alloys. Results of lattice spacing measurements for alloys of different Cu/Zn ratio are available.

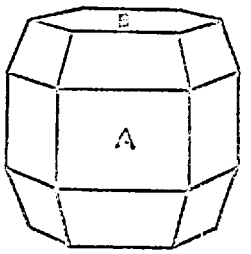

FIG. 16

Present results

As discussed in paragraph 3, some of the transition metal solutes contribute a paramagnetic term to the susceptibility of the alloy. If this term is taken to be the difference of the susceptibility of the ternary alloy and that of the solvent, in some cases no Curie-Weiss law is followed and the results can not be interpreted in terms of an existing model. If it is accepted that the presence of the impurity can change the susceptibility of the matrix, the total

susceptibility can be written as the sum of a temperature-independent term and a paramagnetic contribution which follows a Curie-Weiss law. This procedure has therefore been followed. The results, as derived in paragraph 3 are shown in Table 1. An argument in favour of this interpretation is that the values of θ obtained from the plot $\frac{1}{\chi - \chi_m}$ vs T are in some cases too large to represent the interactions between solute moments in dilute solutions as considered here.

Table 1

solvent	Zn-rich ε-brass				Cu-rich θ-brass			
solute	$\chi_o \times 10^6$ emu/g	θ °K	μ_{eff} μ_B	H_{dep} °K	$\chi_o \times 10^6$ emu/g	θ °K	μ_{eff} μ_B	H_{dep} °K
pure	-0.31	-	-	-	-0.28	-	-	-
Cr	x	x	x	x	-0.31	+2	0.7	1.8
Mn	-0.34	-6	4.1	4.2	-0.21	-0.6	2.3	1.7
Fe	-0.35	-	zero	1.7	-0.24	-1.2	1.5	-
Co	-0.21	-	zero	4.2	-0.32	-	zero	-

In the column H dep is given the temperature at which a field-dependence of was observed. x = not measured.

The difference between χ_o and χ_m.

This difference can be partly due to an experimental error as discussed in Chapter IV, but the χ_o - values for the Zn-rich Zn-Cu-Co and the Cu-rich Zn-Cu-Mn and Zn-Cu-Fe solutions deviate too much and a different mechanism must be operative. The temperature-independent terms in the susceptibility are the diamagnetism, the Pauli-paramagnetism

and the Van Vleck paramagnetism. For an alloy having an electronic structure with a nearly full Brillouin zone which is overlapped by the Fermi surface the diamagnetic susceptibility of the conduction electrons is very sensitive to the shape of the Fermi-surface as was shown by Jones in a treatment of the γ brass alloys.[27] It is thus possible that the perturbation of the lattice and the Brillouin zone structure by the impurity will affect the diamagnetism.

A change in the Pauli-paramagnetism will be the result of a change in the density of Bloch-states at the Fermi-energy. A small effect could be the result of the mixing of the 3d wave functions on the solute atoms and those of the conduction band.

For the Van Vleck term in alloys no theoretical model has been developed nor are experimental data available, so that no estimate can be given.

Although it is thus possible to indicate a mechanism that can account for the difference between χ_o and χ_m no values can be predicted nor reasons given why the magnitude of the effect should be different for different systems.

Interaction between solute moments.

For the solution of Mn in the Zn-rich ε brass the negative value of θ ($-6^{\circ}K$) indicates an antiferromagnetic interaction at high temperatures. The absolute value of θ leads to the expectation that below $6^{\circ}K$ ordering will take place. In agreement with this is that the susceptibility is field-dependent at 4.2° and $1.8^{\circ}K$. The deviation from the Curie-Weiss law at low temperatures indicates a ferromagnetic interaction. This behaviour is the opposite of that

found for Cu-Mn and Zn-Mn solutions where the ϑ values are positive but at low temperatures antiferromagnetic interactions dominate.

For the solution of Cr the Zn-Mn type of behaviour is found, here $\theta = 2^{\circ}K$ and at $1.7^{\circ}K$ the susceptibility is field-dependent and smaller than the value extrapolated from the Curie-Weiss law at higher temperatures.

For the solutions of Mn and Fe in the Cu-rich solvent the θ values are small which is consistent with the fact that the field-dependence of the susceptibility, where observed, is only slight.

The variation of the atomic moment.

The variation of the solute moment with matrix composition is qualitatively different for Mn, Fe and Co as solute. With increasing Cu content the moment for Fe increases from zero to 1.5 μ_B over the phase, that for Mn decreases from 4.2 to 2.3 μ_B while that for Co remains zero. The only theoretical model applicable to this case is that given by Anderson.[16]

If the interactions within the solute atom are not strongly affected by the matrix, a change in the effective moment must be due to a change of the width Δ in energy of the virtual 3d-state, given by $\Delta = \pi < V_{kd}^2 > \rho(E)$ where $\rho(E)$ is the density of Bloch states and V_{kd} the parameter of the interaction between the 3d-state and the Bloch states of the matrix. No data on the electronic specific heat of binary ε brass alloys are available for comparison with the observed moment. The observed variation of μ_{eff} can however not be due to a change of $\rho(E)$ at the Fermi-level because this would imply that the moment would vary in a similar way for Fe, Mn and Co as solute. The

only parameter available is then $\langle V_{kd}^2 \rangle$. If it is assumed that the magnitude of V_{kd} depends on the symmetry of the wave functions of the Bloch electrons (s or p), the interpretation given of lattice spacing data suggests an explanation of the observed change of μ_{eff}. Massalski and King [105] measured the lattice parameters of binary ε phase Cu-Zn alloys of different composition and found that the axial ratio $\frac{c}{a}$ decreases with increasing number of conduction electrons per atom $(\frac{e}{a})$ from the Cu-rich end of the phase up to $\frac{e}{a} = 1.86$. This result was interpreted as due to the fact that in these alloys the Fermi-surface overlaps the Brillouin zone at the point A and the equivalent points in Figure 16 and only there. On this basis the following tentative explanation of the variation of μ_{eff} over the ε phase can be given. It is assumed: 1. that the theory by Anderson is applicable to this case and that the observed variation of μ_{eff} is the result of a variation of the width of the virtual 3d state; 2. that the symmetry of a conduction electron wave function having a $\underline{k}$ vector near the top of the first Brillouin zone (type I symmetry) is different from the symmetry of a state which lies at the bottom of the second zone near A (type II symmetry); 3. that the interaction of the virtual 3d-state associated with an Fe atom with Bloch states of type I is less strong than that with Bloch states of type II. Then a gradual increase of $\frac{e}{a}$, i.e. an increase of the overlap into the second zone and thus of the relative amount of type II Bloch wave function, will lead to an increase of the average interaction $\langle V_{kd}^2 \rangle$ and a broadening of the 3d state, thus reducing the moment.

A proper theoretical treatment along these lines will have to explain why this effect is reversed for Mn as solute where the moment increases with increasing $\frac{e}{a}$ and why in Co no moment is observed at either end of the phase. As long as no other independent estimate of V_{kd} can be given this explanation can only be tentative.

§ 5. Ternary Υ phase alloys. Interpretation of the results.

For all the Υ phase alloys measured the variation of the susceptibility with temperature is similar. The alloys are weakly paramagnetic at 1.8°K, the susceptibility decreases with increasing temperature and is almost constant above 60°K, this constant value being in most cases above that for the pure solvent.

The effective moment per transition metal atom μ_{eff} and the Curie-Weiss constant θ have been determined as for the ε phase alloys. Where the difference between the susceptibility of the alloy χ and that of the solvent χ_m does not follow a Curie-Weiss law, a different value χ_o has been used instead of χ_m, such that a plot of $\frac{1}{\chi - \chi_o}$ vs T is linear. In all cases $\chi_o \gtrsim \chi_m$. The effect of the solute in these alloys is small, and the relative errors in $\chi - \chi_o$ for points above 15°K are considerable. As discussed in paragraph 3 of this section, the temperature of the specimen in the region between 4.2 and 15°K is somewhat doubtful so that, where the susceptibility of the solute system is small, the most useful points to determine μ_{eff} and θ are those below 4.2°K. The most obvious choice of χ_o is the constant high-temperature value. For alloys with composition near the limits of the phase the susceptibility at 77°K is different from that at 300°K. For those alloys the value at 77°K has been taken.

The susceptibility of a number of binary Cu-Zn γ phase alloys was measured by Marcus.[103] These results show only a small temperature dependence below 150°K which suggests that the impurity content of the samples used was low. The binary γ brass Cu-Zn alloy prepared for the work reported here was cast from the same batch of starting materials as used for the ternary alloys. It was originally intended to compare the susceptibility of this alloy with the above-mentioned results in order to determine any systematic difference and to use the reported values for the binary alloys. As discussed in Chapter IV, paragraph 6, no conclusions can be drawn from the susceptibility values for the binary alloy measured here. Because no more Cu from the original batch was available, results on a newly cast alloy would not have given the required information. In the derivation of μ_{eff} and θ for the ternary solution the matrix susceptibility has however not been used. The values reported by Marcus have therefore been used where necessary, i.e. to determine the change of the temperature-independent term

The derivation of the effective moment per transition metal atom, μ_{eff} and the Curie-Weiss constant θ will be discussed below

γ brass (Cu-rich) with 0.03% Mn.

The plot of $\frac{1}{\chi - \chi_o}$ vs T with $\chi_o = -0.38 \times 10^{-6}$ emu/g is given in Figure 17. The line drawn corresponds to $\mu_{eff} = 1.04\,\mu_B$ and $\theta = 0 \pm 0.2$°K. The value for the solvent given by Marcus is -0.35×10^{-6} emu/g the value at 77°K found in the second run on this alloy, -0.36×10^{-6} emu/g, agrees well with this value.

γ brass (middle of the phase) with 0.1% Mn.

With the value χ_o - 0.32 x 10^{-6} emu/g, i.e. the room-temperature value of the measured susceptibility, the plot of $\frac{1}{\chi - \chi_m}$ vs T as shown in Figure 18 is found. The moment corresponding to the Curie-Weiss relation drawn is 1.09μ_B, $\theta = 0^oK$. The value of the susceptibility of the solvent is -0.46 x 10^{-6} emu/g. The difference between this value and χ_o is too large for a systematic error on the points. An error in the composition has also to be considered. In the binary Cu-Zn system the alloy with a susceptibility - 0.32 x 10^{-6} emu/g has a Zn content of 60.4 wt %, as is found from reference 103. If it is assumed that χ_o is equal to the value for the pure solvent it follows that the deviation of the Zn content of this alloy from the intended value is several per cent. The results of the chemical analysis show that in the alloys for which the Cu/Zn was determined the Zn content did not deviate more than 0.2% from the intended value. The increase of 0.14 x 10^{-6} in the temperature-independent term must thus be a genuine property of the alloy.

γ phase (Zn-rich) with 0.1% Mn.

The obvious value for χ_o is 0.42 x 10^{-6} emu/g, i.e. the value at 77° and 295°K. The plot of $\frac{1}{\chi - \chi_o}$ vs T is given in Figure 19, this gives $\mu_{eff} = 0.6\mu_B$, $\theta = 0^oK$. The susceptibility of the pure solvent from reference 103 is - 0.71 x 10^{-6} emu/g. Also in this alloy the large difference between χ_o and χ_m can not be ascribed to an error in the Cu/Zn ratio. If this was the case the Zn content of the alloy would be 62 wt% which is highly unlikely as discussed above.

FIG. 17 39.6% CU-60 4% ZN-0 04% MN

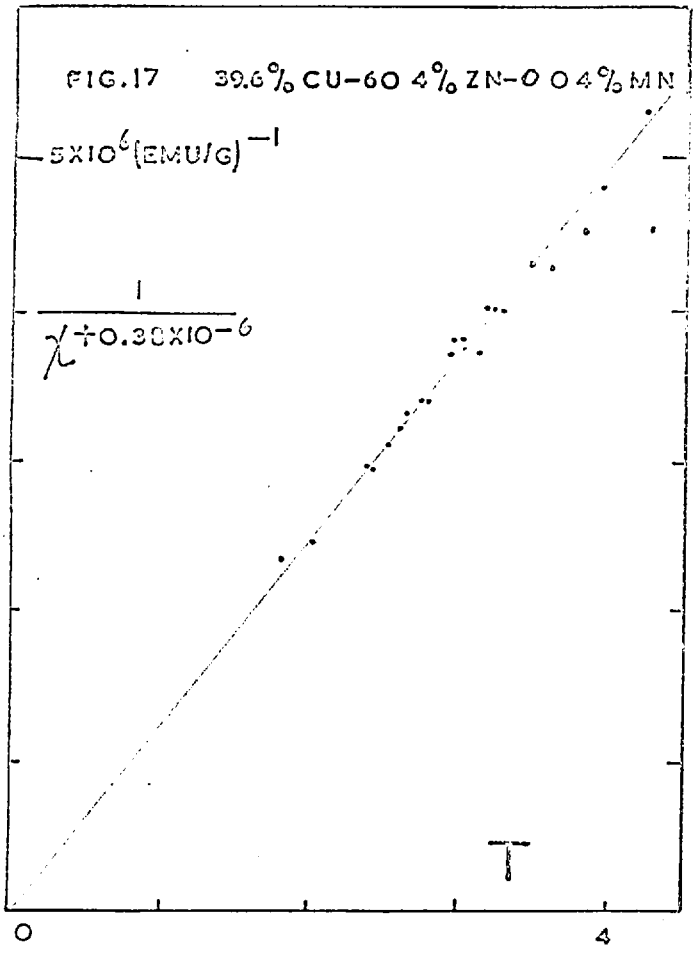

FIG. 19 35.2% CU-6 4.7 % ZN
0.1% MN

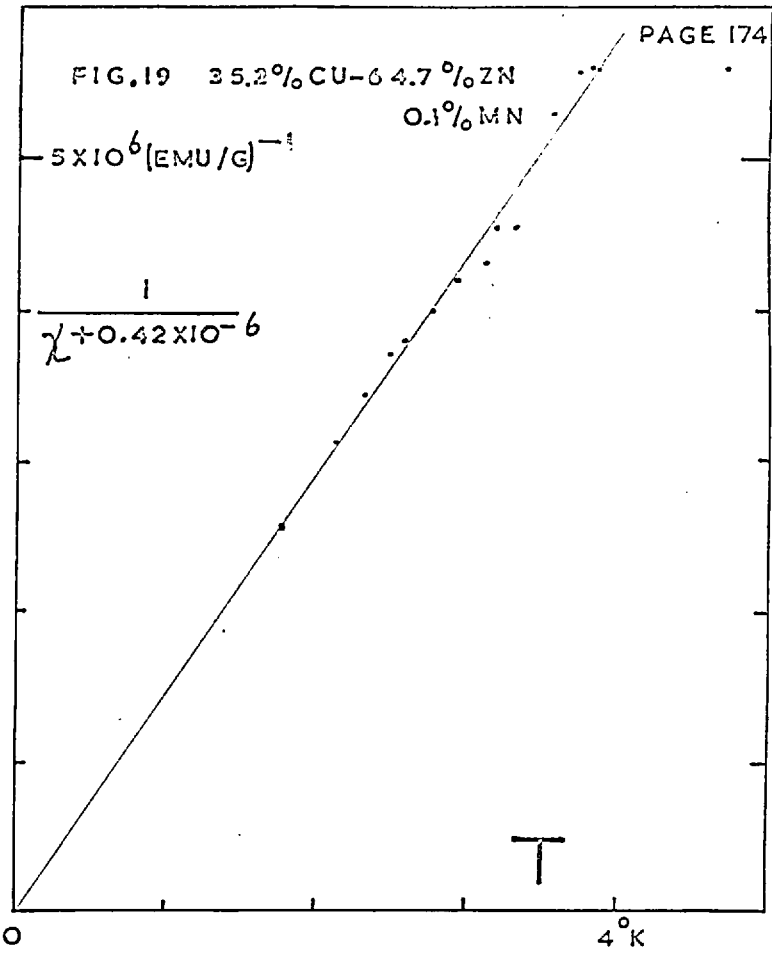

FIG. 18 37.9% CU- 62.0% ZN- 0.1% MN

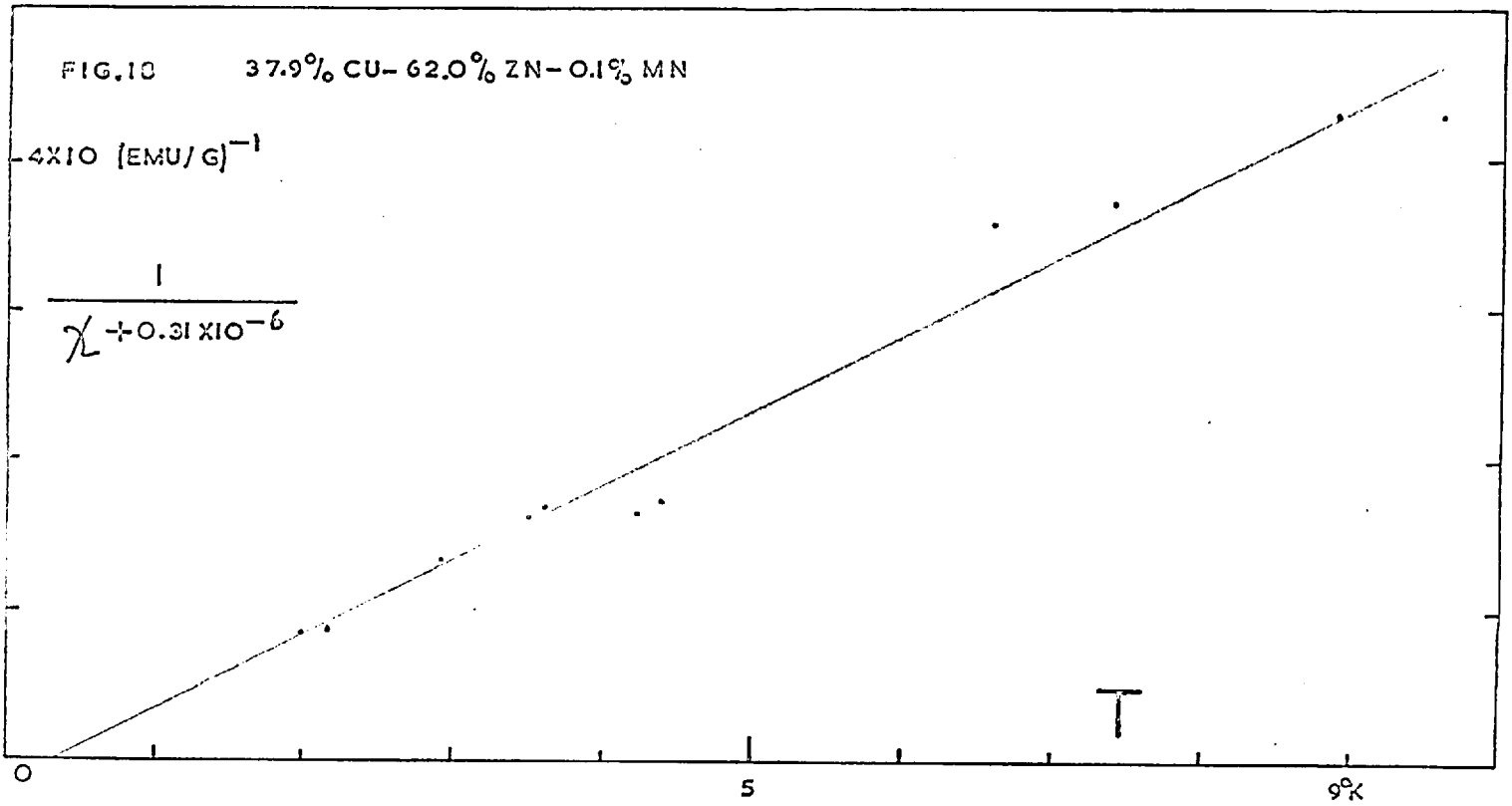

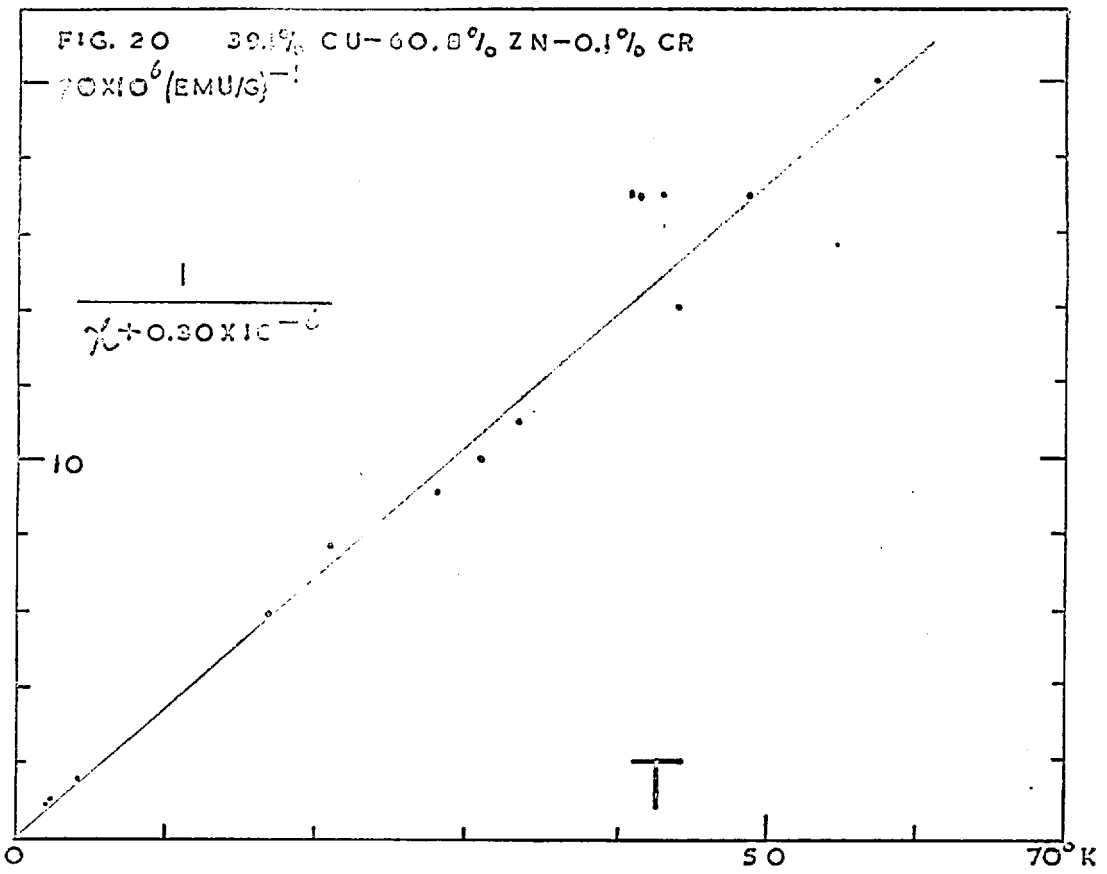
FIG. 20 39.1% CU-60.8% ZN-0.1% CR
20X10⁶ (EMU/G)⁻¹
1/(χ+0.30X10⁻⁶)
10
T
0
50
70° K

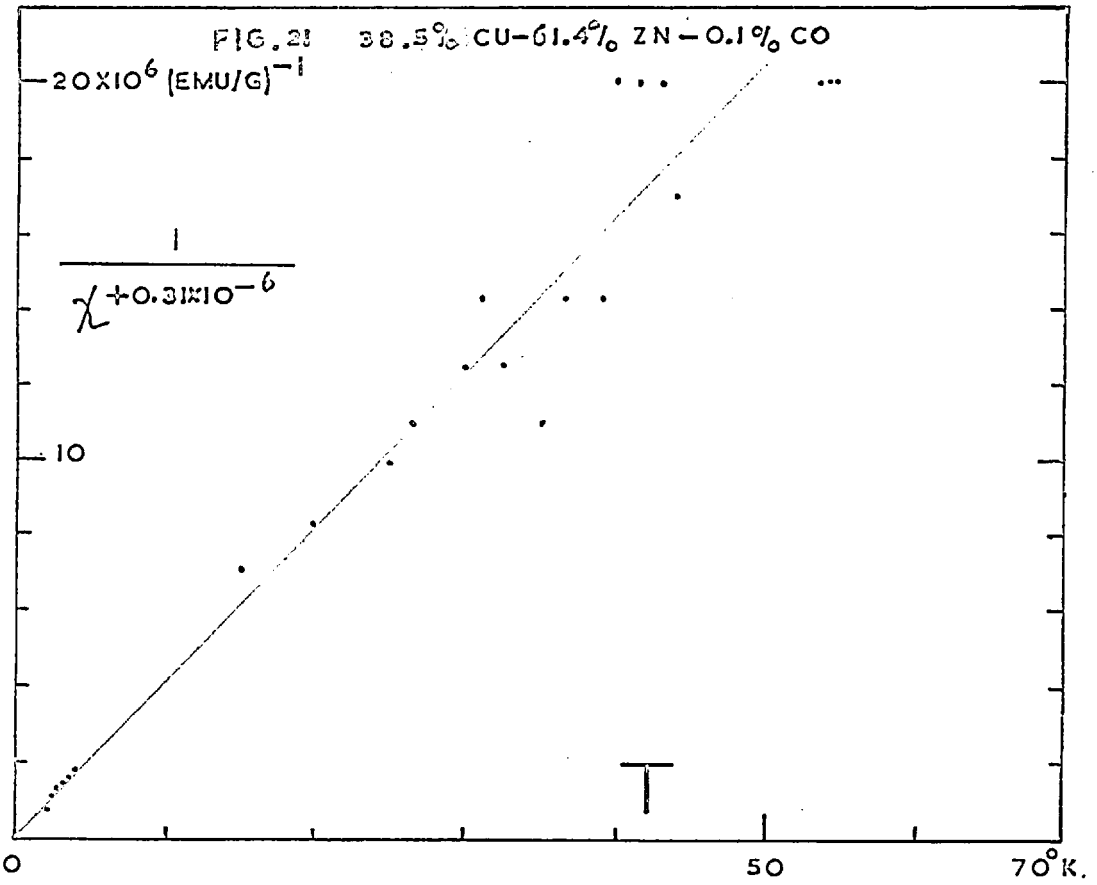
FIG. 21 38.5% CU-61.4% ZN-0.1% CO
20X10⁶ (EMU/G)⁻¹
1/(χ+0.31X10⁻⁶)
10
T
0
50
70°K.

γ phase with 0.1% Cr.

The plot of $\frac{1}{\chi - \chi_o}$ vs T with $\chi_o = -0.30 \times 10^{-6}$ emu/g is given in Figure 20. The line drawn gives a moment of $1.3\mu_B$ per Cr atom, while $\theta = -1^\circ K$. The susceptibility of the pure solvent is -0.37×10^{-6} emu/g.

γ phase with 0.1% Co.

The plot of $\frac{1}{\chi - \chi_o}$ vs T with $\chi_o = -0.22 \times 10^{-6}$ (the value at 295°K) leads to $\mu_{eff} = 1.2\mu_B$ and $\theta = 0^\circ K$. The susceptibility of the pure solvent is -0.43×10^{-6}.

§ 6. Ternary γ phase alloys. Discussion

The binary Cu-Zn γ phase has a complicated cubic structure with 52 atoms per unit cell.[106] This structure can be derived from the body-centred cubic lattice, by considering a cell consisting of 27 b.c.c. unit cells arranged in a cube (Figure 22a) in which the atoms at the eight corners and in the centre of the large cube are removed and several of the other atoms displaced slightly (Figure 22b). The composition of the binary phase is from 58 at % Zn ($\frac{e}{a} = 1.58$) to 66 at % Zn ($\frac{e}{a} = 1.66$). The large Brillouin zone [107] for this structure (Figure 22c) contains 90 states per unit cell, i.e. 1.73 states per atom and is thus for these alloys almost full. The inscribed sphere in this zone contains 1.54 states per atom. Jones [107] predicted a density of states vs energy curve $\rho(E)$ as given in Figure 23 on the following arguments. As long as the Fermi-surface does not touch the zone faces, the density of states is that for a free electron gas. As the number of electrons is increased, the

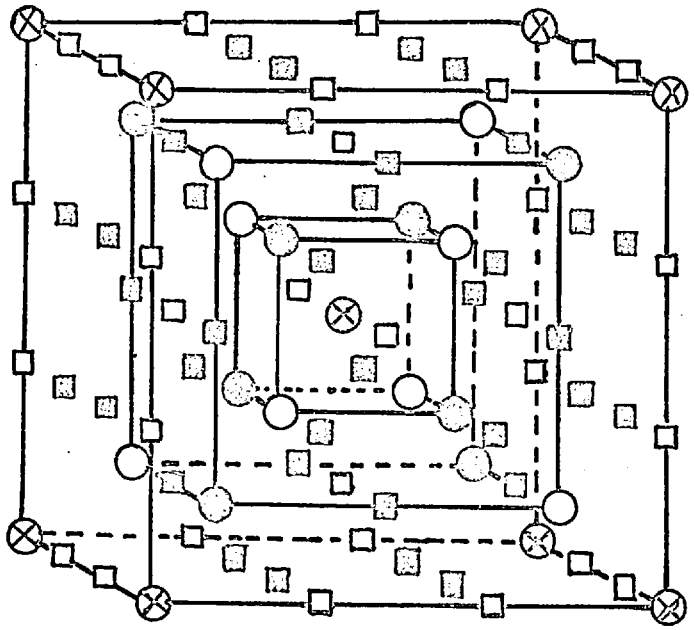

FIG. 22a b.c.c. structure

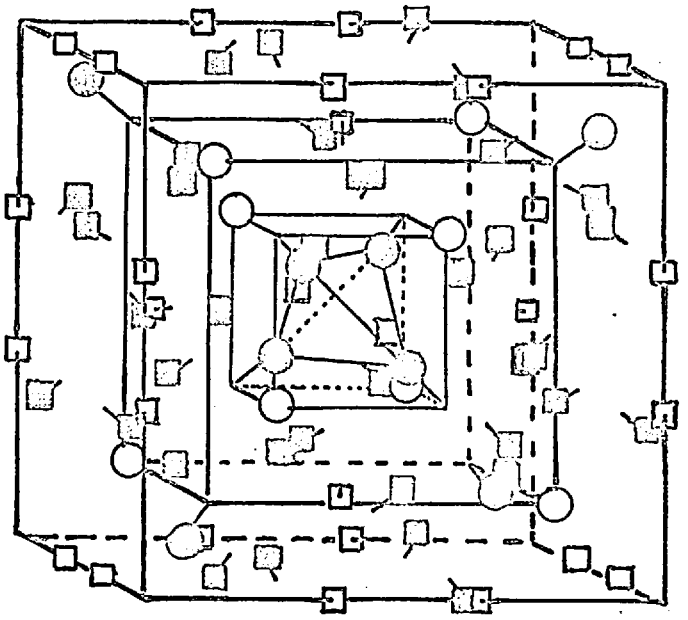

FIG. 22b . γ-brass structure

The γ-brass structure can be obtained from the b.c.c. structure by removing the atoms marked ⊗ and shifting the other atoms as indicated in 22b.

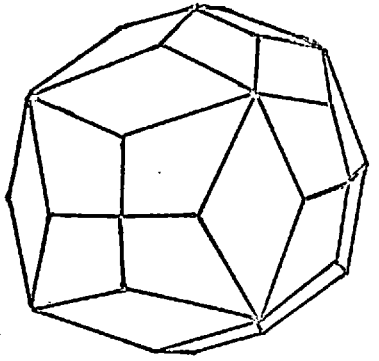

FIG. 22c. Jones zone for γ-brass

Fermi-surface will touch the zone faces when $\frac{e}{a} = 1.54$. If more electrons are added the Fermi-surface will become a truncated sphere within the zone. If no overlap into the next zone takes place the density of states at the Fermi-energy will decrease with increasing $\frac{e}{a}$ and start increasing again when overlap takes place. This model has been confirmed by specific heat measurements by Veal and Rayne,[108] the density of states as derived from these data is also shown in Figure 23. The diamagnetic susceptibility of these alloys is large and shows a strong variation with alloy composition as shown in Figure 24. The large values were ascribed by Jones to an overlapping of the zone by the Fermi-surface.[27]

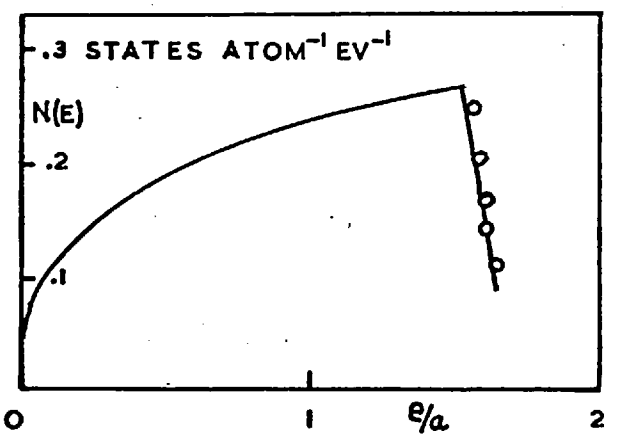

FIG.23. The density of states for an alloyhaving the γ brass structure, after ref. 107. Experimental points from ref. 108.

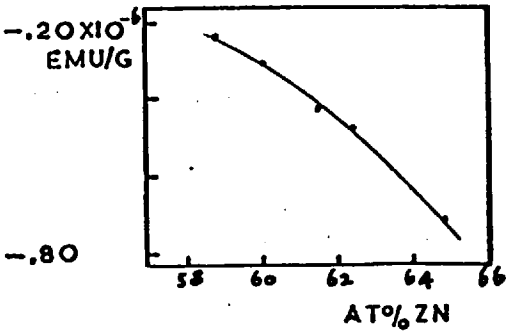

FIG.24 . The magnetic susceptibility of γ phase Cu-Zn alloys. alloys. After ref.103.

Present results.

As discussed in the previous paragraph the susceptibility of the ternary alloys has been written as $\chi = \chi_o + \frac{N\mu_{eff}^2}{3k(T-\theta)}$ where χ_o is in general not equal to the value for the solvent, χ_m The results obtained are shown in Table II. In addition to these data it must be noted that the susceptibility has a small field-dependence at 1.8°K

TABLE II

at % Cu in solvent	39	38	40	38	35
solute	Cr	Co	Mn	Mn	Mn
$-\chi_m \times 10^6$ (emu/g)	0.37	0.43	0.35	0.46	0.71
$-\chi_o \times 10^6$ (emu/g)	0.30	0.22	0.37	0.32	0.42
μ/μ_B	1.3	1.2	1.0	1.1	0.6
θ (°K)	-1	0	0	0	0

The difference $\chi_o - \chi_m$.

The first question is to account for the temperature-independent term $\chi_o - \chi_m$ which is zero for the alloy at the Cu-rich end of the phase and increases with increasing Zn content. The large values of the diamagnetic susceptibility of the binary Υ brass alloys were ascribed by Jones [27] to small pockets of occupied states outside the zone in Figure 22. If the solute perturbs the periodicity of the lattice and thus the Brillouin zone structure, appreciably, a modification of the diamagnetism will also be expected.

It must be noted that at the Zn-rich end of the phase where the largest overlapping is expected and the diamagnetism is strongest, also the term $\chi_o - \chi_m$ is large.

Interactions between atomic moments.

From the values of the interaction-parameter θ and the small field-dependence of the susceptibility at 1.8°K it is seen that no significant interactions between the moments take place.

The effective atomic moment.

The most important result is the small magnitude of μ_{eff} for Mn as solute. The values found for Mn in solution in other alloys are: in the Cu-Zn α phase $4.8 \pm 0.1 \mu_B$, in the Cu-Zn ε phase from 2.3 to 4.1 μ_B and in Zn 4.8 μ_B. A possibility that has to be considered is that only a small fraction of the Mn atoms carries a moment. If this moment is equal to that in pure Cu or Zn this means that only 4% of the solute carries a moment. This in turn would imply that only on a small fraction of the lattice sites the conditions for the magnetization of a Mn atom are favourable. A difference between the conditions on different sites can arise if an ordered structure exists in this phase, as it does in the Cu-Zn β phase. No evidence of order in the γ phase exists however.

The other possibility is to interpret the data in terms of the theory by Anderson as was done in paragraph 4. Also here there is no reason to assume a strong modification of the Coulomb-and exchange-interactions within the solute atoms, so that the observed values of μ_{eff} must be ascribed to a large width of the virtual 3d-state $\Delta = \pi \langle V_{kd}^2 \rangle \rho(E)$ with V_{kd} and $\rho(E)$ as defined in paragraph 4.

If a free-electron model holds the values of the density of states at the Fermi-energy are between 0.1 and 0.3 states per atom per eV, which is of the same order of magnitude as for Cu or Zn. Also the strong decrease of $\rho\,(E_F)$ with increasing $\frac{e}{a}$ ratio would require an increase of μ_{eff} in this direction, while the experiments show a decrease. The explanation will then have to be sought in the magnitude of $< V_{kd}^{\,2} >$ and its variation with $\frac{e}{a}$. The explanation suggested for the variation of μ_{eff} over the ε phase in paragraph 4 also applies to the solutions of the transition metals in γ brass, because both phases have a nearly full Brillouin zone.

CHAPTER VI

SOLUTIONS OF FE IN OTHER TRANSITION METALS.

The curves of the electrical resistivity as function of temperature for dilute Mo-Fe, Rh-Fe and Ir-Fe alloys show anomalies at low temperatures. These anomalies are however qualitatively different for the different systems. Because the mechanism which causes a resistance anomaly often also has an effect on the magnetic susceptibility, this last property was measured for one alloy of each of the above-mentioned systems.

The alloys will be treated in separate paragraphs, because of the large difference between the properties of different systems. The remarks made in the introduction to Chapter V also apply to the measurements reported here.

§§ 1. Mo-Fe

In a Mo - 0.65 at % Fe alloy a maximum at $4^{\circ}K$ and a minimum at $22^{\circ}K$ were observed in the resistivity vs temperature curve. These anomalies are similar to those found for Cu-Mn alloys. To investigate if any magnetic order sets in at a temperature near that of the maximum, the susceptibility was measured from $1.7^{\circ}K$ upwards.

Results

The susceptibility in a field of 8000 Oe as a function of temperature is shown in Figure 1. Some field-dependence was observed at $4.2^{\circ}K$, the values in different fields are

H Oe	χ x 10^6 emu/g
4200	16.06
6350	15.93
8100	13.95

FIG. 1 MO – 0.65% FE

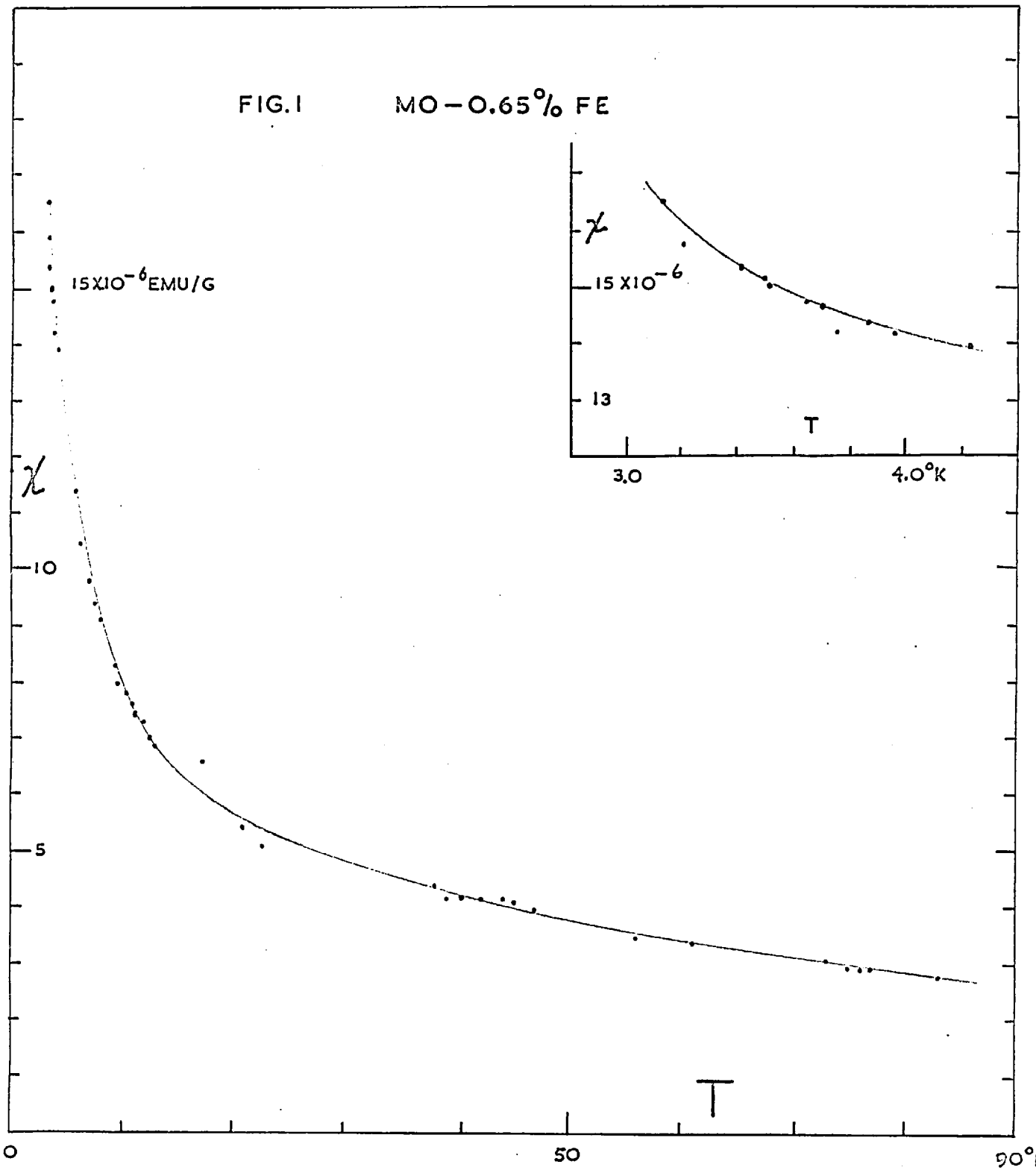

Discussion

The most important result is that at $4^{o}K$ no ferromagnetic or clear cut antiferromagnetic order sets in. Because no results for pure Mo have been reported and a plot of χ vs $\frac{1}{T}$ is not linear for high temperatures no value for the atomic moment can be derived. Clogston et.al [78] reported for this system an effective moment of $2.9\mu_B$ per Fe atom. Also in the alloys discussed in Chapter III, Sec. A, no indication of long-range magnetic order were found at the temperature of the resistivity maximum. For these systems a susceptibility maximum was however observed in alloys of higher solute concentration.

§ 2. Rh-Fe.

As discussed in Chapter III, a resistivity anomaly of a type not yet observed in any other system has been found in dilute solutions of Fe in Rh. For a Rh - 0.85 at % Fe alloy the magnetic susceptibility was measured from 1.7^{o} to $295^{o}K$.

Results.

The susceptibility of this alloy did not show a field-dependence at any temperature, plots of χH vs H are given in Figure 2. The susceptibility in a field of 8000 Oe as a function of temperature is shown in Figure 3.

The reciprocal of the difference of the susceptibility of this alloy and pure Rh [83] as a function of temperature is given in Figure 4a, which shows that a Curie-Weiss law is not obeyed over the whole temperature-range. The line drawn in Figure 4a corresponds to a moment per Fe atom $\mu_{eff} = 3.4\,\mu_B$ while $\theta = -41^{o}K$. The change of the

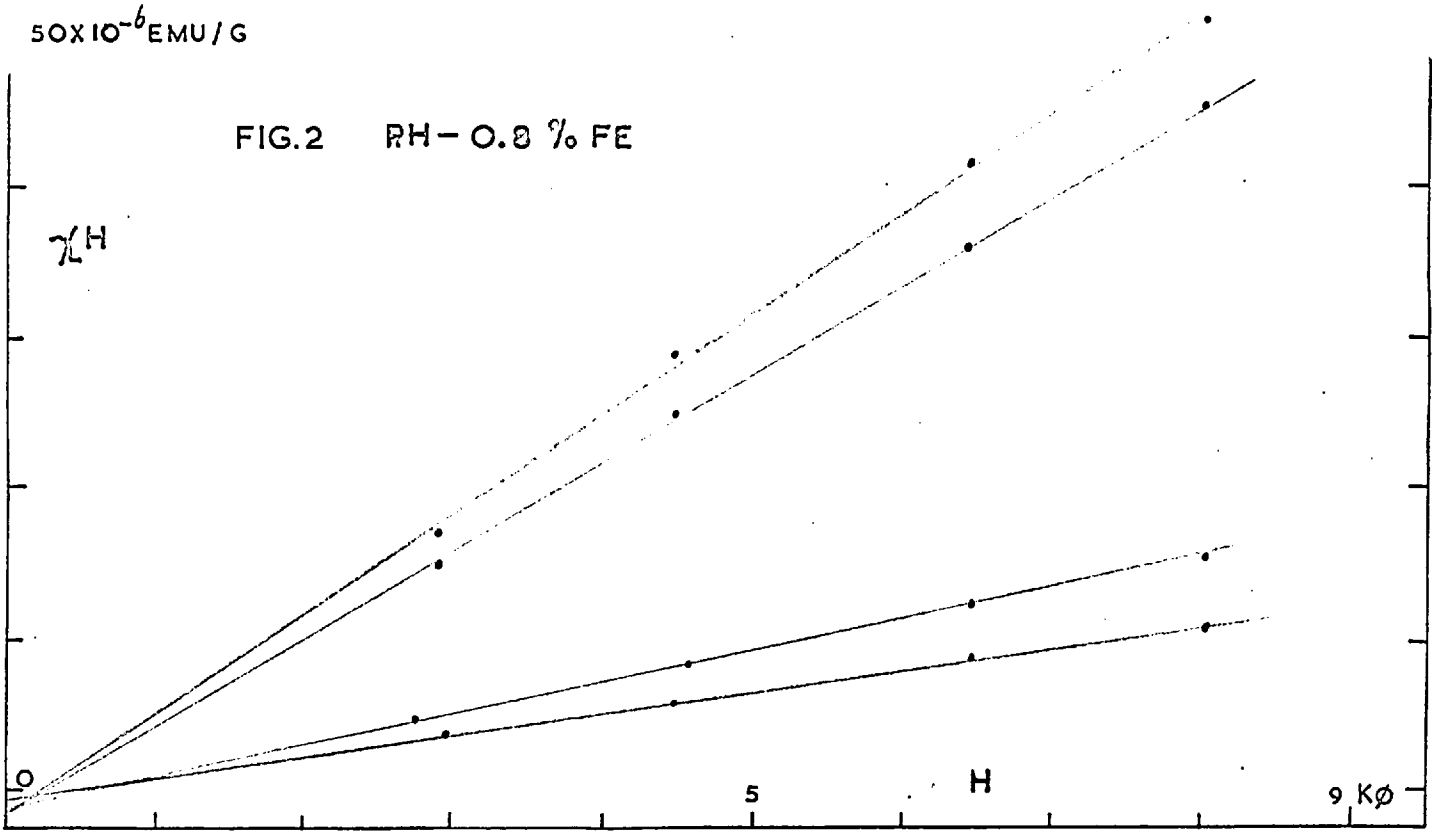

FIG. 2 RH – 0.8 % FE

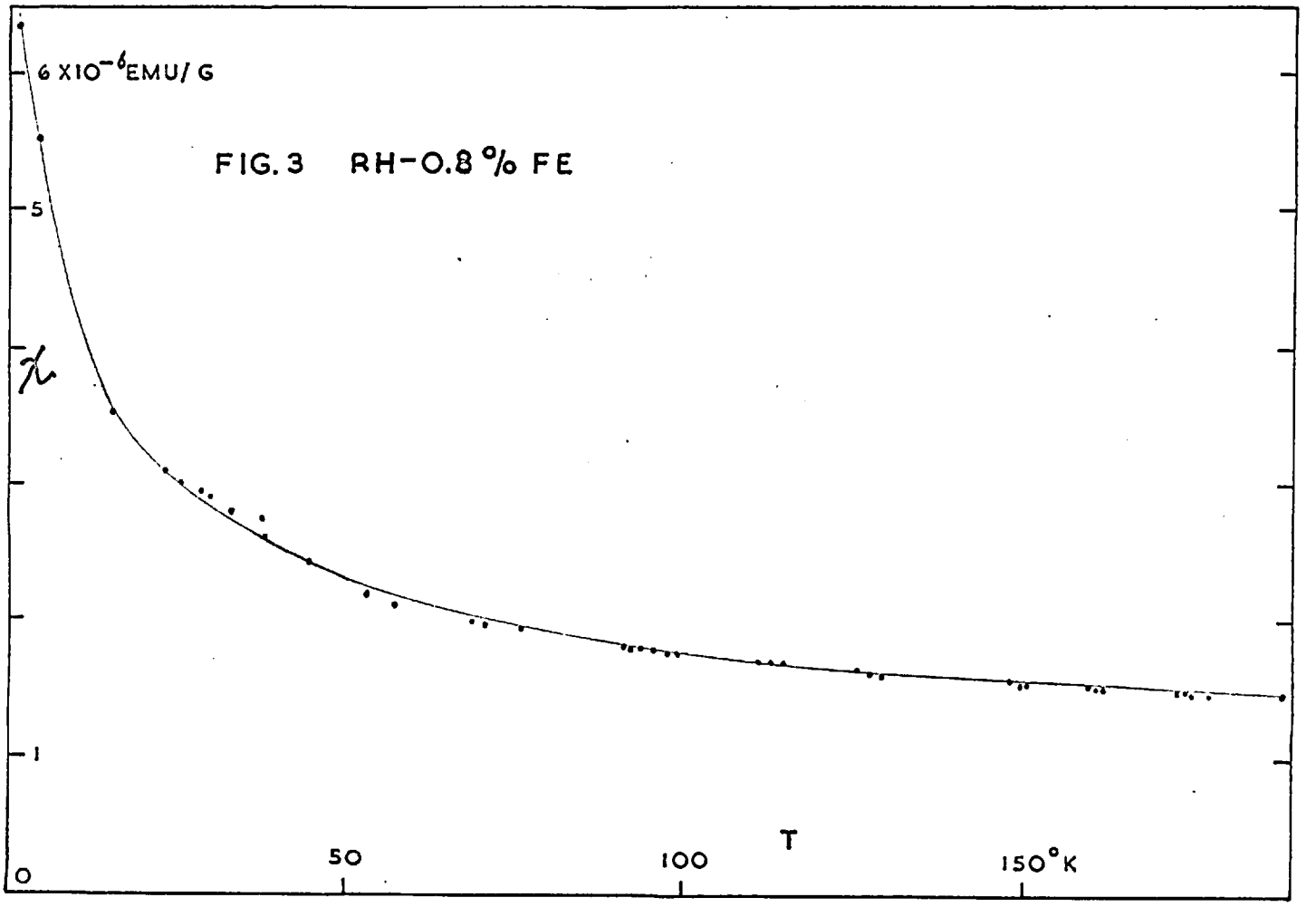

FIG. 3 RH – 0.8 % FE

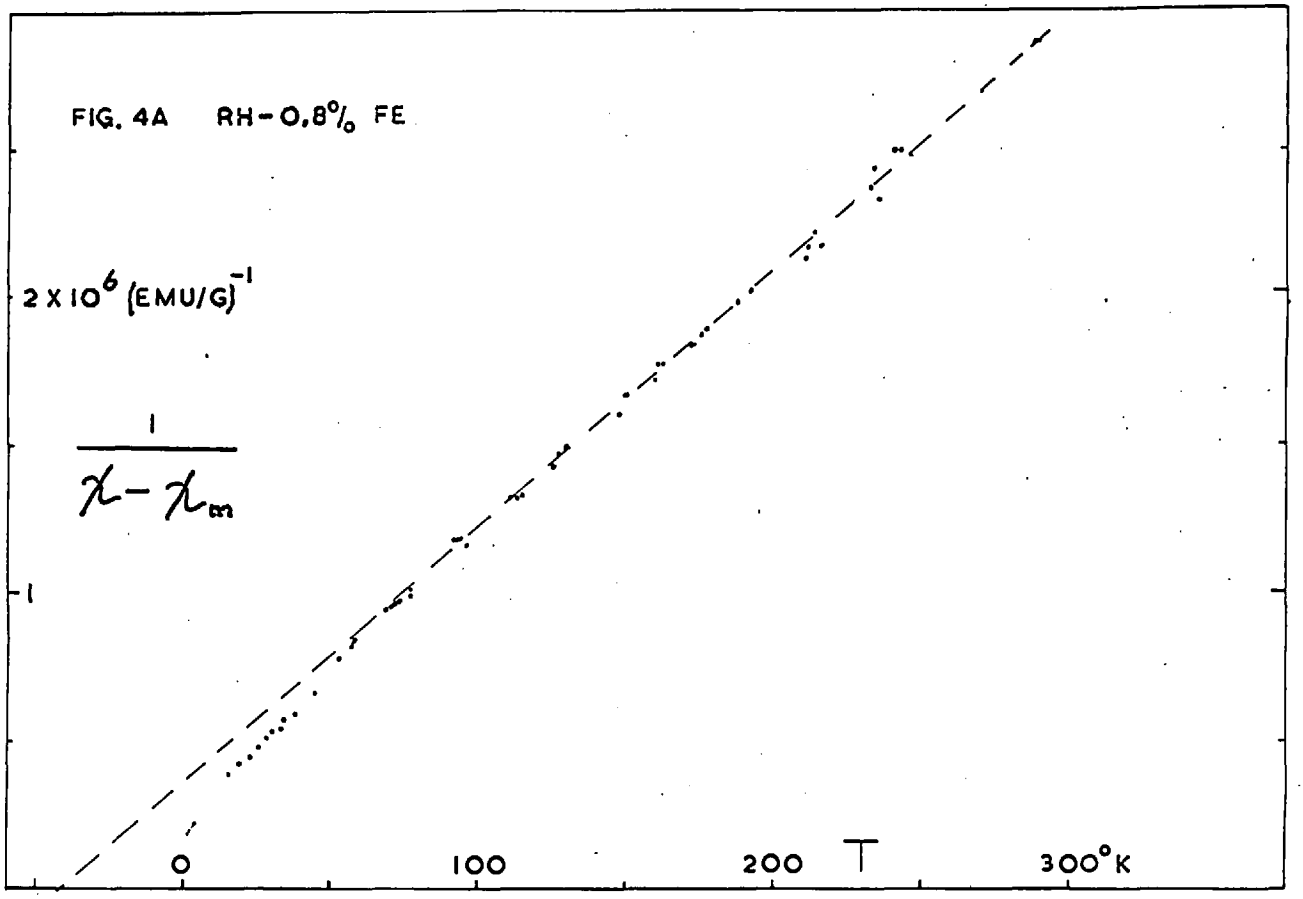
FIG. 4A RH-0.8% FE
2 X 10^6 (EMU/G)^-1
1/(χ - χm)
1
0
100
200
T
300°K

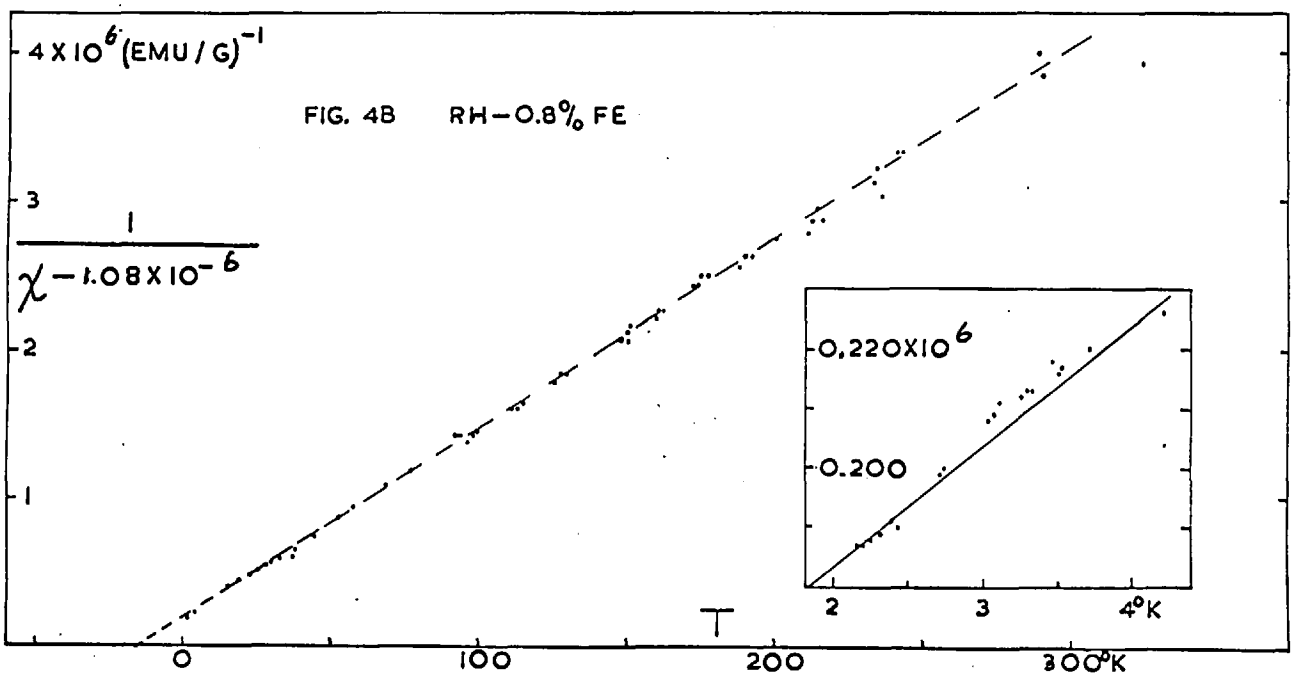
4 X 10^6 (EMU/G)^-1
FIG. 4B RH-0.8% FE
3
1/(χ - 1.08 X 10^-6)
2
1
0
100
200
T
300°K
0.220X10^6
0.200
2
3
4°K

slope at low temperatures can be reduced considerably by replacing χ_m, which varies from 0.92×10^{-6} emu/g at 20°K to 0.99×10^{-6} emu/g at 300°K, by a constant term $\chi_o = 1.08 \times 10^{-6}$ emu/g as is shown in Figure 4b. The curvature can however not be made to disappear with this procedure. The line drawn in Figure 4b gives $\mu_{eff} = 2.8\mu_B$, $\theta = -15°K$. Below 4.2°K no Curie-Weiss law is obeyed as is shown in Figure 4b. The best straight line through the points corresponds to $\mu_{eff} = 2.3\mu_B$, $\theta = -7.5°K$. Clogston et.al. [78] reported for this solution a simple Curie-Weiss behaviour with $\mu_{eff} = 3.0\mu_B$, $\theta = -14°K$ Although it is clear that Fe carries a moment in this solution the susceptibility as measured here can not be described by a simple Curie-Weiss law.

Discussion.

The following conclusions can be drawn from the experimental results reported here and those for the electrical resistivity in reference 84.

1. The absence of a field-dependence of the susceptibility shows that the moments on the Fe atoms do not interact.

2. The fact that the difference of the resistivity of Rh-Fe solutions and that of pure Rh, $\Delta\rho$, is proportional to the Fe concentration c suggests that this extra resistivity is due to the scattering of conduction electrons by single Fe atoms.

3. Then the strong increase of $\frac{\Delta\rho}{c}$ with temperature indicates that as the temperature is raised the solute atoms make a transition into a state where the atoms have a larger cross-section for conduction-electron scattering.

4. At high temperatures apparent Curie-Weiss behaviour for the susceptibility is found. The value of θ ($= -41^{\circ}K$) can however not be ascribed to interactions between Fe atoms because at 1.8° and $4.2^{\circ}K$ the magnetization of the alloy is proportional to the applied field.

The change of the slope of the curve in Figure 4a is similar to that found for the hydrated sulphate of Nd [7] where the curvature can be ascribed to the fact that excited states in which the atom carries a different moment from that of the ground state, become occupied as the temperature is raised. This explanation applied to Rh-Fe is consistent with the interpretation of the resistivity results given above. In this case the existence is required of energy levels which are narrow compared to kT for $T \lesssim 300^{\circ}K$, but in a metallic structure such sharp states can not exist. As discussed in Chapter I, the width of the 3d-level of a solute atom can be estimated at at least 0.1 eV ($\sim 1000^{\circ}K$). As was shown however by Korringa and Gerritsen (Chapter III, Sec.E, 4a) the resistivity of a number of Cu and Au based solid solutions can be described formally in terms of a one-electron theory if the existence of sharp resonant states near the Fermi-energy is postulated. The possibility that the χ vs T curve for this Rh-Fe alloy can be described in terms of a thermal excitation of the Fe atoms has therefore been investigated.

Let μ_1 be the moment of an Fe atom in the ground state, μ_2 that in the excited state and N_i the number of Fe atoms having a moment μ_i ($i = 1,2$).

The susceptibility can then be written as $\chi = \frac{N_1 \mu_1^2}{3kT} + \frac{N_2 \mu_2^2}{3kT}$ (1), if the solute atoms do not interact. If, as in the theory given for paramagnetic salts the ratio $\frac{N_1}{N_2}$ is determined by a Boltzmann distribution and if u is the energy difference between the ground-state and the excited state, then $\frac{N_1}{N_2} = e^{-u/kT}$ (2) which leads with equ (1) to

$$\chi = \frac{N \mu_1^2 (1 + W_p^2)}{3kT (1 + W)} \qquad (3)$$

where $p \equiv \frac{\mu_1}{\mu_2}$

$N \equiv N_1 + N_2$

$W = e^{-u/kT}$

A curve of $\frac{1}{\chi}$ vs T for u = 20°K and p = 2 is given in Figure 5. Above $T = \frac{u}{k}$ the curve $\frac{1}{\chi}$ vs T lies close to a straight line, which intersects the temperature-axis at $T = \theta' \equiv \frac{1}{2} \frac{1 - p^2}{1 + p^2} \cdot \frac{u}{k}$ (4)

B

Because the slope of the experimental $\frac{1}{\chi}$ vs T curve (Figure 4) is larger at high than at low temperatures a value of $p > 1$ is needed to fit equ (3) to the observed points. From (4) it follows then that $\theta' < o$, while $|\theta'| < \frac{1}{2} \frac{u}{k}$. The experimental values of $\frac{1}{\chi}$ at low temperatures make it necessary to have a sharp rise from T = 0°K to T = 2°K and a flattening out as the temperature is increased, so that a value of a few degrees K for $\frac{u}{k}$ is needed. But this implies that $|\theta'|$ is at most a few degrees K while the graphs 4a and 4b show that the experimental value is at least 15°K. The observed χ vs T curve can thus not be fitted to equ (3).

FIG. 5

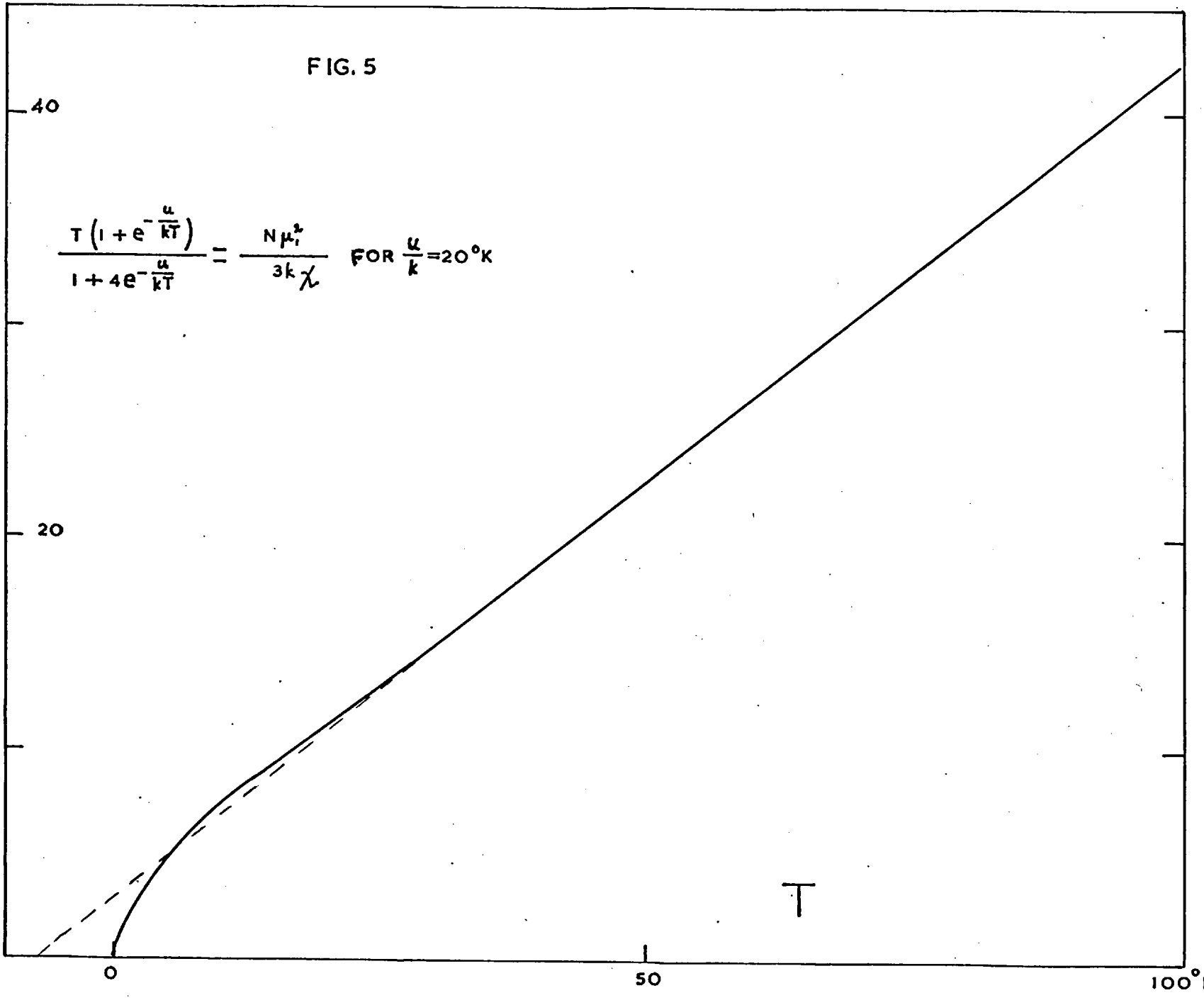
40
20
$\frac{T\left(1+e^{-\frac{u}{kT}}\right)}{1+4e^{-\frac{u}{kT}}} = \frac{N\mu_1^2}{3k\chi}$ FOR $\frac{u}{k}$=20°K
T
0
50
100°K

It might be possible that if a molecular field is introduced this procedure will be successful. As said above, however, down to 1.7°K no interaction between the atomic moments seem to take place. Further if the solute moment changes the molecular field acting on a particular Fe atom will change, so that the interaction parameters will be temperature-dependent and the model will then contain too many variable parameters to be useful. That this very simple model does not apply does not rule out the possibility of an excitation of the Fe atoms.

As an extension of the theory given by Anderson, the change of the atomic moment with temperature was discussed by White and Clogston (Chapter I). For a virtual state with a width of 0.1 eV or more and a change in temperature of 100°K, the predicted change of the moment is however too small to account for the Rh-Fe results.

A different possibility is to ascribe the change in slope of the $\frac{1}{\chi}$ vs T curve to a change in the moment associated with an Fe atom by a polarization of the Rh atoms which are nearest neighbours to that Fe atom. This effect has been shown to occur in Pd-Fe (Chapter III, Sec. F, 3) and can be described satisfactorily by the theory developed by Clogston et.al.[78] To explain the observed susceptibility curve for Rh-Fe, this effect will have to be strongly temperature-dependent. Because the density of states at the Fermi-energy of Rh is a steep and non-linear function of energy, a change of temperature is expected to have a similar effect on the magnetic properties as the addition of electrons to the system and, as was shown by Clogston et.al., the addition of Pd to Rh-Fe increases the moment considerably. An estimate of this effect is made below.

According to the model developed in reference 78 the difference between the numbers of spin-up and spin-down states, having energy E, on a solvent atom nearest neighbour to a solute atom is approximately $\frac{d}{dE}\ (\rho(E)\ S_o J')$, where $\rho\ (E)$ is the density of states in energy for the solvent, S_o the spin on a solute atom, and J the exchange-integral between a solute atom and a nearest neighbour solvent atom. The magnetic moment on such a solvent atom in Bohr-magnetons is then at temperature T : $m = \int_{-\infty}^{+\infty} \frac{d}{dE}(2\rho(E)\ S_o J')\ f\ (E,T)\ dE$ (5)

where f (E,T) is the Fermi-Dirac distribution function. As was shown by Kriessman and Callen,[87] a good approximation to f (E,T) is the function $f^*(E,T)$ which is defined as

$$\left.\begin{aligned} f^*(E,T) &= 1 \quad \text{for } E < E_F - \delta \\ f^*(E,T) &= 1 - \frac{E - E_F + \delta}{2\delta} \quad \text{for } E_F - \delta < E_F < E_F + \delta \\ f^*(E,T) &= 0 \quad \text{for } E > E_F + \delta \end{aligned}\right\} (6)$$

here E_F is the Fermi-energy and $\delta = 2.77kT$. If f(E,T) is replaced by $f^*(E,T)$ equ (5) gives

$$m = \int_{E_b}^{E_F-\delta} \frac{d}{dE}\left\{2\rho(E)\ S_o J'\right\}\ dE + \int_{E_F-\delta}^{E_F+\delta} \frac{d}{dE}\left\{2\rho(E)\ S_o J'\right\}\left\{1 - \frac{E - E_F}{2\delta} + \delta\right\}\ dE \qquad (7)$$

where E_b is the bottom of the band. If $\rho(E)$ is written as

$\rho(E) = \rho(E_o) + a(E - E_o)^2$ (8) equ (7) gives

$m = 2\ S_o J \left\{\rho(E_F) + \frac{1}{3}\ a\delta^2\right\}$ (9).

The density of states as found from the electronic specific heat of Ru, Rh and Pd can be fitted roughly to equ (8) with $\rho\ (E_o)$ the density

of states at the Fermi-energy of Ru ($\approx$0.7 states per atom per eV) and a = 0.4 states per atom per $(eV)^3$. The term $\frac{1}{3} a\delta^2$ in equ (9) has for T = 100°K the value 2 x 10^{-4} $(eV)^{-1}$ while for Rh, $\rho(E_F) \approx 1$ $(eV)^{-1}$, so that this effect does not explain the observed result.

A last possibility is that the Fe atoms follow a normal Curie-Weiss law and that the Pauli-paramagnetic susceptibility of the 4d band, χ_p, is different from that in Rh and strongly temperature-dependent. As was shown in reference 87 the temperature-dependence of χ_p for a pure transition metal can be related directly to the shape of the density of states vs energy curve of the unfilled d-band, $\rho(E)$, near the Fermi-energy E_F. A sharp peak on $\rho(E)$ near E_F will give rise to a strong variation of χ_p with temperature. The susceptibility of pure Rh is only slightly temperature-dependent below 300°K. This interpretation thus implies that in Rh-Fe the presence of the solute disturbs the 4d-band of the matrix such that a sharp peak in the density of states curve appears near the Fermi-energy. As long as no other evidence of such a peak has been found this explanation is too far-fetched to be accepted.

§§ 3. Ir - Fe

Because Ir is below Rh in the periodic table of elements a measurement was made of the susceptibility of a solution of 0.8 at % Fe in Ir to investigate if in this system magnetic anomalies appear.

Results.

The susceptibility is field-independent at all temperatures down to 1.8°K. A plot of χ vs T is given in Figure 9.

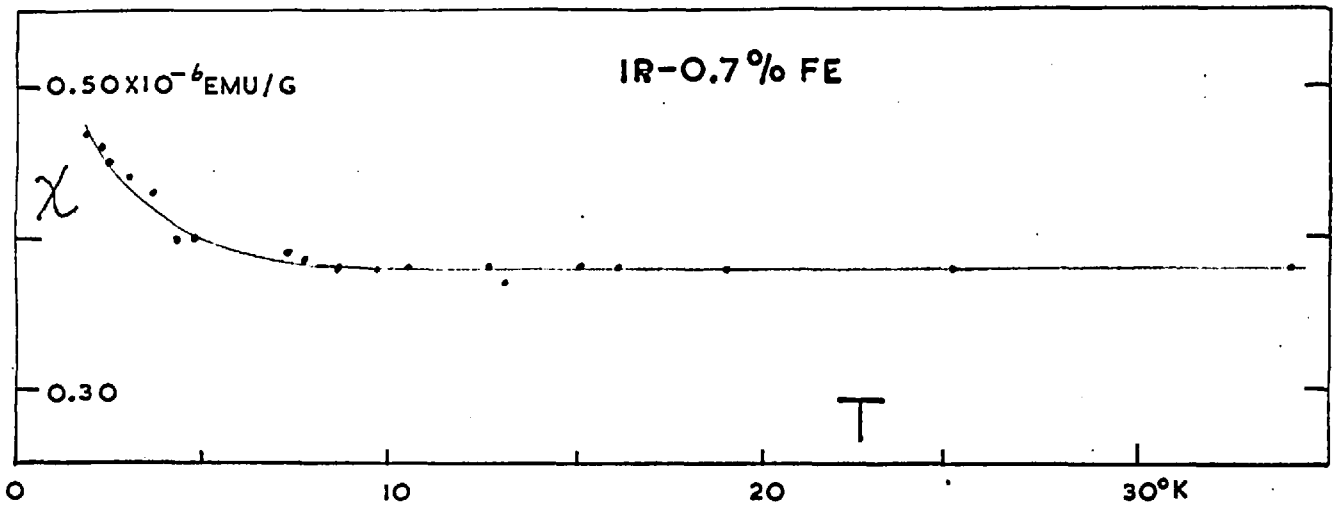
IR-0.7 % FE
0.50X10⁻⁶EMU/G
χ
0.30
T
0
10
20
30°K

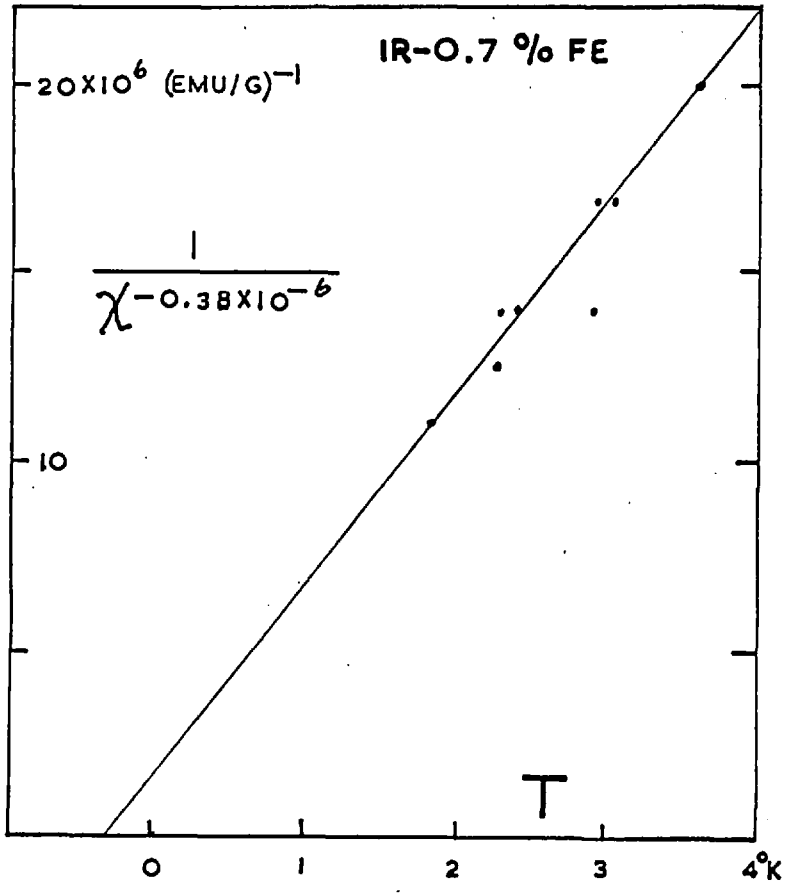
IR-0.7 % FE
20X10⁶ (EMU/G)⁻¹
1
χ−0.38X10⁻⁶
10
T
0
1
2
3
4°K

Derivation of the effective atomic moment.

A plot of $\frac{1}{\chi - \chi_m}$ vs T with χ_m the value for pure Ir, is not linear. From Figure 6 it is seen that from 10° to 30°K, χ is constant at $+ 0.38 \times 10^{-6}$ emu/g. In Figure 7 a plot of $\frac{1}{\chi - \chi_o}$ vs T with χ_o equal to this value is given. The effect of the solute is small so that the errors on the points are large. The line drawn corresponds to a moment per Fe atom $\mu_{eff} = 0.2\mu_B$, while $\theta = -0.4^{\circ}$K.

This results shows that the state of an Fe atom in solution in Ir is essentially different from that of such an atom in Rh-Fe. The fact that the atomic moment is extremely small can not be interpreted readily in terms of any existing theoretical model.

SUMMARY

The magnetic susceptibility has been measured for ternary solutions of Cr, Mn, Fe and Co in Cu-Zn alloys of different composition, and found to obey a Curie-Weiss law.

For a given solute the atomic moment per solute atom varies strongly with composition of the solvent. Also the results for different solutes are qualitatively different. The only existing theoretical model which is expected to be applicable to these alloys is that given by Anderson. An essential parameter in this model is the interaction between the 3d electrons on a solute atom and the conduction electrons of the matrix. At the present state of the theory it is not possible to give an estimate of this parameter. It can thus not be shown that this theory describes the observed results. If it is assumed that the theory is applicable some qualitative conclusions on the variation of the interactions mentioned with the electronic structure of the matrix can be drawn.

Also measured were some solutions of Fe in other transition metals. The results for a Mo-Fe alloy show that the resistivity maximum does not correspond to the onset of long-range ferromagnetic ordering. For a Rh-Fe solution it was confirmed that the mechanism responsible for the resistivity-anomaly also gives rise to an anomaly in the magnetic behaviour, and that this anomaly is not due to interactions between solute atoms. In Ir-Fe no anomaly was observed, the solute atomic moment in this solution is extremely small.

Suggestions for further work.

Due to metallurgical difficulties no solutions of Fe in γ phase Cu-Zn alloys were measured here. When the metallurgy of this ternary system will have been investigated and a procedure developed for casting these alloys, susceptibility measurements on solutions in matrices of different composition might contribute to the clarification of the striking results for solutions of Mn in this solvent.

In the binary Cu-Zn β-phase an ordered structure exists. If solid solutions of metals of the first transition group in this matrix exist, the effect of order in the solvent lattice on the solute moment can be investigated.

In analogy with the results for the solutions of transition metals in noble metals, also in the alloys considered in this work resistivity anomalies are expected at low temperatures. The preparation of specimens of γ brass alloys for resistivity measurements will be difficult, because the brittleness of this material makes it impossible to draw wires.

The magnetic properties of primary Cu-Fe solutions have not been investigated below $14^{\circ}K$. The available results suggest that at low temperatures magnetic ordering will take place. Because of the low solubility of Fe in Cu the danger exists of a ferromagnetic or superparamagnetic precipitate in the samples, which will therefore have to be cast and annealed with great care.

To investigate further the observed analogy between the Mo-Fe and Cu-Mn systems the susceptibility of Mo-Fe alloys containing about 5% Fe could be measured. If the behaviour of the systems is analogous a susceptibility-maximum is expected in this alloy.

APPENDIX A.

Details of the preparation of the Cu-An based alloys, as described in Chapter IV, part A. The indications in the columns "source" refer to the starting material used.

nr	wt% Zn	source wt% Zn	source wt% Cu	source Cu	trans. metal	melted temp. °C	melted time hrs	annealed temp. °C	annealed time days	analysis wt% trans. metal.
1	100	A	-	-	none	450	1/3	-	-	-
2	99.9	A	-	-	Fe	450	1	-	-	-
3	99.9	A	-	-	Fe	800	5	-	-	0.090
4	85.0	L	15.0	JM	none	700	2	420	8	-
5	84.9	L	15.0	JM	Mn	700	2	420	8	0.131
6	84.9	L	15.0	JM	Fe	700	2	420	8	0.090
7	84.9	L	15.0	JM	Co	700	2	420	8	0.090
8	81.0	L	19.0	S	none	750	1	400	14	-
9	80.8	L	19.2	S	Cr	750	1½	500	4	0.030
10	81.0	L	18.9	S	Mn	800	2	500	4	0.100
11	80.9	L	19.0	S	Fe	800	3	500	4	0.090
12	81.1	L	18.8	S	Co	770	1½	500	4	0.090
13	62.3	L	37.7	S	-	900	1½	700	5	-
14	61.5	L	38.4	S	Cr	860	3	700	5	0.075
15	61.0	L	38.9	JM	Mn	860	3	700	5	0.032
16	62.7	L	37.2	S	Mn	900	3½	700	5	0.080
17	65.3	L	34.6	JM	Mn	860	3	700	5	0.080
18	62.1	L	37.8	S	Co	860	3	700	5	0.085

APPENDIX B

The energy of the electromagnetic field is

$$\frac{1}{8\pi}\int \underline{B}\cdot\underline{H}\,dv = \int \frac{H^2}{8}\,dv + \tfrac{1}{2}\int \underline{M}\cdot\underline{H}\,dv$$

$\underline{M}$ is the magnetization per unit volume v the volume. The change in energy as a result of the introduction of a paramagnetic sample in the field is $\Delta E = \frac{1}{2}\int \underline{M}.\underline{H}\,dv$ and the force on the sample in the z-direction $f_z = -\frac{\partial(\Delta E)}{\partial z} = -\frac{1}{2}\frac{\partial}{\partial z}\int \underline{M}\cdot\underline{H}\,dv$.

If $\underline{M}$ and $\underline{H}$ do not vary over the volume of the specimen and if $\underline{H} = \underline{H}(z)$ and $\underline{M} = \underline{M}(z)$: $f_z = -\frac{1}{2} V \frac{\partial}{\partial z}(\underline{H}.\underline{M}) = -\frac{1}{2}\left(M + H\frac{dM}{dz}\right)\frac{dH}{dz}$.
If M^* is the magnetization per unit mass,

$f_z = -\frac{1}{2} m \left(M^* + H\frac{dM^*}{dz}\right)\frac{dH}{dz}$, where m is the mass of the sample.

APPENDIX C

MAGNET CIRCUIT

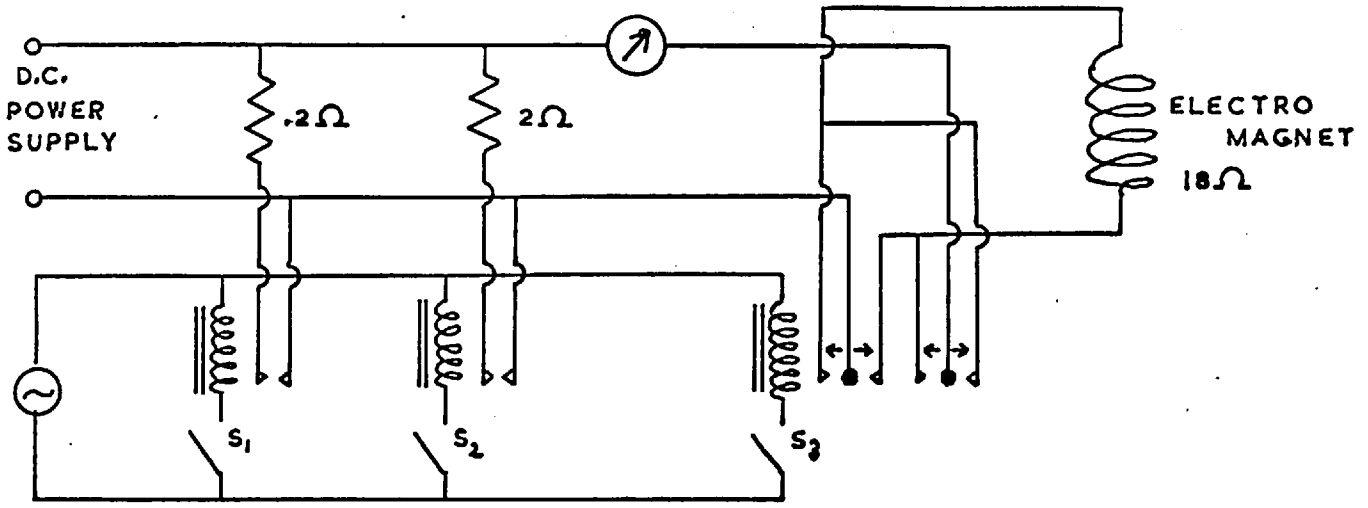

CONTROL OF THE MAGNET CURRENT

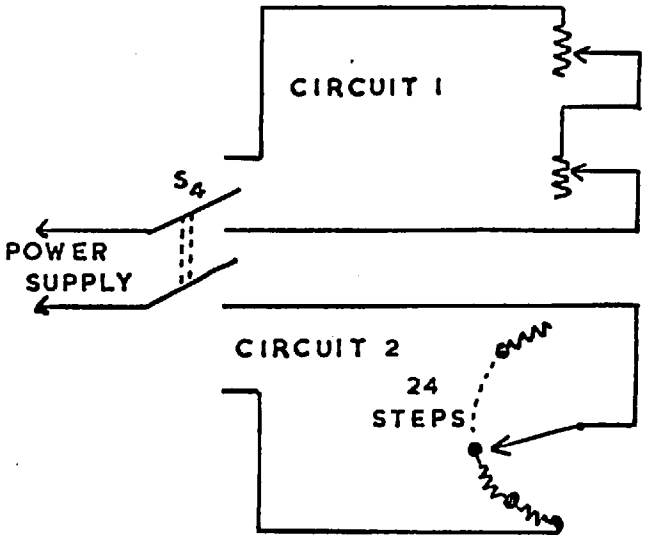

CIRCUIT 1 FOR CONTINUOUS ,

CIRCUIT 2 FOR STEPWISE

VARIATION OF THE MAGNET

CURRENT .

OVER S_3 IS A LID L_3

OVER S_1, S_2, L_3 AND S_4 A LID L_1

ALARM CIRCUIT

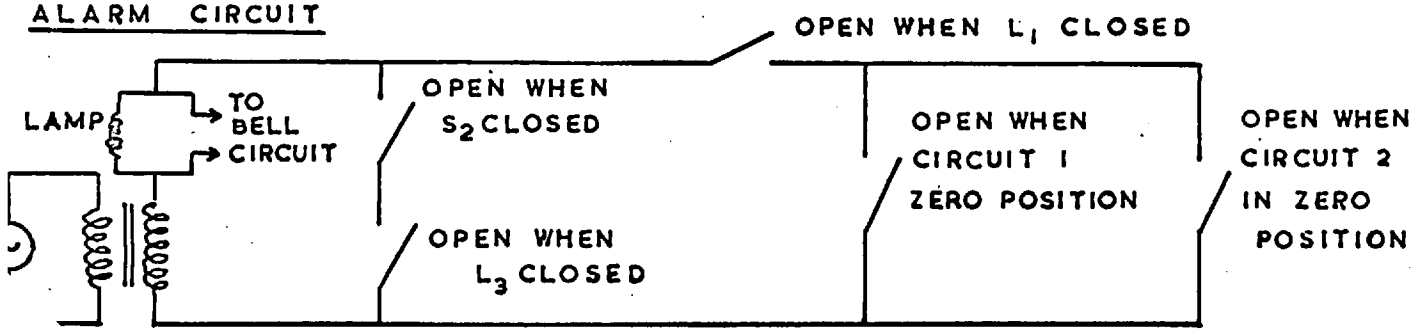

APPENDIX D.

As a check on the thermometry the susceptibility of manganous ammonium sulphate was measured. In Table I is given the temperature of the salt as found from the susceptibility, in the Tables II and III the corresponding readings of the carbon resistance thermometer and the thermocouple.

I	II	III
temp. salt	temp. carbon resistor	temp. thermocouple
^{o}K	^{o}K	^{o}K
13.9	13.6	
15.7	14.6	
16.8	16.4	
18.9	18.3	
22±1	20.2	20.5
24.7	25.2	25
26.6	26.4	26
37.8	36.5	37
58.9		56.5
56.1		57
59.4		60
76.2		77

REFERENCES

1. H. Jones. Phil. Mag. 44, 907, 1953

2. B.R. Coles. Phil. Mag. 44, 915, 1953

3. J. Friedel. Nuovo Cimento, Supp. Vol. 7, 287, 1958.

4. J.M. Ziman, Electrons & Phonons, Clarendon Press, 1960, p.159.

4a. idem p. 348.

5. G.G.E. Low, M.F. Collins. J. App. Phys. 34, 1195, 1963

   M.F. Collins, G.G. Low, Conf. Electronic Structure of Alloys, Sheffield 1963.

   M.F. Collins, Conf. Electronic Structure of Alloys, Sheffield 1963.

6. G.F. Koster, J.C. Slater, Phys. Rev. 96, 1208, 1954.

7. E.C. Stoner, Magnetism and Matter, Methuen, 1934, p.306.

8. C.G. Shull, M.K. Wilkinson, Phys. Rev. 97, 304, 1955.
   See also Ref. 5.

9. L.I. Schiff, Quantum Mechanics, McGraw-Hill, 2nd. ed, 1955, p.113

   V. Rojansky, Introductory Quantum Mechanics, Prentice-Hall, p.222.

10. A. Blandin, J. Friedel, J. Phys. Rad. 20, 160, 1959
    See also: P. de Faget de Casteljau, J. Friedel, J. Phys. Rad. 17,27, 1956

11. J. Friedel, Ann. Physique 9, 166, 1954

12. J. Friedel, Can. J. Phys. 34, 1190, 1956

13. K.D. Bowers, J. Owen, Repts. Prog. Phys. 18, 305, 1955.

14. P.A. Wolff, Phys. Rev. 124, 1030, 1961
    For the principles of the scattering theory used in this paper see:
    Ta-You Wu, Takashi Ohmura, Quantum Theory of Scattering, Prentice-Hall, 1962.

15. A.M. Clogston, Phys. Rev. 125, 439, 1962.

16. P.W. Anderson, Phys. Rev. 124, 41, 1961.

17. J.A. White, A.M. Clogston, J. App. Phys. 34, 1187, 1963.

18. C. Zener, Phys. Rev. 81, 440, 1951.

19. T. Kasuya, Progr. Theoret. Phys. 16, 45, 1956.

20. K. Yosida, Phys. Rev. 106, 893, 1957

21. A. Blandin, Thesis, Paris, 1961.

21a. W. Kohn, S.H. Vosko. Phys. Rev. 119, 912, 1960.

22. A.W. Overhauser, J. Phys. Chem. Solids 13, 71, 1960.

23. A.A. Abrikosov and L.P. Gorkov, Soviet Physics. JETP 16, 382, 1963.

24. J.H. Van Vleck, The Theory of Electric and Magnetic Susceptibilities, Oxford University Press , 1932.

25. C. Kittel, Introduction to Solid State Physics, 2nd.ed. Wiley, 1956.

26. A.J. Dekker, Physica 24, 697, 1958.

27. N.F. Mott, H. Jones, The Theory of the Properties of Metals and Alloys, Oxford University Press, 1936.

28. E.C. Stoner, Proc. Roy. Soc. A165, 372, 1938 and A169, 339, 1939. See also: A.H. Wilson Theory of Metals, Cambridge University Press, 2nd. ed. 1958, p.182.

29. E.P. Wohlfarth, Phil. Mag. 43, 374, 1951.

30. E.P. Wohlfarth, Proc. Phys. Soc. 60, 360, 1948.

31. E.P. Wohlfarth, Phil. Mag. 40, 1085, 1949.

32. E.P. Wohlfarth, J. Phys. Chem. Solids 1, 35, 1956-7.

33. A.B. Lidiard, Proc. Roy. Soc. A224, 161, 1954

34. L.M. Corliss, J.M. Hastings, R.J. Weiss. Phys. Rev. Letters 3, 211,1959.

35. A.W. Overhauser, Phys. Rev. 128, 1437, 1962.

36. R.E. Peierls, Quantum Theory of Solids, Clarendon Press, 1955.

37. J.E. Hebborn, J.M. Luttinger, E.H. Sondheimer, P.J. Stiles, J. Phys. Chem. Solids 25, 741, 1964

38. M. Hansen, Constitution of Binary Alloys, McGraw-Hill, 1958.

39. J. Owen, M.E. Browne, V. Arp, A.F. Kip, J. Phys. Chem. Solids 2, 85, 1957.

40. A. van Itterbeek, W. Peelaers, F. Steffens, App. Sci.Res. B8, 337, 1960.

41. I.S. Jacobs, R.W. Schmitt, Phys. Rev. 113, 459, 1959.

42. A.R. Kaufmann,S.T. Pan, J.R. Clark, Rev. Mod. Phys. 17, 87, 1945.

43. O.S. Lutes, J.L. Schmit, Phys. Rev. 134, A676, 1964

44. A. Kjekshus and W.B. Pearson, Can.J. Phys. 40, 98, 1962.

45. For a survey of the experimental work on the resistivity and magnetoresistance of dilute alloys, see A.N. Gerritsen, Physica 25, 489, 1959.

46. R.W. Schmitt, I.S. Jacobs, J. Phys. Chem.Solids 3, 324, 1957.

47. G.H. Wannier, Elements of Solid State Theory, Cambridge University Press, 1959, p.89.

48. J.E. Zimmerman and F.E. Hoare. J. Phys. Chem.Solids, 17, 52, 1960.

49. J. de Nobel, F.J. du Chatenier, Physica 25, 969, 1959.

50. J.P. Franck, F.D. Manchester, D.L. Martin, Proc.Roy.Soc. A263,494,1961

51. J. de Nobel, F.J. du Chatenier. Proceedings 8th. Int. Conf. Low Temp. Phys. London. p350 Butterworth, 1963, 241.

52. D.K.C. MacDonald, W.B. Pearson, I.M. Templeton
Proc. Roy. Soc 266, 161, 1962.

52a. A.V. Gold, D.K.C. MacDonald, W.B. Pearson, I.M. Templeton,
Phil. Mag. 5, 765, 1960.

53. E. Hildebrand, Ann. Physik 30, 593, 1936.

54. E. Bitter, A.R. Kaufmann, C. Starr, S.T. Pan,
Phys. Rev. 60, 134, 1941.

55. B. Knook, Thesis, Leiden, 1962.

56. J.S. Dugdale, D.K.C. MacDonald, Can.J. Phys. 35, 271, 1957.

57. L.T. Crane, J.E. Zimmermann, Phys. Rev. 123, 113, 1961.

58. L.T. Crane, Phys. Rev. 125, 1902, 1962.

59. E.W. Pugh, B.R. Coles, A. Arrott, J.E. Goldman,
Phys. Rev. 105, 814, 1957.

60. E.W. Pugh, F.M. Ryan, Phys. Rev. 111, 1038, 1958.

61. G.J. Los, A.N. Gerritsen, Physica 23, 633, 1957.

62. G.L. Guthrie, S.A. Friedberg, J.E. Goldman,
Phys. Rev. 113, 45, 1959.

63. E.W. Collings, F.T. Hedgcock,
Phys. Rev. 126, 1654, 1962.

64. E.W. Collings, F.T. Hedgcock, W.B. Muir,
Proc. 8th. Int. Conf. Low Temp. Phys. London, Butterworth, 1963,p.253.

65. D.A. Spohr, R.T. Webber, Phys. Rev. 105, 1427, 1957.

66. Y. Muto, Y. Tawara, Y. Shibuya, T. Fukuroi,
J. Phys. Soc. Japan 14, 380, 1959.

67. Y. Muto, J. Phys. Soc. Japan 15, 2119, 1960.

68. R.T. Webber, Phys. Rev. 105, 1437, 1957.

69. J.K. Logan, J.R. Clement, H.R. Jeffers, Phys. Rev. 105, 1435,1957.

70. D.L. Martin, Con.J. Phys. 39, 1385, 1961.

71. M.A. Taylor, J.P. Burger, J. Wucher, J.Phys. Rad. 20, 829, 1959.

72. F.T. Hedgcock, W.B. Muir,E. Wallingford.
Can.J. Phys. 38, 376, 1960.

G. Gaudet, F. T. Hedgcock, G. Lamarche, E. Wallingford.
Can.J. Phys. 38, 1134, 1960.

73. D.L. Martin, Proc. Phys. Soc. 78, 1489, 1961.

74. B. Henderson, G.V. Raynor, J. Phys. Rad. 23, 685, 1962.

75. H.P. Myers, R. Westin, Phil. Mag. 8, 669, 1963.
and 8, 1969, 1963.

76. B. Henderson, G.V. Raynor, J. Phys. Chem.Solids 25, 191, 1964.

77. B. Henderson, G.V. Raynor, Proc.Roy.Soc. A267, 313, 1962.

78. A.M. Clogston, B.T. Matthias, M. Peter, H.J. Williams, E. Corenzwit,
R.C. Sherwood. Phys. Rev. 125, 541, 1962.

79. D. Gerstenberg, Ann. Physik 2, 236, 1958.

80. J. Crangle, Phil. Mag. 5, 335, 1960.

81. R.M. Bozorth, P.A. Wolff, D.D. Davis, V.B. Compton, J.H.Wernick,
Phys. Rev. 122, 1157, 1961.

82. R.M. Bozorth, D.D. Davis, J.H. Wernick.
J.Phys. Soc. Japan 17, supp.B-I, 112 (1962).

83. F.E. Hoare, J.C. Matthews, Proc.Roy.Soc. A212, 137, 1952.

84. B.R. Coles, Phil. Mag, 8, 335, 1963 , Phys. Letters 8, 243, 1964.

85. J.A. Cape, R.R. Hake,
International Conference on Magnetism, Nottingham 1964, (to be published).

86. B.W. Veal, J.A. Rayne, Phys. Rev. 130, 2156, 1963.

87. C.J. Kriessman, M.B. Callen, Phys. Rev. 94, 837, 1954.

88. J. Korringa, A.N. Gerritsen, Physica 19, 457, 1953.

89. J. Korringa, Physica 19, 816, 1953.

90. R.W. Schmitt, Phys. Rev. 103, 83, 1956.

91. K. Yosida, Phys. Rev. 107, 396, 1957.

92. A.D. Brailsford, A.W. Overhauser,
Phys. Rev. Letters, 3, 331, 1959.
J. Phys. Chem.Solids, 15, 140, 1960.

93. A.J. Dekker, Physica 25, 1244, 1959.

94. W. Marshall, Phys. Rev. 118, 1519, 1960.

95. A.M. Guenault, D.K.C. MacDonald, Phil. Mag,6, 1201, 1961.

96. A.R. de Vroomen, M.L. Potters, Physica 27, 1083, 1961.

97. G.G. Low, International Conference on Magnetism,
Nottingham 1964 (to be published).

98. T.B. Massalski, H.W. King, Alloy Phases of the Noble Metals.
Pergamon Press, 1961.

99. B. Henderson, R.J.M. Willcox, Phil. Mag. 9, 829, 1964.

100. E. Raub, private communication.

101. D. Griffiths, thesis Imperial College, 1961 and
J. Sci. Inst. 38, 463, 1961.

102. R.L. Powell, M.D. Bunch, R.J. Corruccini, Cryogenics 1, 239, 1961.

103. J.A. Marcus, Phys. Rev. 76, 621, 1949.

104. J.G. Daunt, A.A. Silvidi, Phys. Rev. 77, 125, 1950.

105. T.B. Massalski, H.W. King, Acta. Met. 10, 1171, 1962.

106. A.J. Bradley, J. Thewlis,
Proc. Roy. Soc. A112, 678, 1926.

107. H. Jones, The Theory of Brillouin zones and Electronic States in Crystals, North Holland Publishing Co. 1960.

108. B.W. Veal, J.A. Rayne, Phys. Rev. 132, 1617, 1963.